AD-A154 601 A MATHEMATICAL DESCRIPTION OF THE PULSAR DOPPLER SATELLITE TRACKING DATA EDITOR(U) NAVAL SURFACE WEAPONS CENTER DAHLGREN VA A D PARKS ET AL. SEP 82 1/3

UNCLASSIFIED NSWC/TR-82-391 F/G 17/3 NL

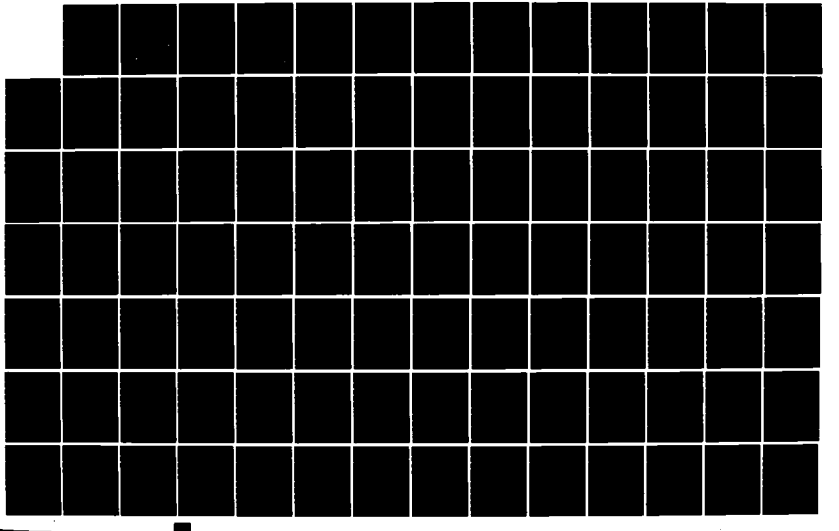

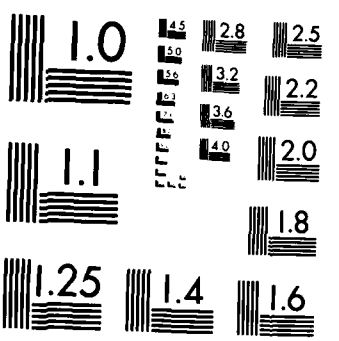

(2)

NSWC TR 82-391

A MATHEMATICAL DESCRIPTION OF THE PULSAR DOPPLER SATELLITE TRACKING DATA EDITOR

BY A. D. PARKS T. I. HICKS

STRATEGIC SYSTEMS DEPARTMENT

SEPTEMBER 1982

Approved for public release; distribution unlimited.

NAVAL SURFACE WEAPONS CENTER

Dahlgren, Virginia 22448 • Silver Spring, Maryland 20910

REPORT DOCUMENTATION PAGE

READ INSTRUCTIONS BEFORE COMPLETING FORM

1. REPORT NUMBER: NSWC TR 82-391	2. GOVT ACCESSION NO.: AD-A154 601
3. RECIPIENT'S CATALOG NUMBER:	
4. TITLE (and Subtitle): A MATHEMATICAL DESCRIPTION OF THE PULSAR DOPPLER SATELLITE TRACKING DATA EDITOR	5. TYPE OF REPORT & PERIOD COVERED: Final
	6. PERFORMING ORG. REPORT NUMBER:
7. AUTHOR(s): A. D. PARKS, T. I. HICKS	8. CONTRACT OR GRANT NUMBER(s):
9. PERFORMING ORGANIZATION NAME AND ADDRESS: Naval Surface Weapons Center (K13), Dahlgren, VA 22448	10. PROGRAM ELEMENT, PROJECT, TASK AREA & WORK UNIT NUMBERS: 63701B
11. CONTROLLING OFFICE NAME AND ADDRESS: Defense Mapping Agency, Washington, DC 20370	12. REPORT DATE: September 1982
	13. NUMBER OF PAGES: 198
14. MONITORING AGENCY NAME & ADDRESS (if different from Controlling Office)	15. SECURITY CLASS. (of this report): UNCLASSIFIED
	15a. DECLASSIFICATION/DOWNGRADING SCHEDULE:

16. DISTRIBUTION STATEMENT (of this Report)

Approved for public release; distribution unlimited.

17. DISTRIBUTION STATEMENT (of the abstract entered in Block 20, if different from Report)

18. SUPPLEMENTARY NOTES

19. KEY WORDS (Continue on reverse side if necessary and identify by block number)

PULSAR Doppler satellite tracking data editor
Satellite tracking, PULSAR Doppler satellite

20. ABSTRACT (Continue on reverse side if necessary and identify by block number)

This document provides a detailed discussion of both the mathematical and processing methodologies employed by the PULSAR Doppler satellite tracking data editor. Included are descriptions of coordinate reference frames; force models; variational equations; time calibration procedures; observation correction methods; the state estimation and parameter improvement process; data quality statistics; and associated numerical techniques.

FOREWORD

The PULSAR system has been developed to provide a sophisticated Doppler satellite tracking data editing capability. This system utilizes not only coarse editing methods, but also statistical techniques for observation editing within a station pass. Pass consistency editing is also employed to identify and edit entire passes of unacceptable tracking data.

This document provides a self-contained detailed description of the mathematical and processing methodologies used by the PULSAR system. Included are discussions of pertinent coordinate reference frames; force models; variational equations; time calibration procedures; observation correction methods; the state estimation and parameter improvement process; data quality statistics; and associated numerical techniques.

Released by:

O. F. BRAXTON, Head

Strategic Systems Department

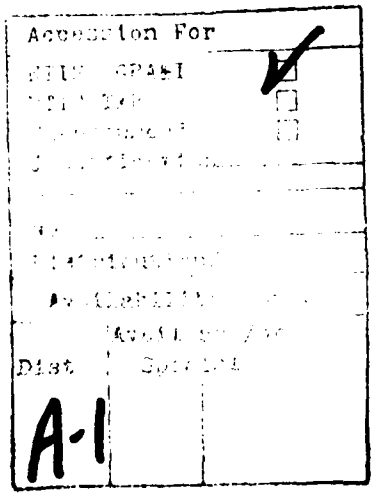

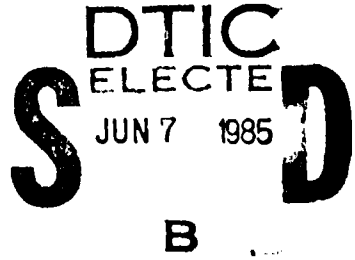

CONTENTS

CONTENTS (con't)

CONTENTS (Con't)

CONTENTS (con't)

ILLUSTRATIONS

TABLES

SECTION 1
INTRODUCTION

An overview of the Doppler satellite tracking data processing system with which this document is largely concerned is shown in Figure 1-1. In this figure the system's data processing steps are represented by circles and locations which provide support data or use the processed results are represented by rectangles. Also shown is the basic data flow between processing steps. Note that only those processing steps enclosed by the dashed box are performed by the PULSAR data editor.

The following sections discuss in detail both the mathematical and the processing methodologies employed by those processing steps enclosed within the PULSAR functional boundary. Included in this discussion are descriptions of pertinent coordinate reference systems; the force model and variational equations used by PULSAR; the time calibration procedures; observation correction methods; the state estimation and parameter improvement process; data quality statistics; as well as numerical techniques applied during processing. Since the analysis reporting function is essentially a bookkeeping procedure and is non-mathematical in nature, it is not discussed within this document. It should be mentioned that the PULSAR program is an outgrowth of the CELEST[1] program used at NSWC for many years and, as a result, both programs share common fundamental algorithms. Although this document is self-contained, the reader may wish to consult reference 1 for supporting background material.

---

[1] O'Toole, J.W., CELEST Computer Program for Computing Satellite Orbits, NSWC/DL TR-3565, Dahlgren, Virginia, 1976.

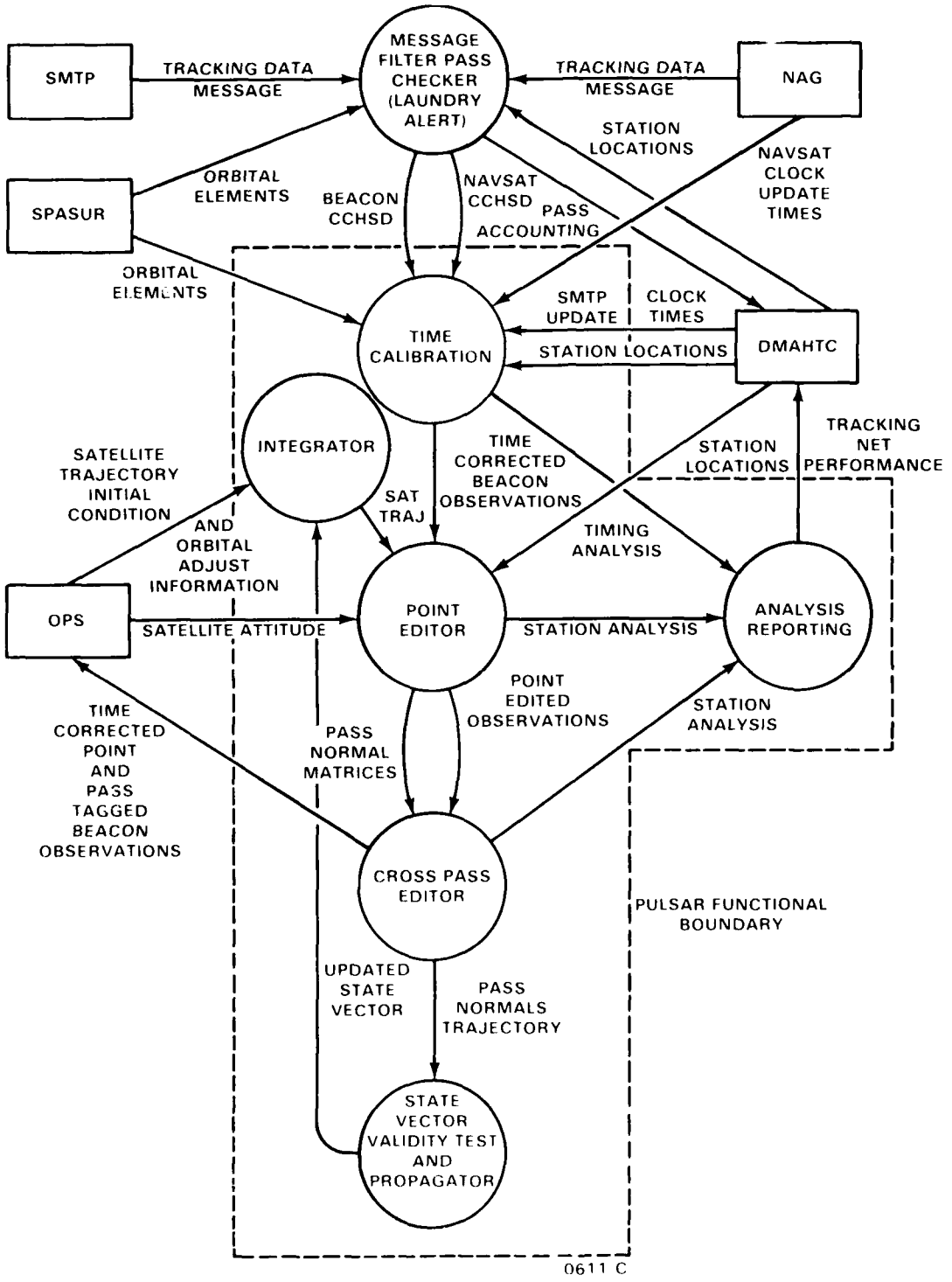

Figure 1-1. Doppler Satellite Tracking Data Processing

SECTION 2

COORDINATE REFERENCE SYSTEMS AND TRANSFORMATIONS

A number of coordinate reference frames are used by the PULSAR data editing system. These include the following:

(i) the basic inertial system;
(ii) the mean of date system;
(iii) the true of date system;
(iv) the instantaneous earth-fixed system;
(v) the earth-fixed reference ellipsoid system;
(vi) the geographical coordinate system; and
(vii) the time of closest approach (t_{ca}) reference system.

Each of these reference systems, as well as transformations between them, will be discussed in some detail in the following subsections.

2.1 EQUATORIAL INERTIAL COORDINATE SYSTEMS

Reference systems (i), (ii), and (iii) above are categorized as equatorial inertial systems. However, before undertaking a description of those inertial coordinate systems, it is necessary to define certain terms of reference. Fundamental to understanding those coordinate frames is the concept of the celestial sphere. This is an imaginary sphere of infinite radius the "center" of which is coincident with the center of the earth. The basic components of a system using the celestial sphere are the celestial equator, celestial poles, ecliptic and equinox. The celestial equator and celestial poles are obtained by projecting the earth's equator and poles onto the celestial sphere. The projection of the apparent path of the sun onto the celestial sphere forms a great circle inclined to the celestial equator at an angle of approximately 23.5°. This great circle is called the ecliptic and the inclination angle is called the obliquity of the ecliptic. The ecliptic intersects the celestial equator at two points called the vernal equinox and the autumnal equinox, i.e. the ascending and descending nodes, respectively, of the sun's apparent orbit. For historical reasons the vernal equinox is commonly referred to as the first point of Aries and is labeled with the symbol ♈. A depiction of the celestial sphere and it's components is given in Figure 2-1.

Table 2-2. Arguments of the Nutation Sine and Cosine Series (B1950.0)

i	a_i	b_i	c_i	d_i
1.	12.11684352	-0.0529538653	0.15595(-11)	0.4600(-19)
2.	200.01154773	1.9712946873	0.45354(-12)	0.2800(-19)
3.	24.23368705	-0.1059077306	0.31190(-11)	0.9200(-19)
4.	126.73383654	26.3527929915	-0.16941(-11)	0.1060(-18)
5.	357.92523074	0.9856002627	-0.11576(-12)	-0.6800(-19)
6.	214.53145564	13.0649926982	0.69061(-11)	0.2950(-18)
7.	197.93677848	2.9568949501	0.33776(-12)	-0.4000(-19)
8.	114.61699301	26.4057468568	-0.32537(-11)	0.6000(-19)
9.	341.26529219	39.4177856897	0.52119(-11)	0.4010(-18)
10.	202.08631698	0.9856944245	0.56929(-12)	0.9600(-19)
11.	287.80916684	-11.3165056059	0.90538(-11)	0.2170(-18)
12.	187.89470420	2.0242485526	-0.11059(-11)	-0.1800(-19)
13.	272.20238089	13.2878002932	-0.86003(-11)	-0.1890(-18)
14.	286.72228880	24.3814983042	-0.21477(-11)	0.7800(-19)
15.	266.64829917	13.0120388329	0.84656(-11)	0.3410(-18)
16.	157.58538787	-13.1179465635	-0.53466(-11)	-0.2490(-18)
17.	198.92466969	37.6692985975	-0.10748(-10)	-0.1110(-18)
18.	45.55408171	0.2757614603	-0.17066(-10)	-0.5300(-18)
19.	142.34062249	1.7484870922	0.15960(-10)	0.5120(-18)
20.	329.14844866	39.4707395551	0.36524(-11)	0.3550(-18)
21.	53.45612534	50.7342912957	-0.38419(-11)	0.1840(-18)
22.	69.06291129	26.1299853965	0.13812(-10)	0.5900(-18)
23.	54.54300338	15.0362873855	0.73596(-11)	0.3230(-18)
24.	195.79674734	52.4827783880	0.12118(-10)	0.6960(-18)
25.	102.50014948	26.4587007221	-0.48132(-11)	0.1400(-19)

The quantities in the parentheses are the exponents of 10.

Table 2-1. Coefficients of the Nutation Sine and Cosine Series (B1950.0) (Con't)

	$\alpha_i + \beta_i T$	$\gamma_i + \delta_i T$
.	-0.111(-06)	0.0
.	0.111(-06)	0.0
.	0.111(-06)	0.0
.	-0.111(-06)	0.55(-07)
.	-0.83(-07)	0.55(-07)
.	0.83(-07)	-0.55(-07)
.	-0.83(-07)	0.0
.	0.83(-07)	0.0
.	-0.83(-07)	0.0
.	-0.83(-07)	0.0
.	-0.55(-07)	0.0
.	-0.55(-07)	0.0
.	-0.55(-07)	0.0
.	0.55(-07)	0.0
.	-0.55(-07)	0.0
.	-0.55(-07)	0.0
.	-0.55(-07)	0.0
.	0.55(-07)	0.0
.	-0.55(-07)	0.0
.	0.0	0.0
.	0.0	0.0
.	0.0	0.0
.	0.0	0.0
.	0.0	0.0

. Coefficients numbered 70 through 106 are all zero for this (B1950.0) version of the transformation.

Table 2-1. Coefficients of the Nutation Sine and Cosine Series (B1950.0) (con't)

i	$\alpha_i + \beta_i T$	$\gamma_i + \delta_i T$
26.	-0.583(-06)	0.0
27.	0.527(-06)	-0.277(-06)
28.	0.443(-06) - 0.3(-08)T	0.0
29.	-0.416(-06)	0.222(-06)
30.	-0.415(-06) + 0.3(-08)T	0.194(-06)
31.	0.388(-06)	-0.194(-06)
32.	-0.361(-06)	0.194(-06)
33.	0.277(-06)	0.0
34.	-0.277(-06)	0.138(-06)
35.	-0.250(-06)	0.138(-06)
36.	-0.194(-06)	0.0
37.	0.194(-06)	-0.83(-07)
38.	0.166(-06)	0.0
39.	-0.166(-06)	0.83(-07)
40.	-0.166(-06)	0.83(-07)
41.	-0.166(-06)	0.83(-07)
42.	0.166(-06)	-0.55(-07)
43.	-0.138(-06)	0.83(-07)
44.	-0.138(-06)	0.83(-07)
45.	-0.138(-06)	0.83(-07)
46.	-0.138(-06)	0.83(-07)
47.	0.138(-06)	-0.83(-07)
48.	-0.111(-06)	0.55(-07)
49.	0.111(-06)	-0.55(-07)
50.	-0.111(-06)	0.0

Table 2-1. Coefficients of the Nutation Sine and Cosine Series (B1950.0)

i	$\alpha_i + \beta_i T$		$\gamma_i + \delta_i T$	
1.	-0.4789274(-02)	-0.4825(-05)T	+0.2558460(-02)	+ 0.252(-06)T
2.	-0.353601(-03)	-0.36(-07)T	0.153348(-03)	- 0.80(-07)T
3.	0.58002(-04)	+0.5(-08)T	-0.25105(-04)	+ 0.11(-07)T
4.	-0.56586(-04)	-0.5(-08)T	0.24548(-04)	- 0.14(-07)T
5.	0.34984(-04)	-0.86(-07)T	0.0	
6.	0.18751(-04)	+0.27(-08)T	0.0	
7.	-0.13788(-04)	+0.33(-07)T	0.5991(-05)	- 0.17(-07)T
8.	-0.9505(-05)	-0.11(-07)T	0.5083(-05)	
9.	-0.7250(-05)		0.3137(-05)	- 0.27(-08)T
10.	0.5937(-05)	-0.13(-07)T	-0.2579(-05)	+ 0.83(-08)T
11.	-0.4138(-05)		0.0	
12.	0.3445(-05)	+0.32(-08)T	-0.1833(-05)	
13.	0.3166(-05)		-0.1388(-05)	
14.	0.1666(-05)		0.0	
15.	0.1611(-05)		-0.861(-06)	
16.	-0.1583(-05)		0.833(-06)	
17.	-0.1444(-05)		0.611(-06)	
18.	0.1250(-05)		-0.666(-06)	
19.	0.1250(-05)		0.0	
20.	-0.1222(-05)		0.638(-06)	
21.	-0.888(-06)		0.388(-06)	
22.	0.777(-06)		0.0	
23.	0.722(-06)		-0.305(-06)	
24.	-0.722(-06)		0.305(-06)	
25.	0.694(-06)		0.0	

$T = (JD - 2,433,282.432,459,1) / 36,525.0$
The quantities in the parentheses are the exponents of 10

2.1.4 THE TRUE OF DATE INERTIAL REFERENCE SYSTEM AND THE $\underset{\sim}{C}$ TRANSFORMATION (con't)

$$\bar{\varepsilon}(^\circ) = \begin{cases} 23.44578773 - 0.356304 \times 10^{-6}(t-t_0) - 0.66319 \times 10^{-15}(t-t_0)^2 \\ \quad + 0.10318 \times 10^{-19}\,(t-t_0)^3 \quad , \quad \text{B1950.0} \quad \underline{\text{or}} \quad , \\ 23.43929111 - 0.3560346794 \times 10^{-6}(t-t_0) - 0.122848274 \\ \quad \times 10^{-15}(t-t_0)^2 + 0.103353 \times 10^{-19}(t-t_0)^3 \quad , \quad \text{J2000.0} \end{cases} \tag{8}$$

$$\Delta\psi(^\circ) = \sum_{i=1}^{106} (\alpha_i + \beta_i T) \sin\left[a_i + b_i(t - t_0) + c_i(t - t_0)^2 + d_i\,(t - t_0)^3\right], \tag{9}$$

and

$$\Delta\varepsilon(^\circ) = \sum_{i=1}^{106} (\gamma_i + \delta_i T) \cos\left[a_i + b_i(t - t_0) + c_i(t - t_0)^2 + d_i(t - t_0)^3\right]. \tag{10}$$

Equations (9) - (10) apply for both the B1950.0 and J2000.0 epochs and

$$T = \frac{t - t_0}{36525.0} \quad . \tag{11}$$

Values for the α_i, β_i, γ_i, and δ_i coefficients are given in Tables 2-1 and 2-3. Values for the a_i, b_i, c_i, and d_i coefficients are given in Tables 2-2 and 2-4.

For an arbitrary vector $\vec{X}$, one has the following relationships

$$\vec{X}'' = \underset{\sim}{C}\vec{X}' = \underset{\sim}{C}\,\underset{\sim}{D}\vec{X} \quad , \tag{12}$$

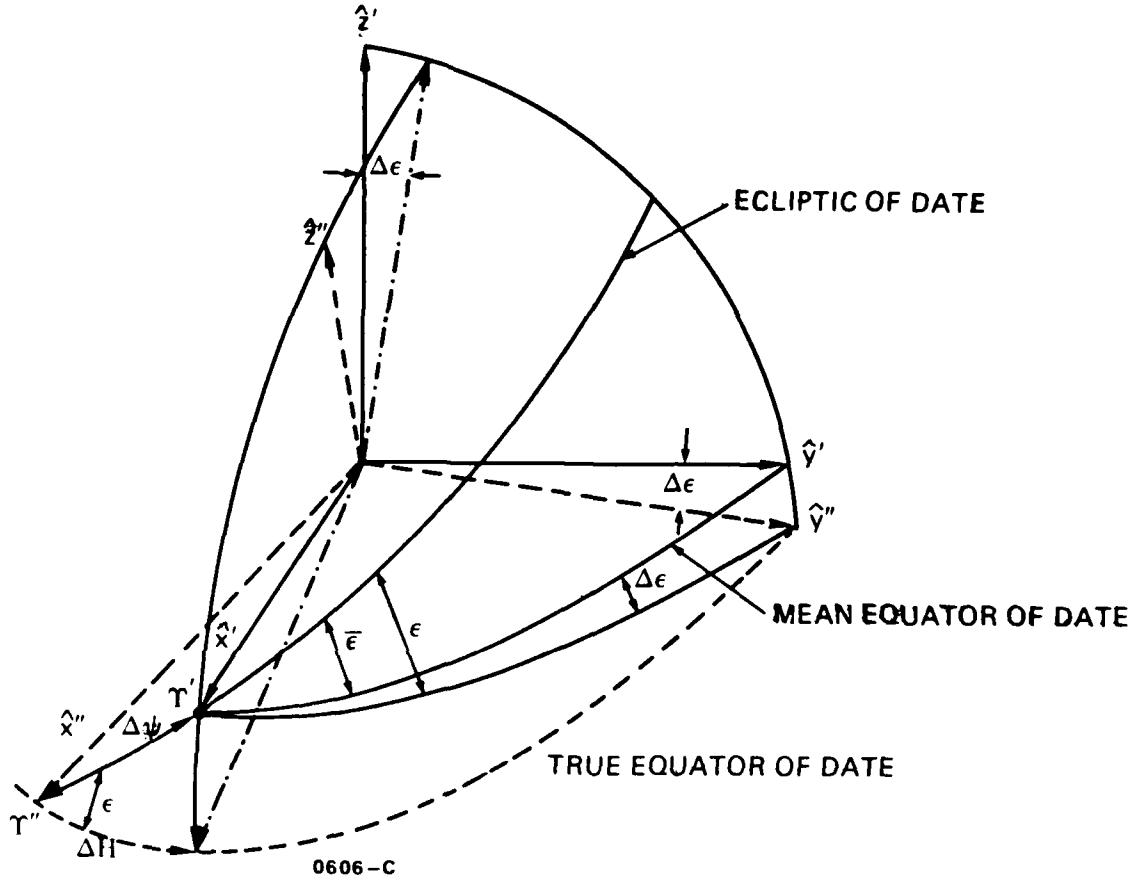

ϵ = TRUE OBLIQUITY OF DATE
$\bar{\epsilon}$ = MEAN OBLIQUITY OF DATE
$\Delta\epsilon$ = NUTATION IN OBLIQUITY
$\Delta\psi$ = NUTATION IN CELESTIAL LONGITUDE
ΔH = $\text{TAN}^{-1}[\text{TAN}\,\Delta\psi\,\text{COS}\epsilon]$

FIGURE 2-4. Nutation Geometry Showing $\Delta\epsilon$ and $\Delta\psi$ Corrections

2.1.4 THE TRUE OF DATE INERTIAL REFERENCE SYSTEM AND THE $\underset{\sim}{C}$ TRANSFORMATION

The true of date system is the inertial reference system at the epoch of date which has its (X, Y, Z) axes defined as follows:

$\hat{X}''$ is the unit vector along the true vernal equinox of date;

$\hat{Z}''$ is the unit vector along the earth's true axis of rotation of date and is positive in the northern hemisphere; and

$\hat{Y}''$ is the unit vector which completes the right-handed orthogonol system with $\hat{X}''$ and $\hat{Z}''$.

The shift from the mean of date system (as defined by precessional motion only) to the true of date system is resolved into nutation induced corrections known as the nutation in ecliptic longitude ($\Delta\psi$) and the nutation in obliquity ($\Delta\varepsilon$). The nutation geometry of Figure 2-4 defines these corrections.

The transformation from the mean of date system to the true of date system is accomplished through application of the $\underset{\sim}{C}$ matrix given by:

$$\underset{\sim}{C} = \begin{pmatrix} \cos\Delta\psi & -\sin\Delta\psi\cos\bar{\varepsilon} & -\sin\Delta\psi\sin\bar{\varepsilon} \\ \cos\varepsilon\sin\Delta\psi & \cos\varepsilon\cos\Delta\psi\cos\bar{\varepsilon}+\sin\varepsilon\sin\bar{\varepsilon} & \cos\varepsilon\cos\Delta\psi\sin\bar{\varepsilon}-\sin\varepsilon\cos\bar{\varepsilon} \\ \sin\varepsilon\sin\Delta\psi & \sin\varepsilon\cos\Delta\psi\cos\bar{\varepsilon}-\cos\varepsilon\sin\bar{\varepsilon} & \sin\varepsilon\cos\Delta\psi\sin\bar{\varepsilon}+\cos\bar{\varepsilon}\cos\varepsilon \end{pmatrix}, \quad (6)$$

where

$$\varepsilon = \bar{\varepsilon} + \Delta\varepsilon \ , \quad (7)$$

2.1.3 THE MEAN OF DATE INERTIAL REFERENCE SYSTEM AND THE $\underset{\sim}{D}$ TRANSFORMATION (con't)

$$\theta(^\circ) = \begin{cases} 0.15242971 \times 10^{-4}\,(t-t_o) - 0.88704407 \times 10^{-13}\,(t-t_o)^2 \\ \quad - 0.23849 \times 10^{-18}\,(t-t_o)^3, \quad \text{B1950.0} \quad \underline{\text{or}}\ , \\ 0.15243067 \times 10^{-4}\,(t-t_o) - 0.88835960 \times 10^{-13}\,(t-t_o)^2 \\ \quad - 0.23847663 \times 10^{-18}\,(t-t_o)^3, \quad \text{J2000.0} \end{cases}$$

In the above expressions

$$t = \begin{cases} \text{Julian Date (JD)}, & \text{B1950.0} \\ \text{Julian Ephemeris Date (JED)}, & \text{J2000.0} \end{cases} ,$$

and (3)

$$t_o = \begin{cases} 2433282.4234591, & \text{B1950.0} \\ 2451545.0\ , & \text{J2000.0} \end{cases} .$$

Thus one may write for an arbitrary vector $\vec{X}$:

$$\vec{X}' = \underset{\sim}{D}\ \vec{X} \quad , \tag{4}$$

where $\vec{X}'$ is the vector in the mean of date system and $\vec{X}$ is the vector in the basic reference system. Note that due to the orthogonality of the $\underset{\sim}{D}$ matrix one has

$$\vec{X} = \underset{\sim}{D}^T\ \vec{X}' \quad . \tag{5}$$

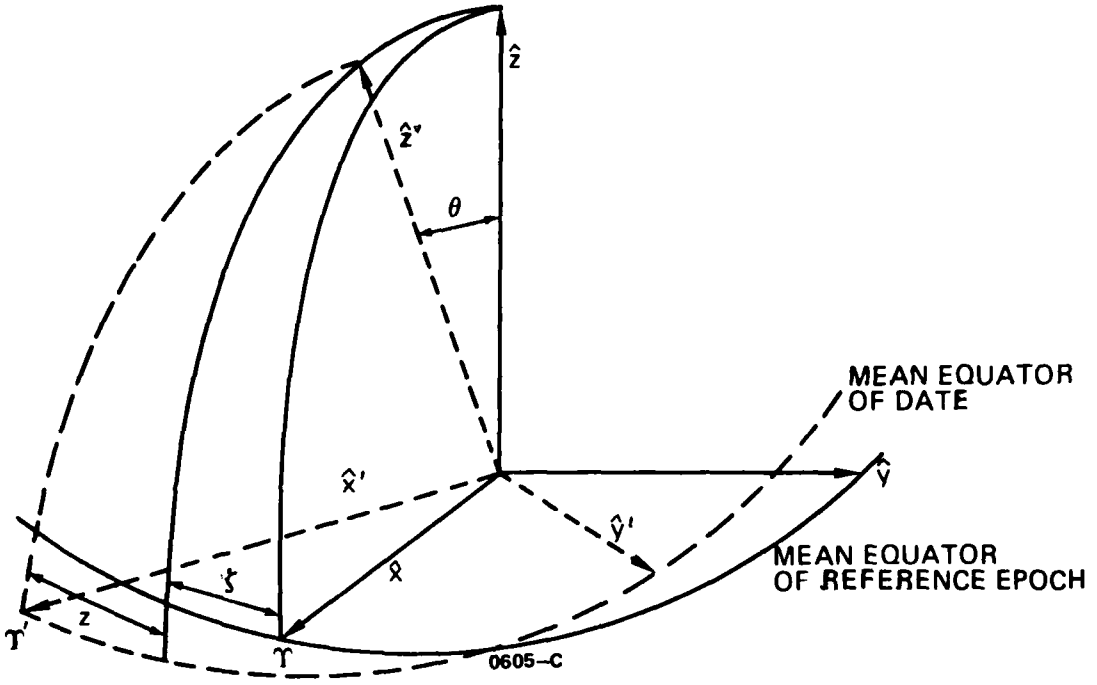

FIGURE 2-3. Precession Geometry Showing ζ, z and θ

2.1.3 THE MEAN OF DATE INERTIAL REFERENCE SYSTEM AND THE $\underset{\sim}{D}$ TRANSFORMATION (con't)

The difference in orientation of axes of the basic and of date inertial systems is a result of the general precession which is discussed in subsection 2.1.1. The complex motion of the general precession can be specified by the three angles ζ, Z, and θ. These angles are defined by the geometry shown in Figure 2-3.

The transformation from the mean equator and equinox of either of the standard epochs (B1950.0 or J2000.0) to the mean equator and equinox of date is given by [1]:

$$\underset{\sim}{D} = \begin{pmatrix} \cos Z\cos\theta\cos\zeta - \sin Z\sin\zeta & -\cos Z\cos\theta\sin\zeta - \sin Z\cos\zeta & -\cos Z\sin\theta \\ \sin Z\cos\theta\cos\zeta + \cos Z\sin\zeta & -\sin Z\cos\theta\sin\zeta + \cos Z\cos\zeta & -\sin Z\sin\theta \\ \sin\theta\cos\zeta & -\sin\theta\sin\zeta & \cos\theta \end{pmatrix} , \quad (1)$$

where

$$\zeta(^\circ) = \begin{cases} 0.17529829 \times 10^{-4}\,(t-t_o) + 0.62884345 \times 10^{-13}(t-t_o)^2 \\ \qquad + 0.10261 \times 10^{-18}(t-t_o)^3, \quad \text{B1950.0} \quad \underline{\text{or}} \\ 0.17539114 \times 10^{-4}\,(t-t_o) + 0.62856673 \times 10^{-13}(t-t_o)^2 \\ \qquad + 0.10260087 \times 10^{-18}(t-t_o)^3, \quad \text{J2000.0} \end{cases}$$

$$Z(^\circ) = \begin{cases} 0.17529829 \times 10^{-4}\,(t-t_o) + 0.22759135 \times 10^{-12}(t-t_o)^2 \\ \qquad + 0.10261 \times 10^{-18}\,(t-t_o)^3, \quad \text{B1950.0} \quad \underline{\text{or}} \\ 0.17539114 \times 10^{-4}\,(t-t_o) + 0.22793143 \times 10^{-12}(t-t_o)^2 \\ \qquad + 0.10376951 \times 10^{-18}(t-t_o)^3, \text{ J2000.0} \end{cases} \quad (2)$$

(con't next page)

[1] Explanatory Supplement to the Astronomical Ephemeris and the American Ephemeris and Nautical Almanac, Her Majesty's Stationery Office, 1961.

2.1.2 PULSAR BASIC INERTIAL REFERENCE SYSTEM

When integrating the satellite equations of motion (see SECTION 5), it is necessary to select a reference frame which is free of all movement. Per the above discussion, this implies that the integration space must be an inertial system fixed to a given equator and equinox, i.e. a standard epoch. PULSAR may optionally adopt as its standard epoch either the Besselian epoch B1950.0 or the Julian epoch J2000.0 so that the basic inertial reference frame is that set of inertial rectangular coordinates associated with either the mean equator and equinox of B1950.0 or J2000.0, respectively. Thus the (X, Y, Z) axes of the basic inertial reference system are defined as follows:

$\hat{X}$ is the unit vector pointing toward the mean vernal equinox of B1950.0 or J2000.0;

$\hat{Z}$ is the unit vector pointing along the earth's mean axis of rotation of B1950.0 or J2000.0 and is positive in the northern hemisphere; and

$\hat{Y}$ is the unit vector which completes the right-handed orthogonal system with $\hat{X}$ and $\hat{Z}$.

2.1.3 THE MEAN OF DATE INERTIAL REFERENCE SYSTEM AND THE $\underset{\sim}{D}$ TRANSFORMATION

The mean of date inertial reference system differs from the basic inertial reference system only in that its reference epoch can be any time, e.g. an observation time. Therefore the (X', Y', Z') axes of this reference frame are defined as follows:

$\hat{X}'$ is the unit vector pointing toward the mean vernal equinox of date;

$\hat{Z}'$ is the unit vector pointing along the earth's mean axis of rotation of date and is positive in the northern hemisphere; and

$\hat{Y}'$ is the unit vector which completes the right-handed orthogonal system with $\hat{X}'$ and $\hat{Z}'$.

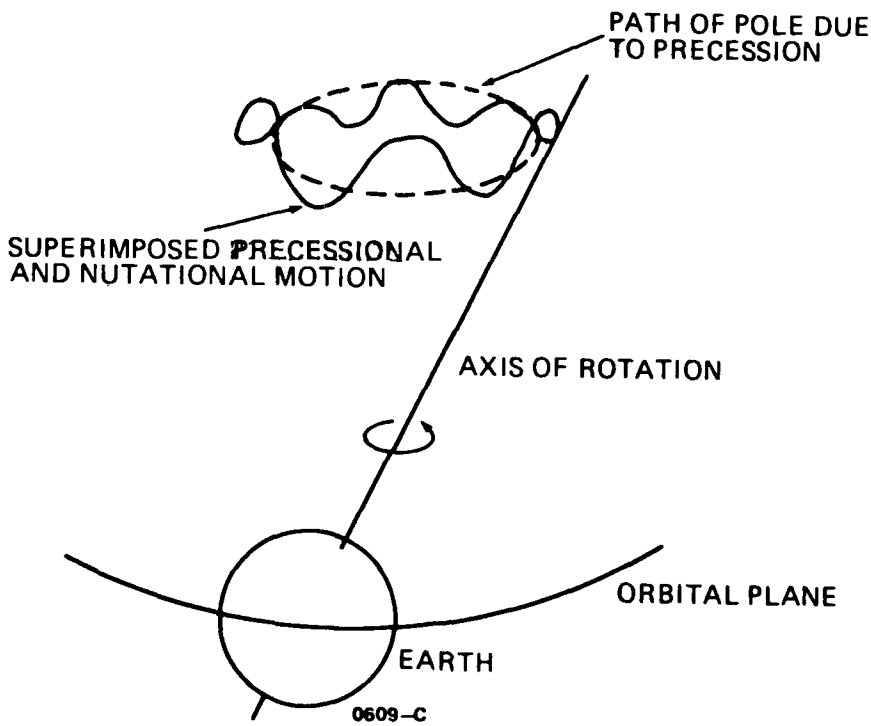

FIGURE 2-2. Precessional and Nutational Motion

2.1 EQUATORIAL INERTIAL COORDINATE SYSTEMS (con't)

All equatorial inertial coordinate systems are formulated using the celestial sphere and its components and are based upon the set of mutually orthogonal axes (X, Y, Z), where X is an axis aligned in the direction of the vernal equinox, Z is aligned in the direction of the celestial pole, and Y is aligned in a manner to complete the right-handed orthogonal system. Unfortunately, this system of coordinates is not fixed in time, but is time varying. This is due to the fact that the equinox undergoes a slow secular movement known as precession and a small periodic variation known as nutation. The complications associated with this motion can be compensated for. This is the subject of the following subsections.

2.1.1 PRECESSION AND NUTATION

The gravitational attractions of the moon and sun upon the earth's equatorial bulge tend to pull the earth's equatorial plane into coincidence with the plane of the ecliptic. However, due to the earth's rotation, these attractions result instead in a conical motion of the earth's axis about the pole of the ecliptic plane (i.e. the intersection with the celestial sphere of an imaginary line projected outwards from the center of the sphere in a direction perpendicular to the plane of the ecliptic). This motion is in the opposite direction to the earth's rotation and has a period of approximately 26,000 years.

This conical motion is usually treated as the sum of two components. One consists of the uniform westward motion of the vernal equinox along the ecliptic. This is called luni-solar precession. The other component of motion is periodic and is called nutation. It describes the departure of the actual position of the pole of the equator from its mean position as defined by precessional motion only.

There are also smaller precessional motions of the ecliptic plane caused by the planetary gravitational attraction and general relativistic effects. These motions are called planetary precession and geodesic precession, respectively. The combined effect of luni-solar precession, planetary precession and geodesic precession is called general precession. The superposition of precessional and nutational motion is depicted in Figure 2-2.

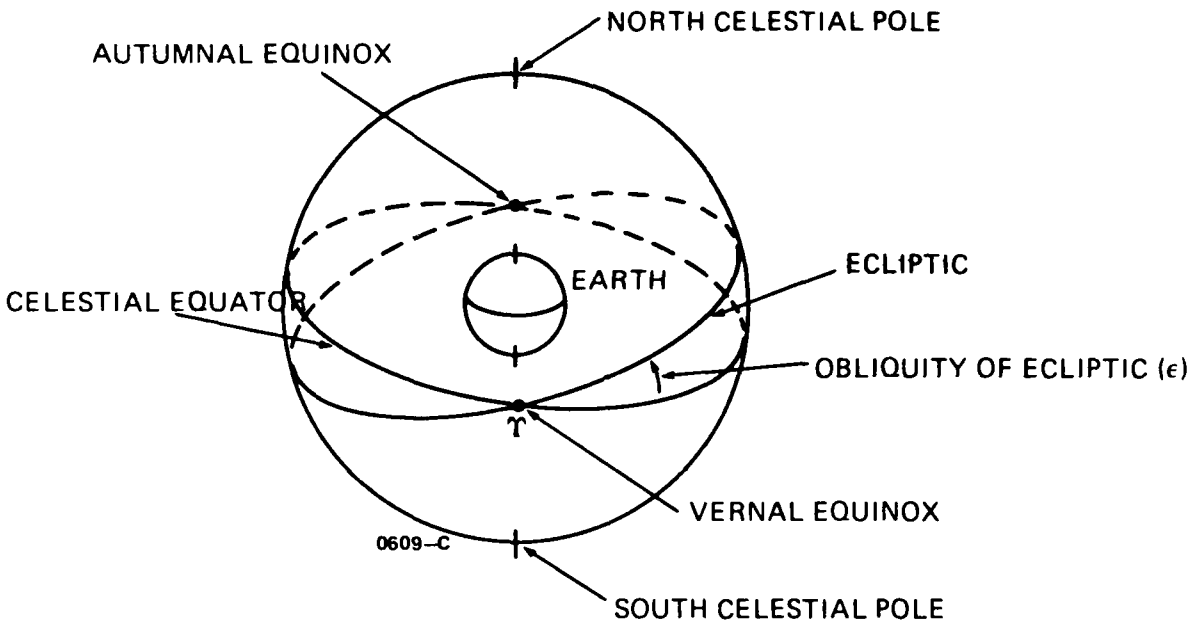

FIGURE 2-1. The Celestial Sphere and Its Components

Table 2-2. Arguments of the Nutation Sine and Cosine Series (B1950.0) (con't)

i	a_i	b_i	c_i	d_i
26.	175.77786068	2.0772024179	-0.26655(-11)	-0.6400(-19)
27.	260.08553736	13.3407541586	-0.10159(-10)	-0.2350(-18)
28.	355.85046149	1.9712005255	-0.23153(-12)	-0.1360(-18)
29.	10.04207427	0.9326463974	0.14437(-11)	-0.2200(-19)
30.	195.86200923	3.9424952128	0.22200(-12)	-0.1080(-18)
31.	84.30767668	11.2635517406	-0.74943(-11)	-0.1710(-18)
32.	153.37058798	37.3935371371	0.63179(-11)	0.4190(-18)
33.	326.56276181	- 0.3287153256	0.18625(-10)	0.5760(-18)
34.	14.19161277	- 1.0385541281	0.16752(-11)	0.1140(-18)
35.	260.08553736	13.3407541586	-0.10159(-10)	-0.2350(-18)
36.	285.73439759	-10.330905343	0.89381(-11)	0.1490(-18)
37.	124.65906729	27.3383932543	-0.18099(-11)	0.3800(-19)
38.	355.78520010	50.5114837007	0.11664(-10)	0.6680(-18)
39.	298.83913233	24.3285444389	-0.58820(-12)	0.1240(-18)
40.	128.80860579	25.3671927287	-0.15784(-11)	0.1740(-18)
41.	267.98758099	63.7992839940	0.30642(-11)	0.4790(-18)
42.	269.07445903	28.1012800838	0.14265(-10)	0.6180(-18)
43.	229.77622103	- 1.8014409576	-0.14400(-10)	-0.4660(-18)
44.	189.96947346	1.0386482898	-0.99022(-12)	0.5000(-19)
45.	85.39455472	-24.4344521695	0.37072(-11)	-0.3200(-19)
46.	41.33928181	50.7872451610	-0.54014(-11)	0.1380(-18)
47.	42.42615985	15.0892412508	0.58001(-11)	0.2770(-18)
48.	192.04424271	0.0530480270	-0.87445(-12)	0.1180(-18)
49.	154.45746602	1.6955332269	0.17519(-10)	0.5580(-18)
50.	143.36114440	12.1907491521	-0.10738(-11)	0.3900(-19)

Table 2-2. Arguments of the Nutation Sine and Cosine Series (B1950.0) (Con't)

i	a_i	b_i	c_i	d_i
51.	71.20294194	-23.3958980414	0.20319(-11)	-0.1460(-18)
52.	216.60622490	12.0793924354	0.70219(-11)	0.3630(-18)
53.	112.03130616	-13.3937080239	0.11719(-10)	0.2810(-18)
54.	183.67990431	52.5357322533	0.10558(-10)	0.6500(-18)
55.	57.67092524	0.2228075950	-0.15506(-10)	-0.4840(-18)
56.	185.81993495	3.0098488154	-0.12217(-11)	-0.8600(-19)
57.	71.17031124	0.8742435461	0.79800(-11)	0.2560(-18)
58.	317.03160513	39.5236934204	0.20929(-11)	0.3090(-18)
59.	212.45668639	14.0505929610	0.67903(-11)	0.2270(-18)
60.	343.34006144	38.4321854270	0.53277(-11)	0.4690(-18)
61.	73.24508049	- 0.1113567166	0.80957(-11)	0.3240(-18)
62.	303.05393222	-26.1829392618	-0.12252(-10)	-0.5440(-18)
63.	333.36324855	-11.0407441456	-0.80121(-11)	-0.3130(-18)
64.	81.17975482	26.0770315311	0.15371(-10)	0.6360(-18)
65.	200.99943894	36.6836983347	-0.10632(-10)	-0.4300(-19)
66.	55.53089459	49.7486910329	-0.37261(-11)	0.2520(-18)
67.	238.76514270	12.9590849676	0.10025(-10)	0.3870(-18)
68.	339.19052294	40.4033859525	0.50962(-11)	0.3330(-18)
69.	50.32820349	65.5477710863	0.19024(-10)	0.9910(-18)
70.	0.0	0.0	0 0	0.0
71.	0.0	0.0	).0	0.0
72.	0.0	0.0	0.0	0.0
73.	0.0	0.0	0.0	0.0
74.	0.0	0.0	0.0	0.0
75.	0.0	0.0	0.0	0.0

Note: Arguments numbered 70 through 106 are all zero for this (B1950.0) version of the transformation.

Table 2-3. Coefficients of the Nutation Sine and Cosine Series (J2000.0)

i	$\alpha_i + \beta_i T$	$\gamma_i + \delta_i T$
1.	-0.477766 (-02) - 0.4838 (-05) T	0.255625 (-02) + 0.247 (-06) T
2.	0.572777 (-04) + 0.5555 (-08) T	-0.24861 (-04) + 0.1398 (-07) T
3.	0.127777 (-05)	-0.666666 (-06)
4.	0.305555 (-06)	
5.	-0.833333 (-07)	0.277777 (-07)
6.	-0.833333 (-07)	
7.	-0.555555 (-07)	0.277777 (-07)
8.	0.277777 (-07)	
9.	-0.366305 (-03) - 0.4444 (-07) T	0.159333 (-03) - 0.8611 (-07) T
10.	0.396111 (-04) - 0.9444 (-07) T	0.150000 (-05) - 0.2777 (-08) T
11.	-0.143611 (-04) + 0.3333 (-07) T	0.622222 (-05) - .1667 (-07) T
12.	0.602777 (-05) - 0.1388 (-07) T	-0.263888 (-05) + .8333 (-08) T
13.	0.358333 (-05) + 0.2777 (-05) T	-0.194444 (-05)
14.	0.133333 (-05)	0.277778 (-07)
15.	-0.611111 (-06)	
16.	0.472222 (-06) - 0.2777 (-08) T	
17.	-0.416666 (-06)	0.250000 (-06)
18.	-0.444444 (-06) + 0.2778 (-08) T	0.194444 (-06)
19.	-0.333333 (-06)	0.166666 (-06)
20.	-0.166666 (-06)	0.833333 (-07)
21.	-0.138888 (-06)	0.833333 (-07)
22.	0.111111 (-06)	-0.555555 (-07)

Table 2-3. Coefficients of the Nutation Sine and Cosine Series (J2000.0) (Con't)

i	$\alpha_i + \beta_i T$	$\gamma_i + \delta_i T$
23.	0.111111 (-06)	-0.555555 (-07)
24.	-0.111111 (-06)	
25.	0.277777 (-07)	
26.	0.277777 (-07)	
27.	-0.277777 (-07)	
28.	0.277777 (-07)	
29.	0.277777 (-07)	
30.	-0.277777 (-07)	
31.	-0.631668 (-04) - 0.5555 (-08) T	0.271388 (-04) - 0.1388 (-07) T
32.	0.197777 (-04) - 0.2777 (-08) T	-0.194444 (-05)
33.	0.107222 (-04) - 0.1111 (-07) T	-0.555555 (-05)
34.	-0.8361111(-05)	0.358333 (-05) - 0.2777(-08)T
35.	-0.438888 (-05)	-0.277777 (-07)
36.	0.341666 (-05)	-0.147222 (-05)
37.	0.175000 (-05)	-0.555555 (-07)
38.	0.175000 (-05) + 0.2777 (-08) T	-0.916666 (-06)
39.	-0.161111 (-05) - 0.2777 (-08) T	0.888888 (-06)
40.	-0.163888 (-05)	0.722222 (-06)
41.	-0.141666 (-05)	0.750000 (-06)
42.	-0.105555 (-05)	0.444444 (-06)
43.	0.805555 (-06)	-0.277777 (-07)
44.	0.805555 (-06)	-0.333333 (-06)
45.	-0.861111 (-06)	0.361111 (-06)

Table 2-3. Coefficients of the Nutation Sine and Cosine Series (J2000.0) (Con't)

i	$\alpha_i + \beta_i T$	$\gamma_i + \delta_i T$
46.	0.722222 (-06)	-0.277777 (-07)
47.	0.583333 (-05)	-0.277777 (-06)
48.	0.444444 (-06)	-0.222222 (-06)
49.	-0.361111 (-06)	0.194444 (-06)
50.	-0.277777 (-06)	0.1388888 (-06)
51.	-0.194444 (-06)	
52.	0.194444 (-06)	-0.833333 (-07)
53.	-0.194444 (-06)	0.833333 (-07)
54.	-0.222222 (-06)	0.833333 (-07)
55.	0.166666 (-06)	
56.	0.166666 (-06)	-0.833333 (-07)
57.	-0.166666 (-06)	0.833333 (-07)
58.	-0.194444 (-06)	0.833333 (-07)
59.	0.166666 (-06)	-0.833333 (-07)
60.	-0.138888 (-06)	0.833333 (-07)
61.	0.138888 (-06)	
62.	-0.138888 (-06)	0.833333 (-07)
63.	-0.111111 (-06)	
64.	0.111111 (-06)	
65.	-0.111111 (-06)	
66.	-0.833333 (-07)	
67.	0.833333 (-07)	
68.	-0.833333 (-07)	0.277777 (-07)
69.	-0.833333 (-07)	0.277777 (-07)
70.	-0.555555 (-07)	0.277777 (-07)

Table 2-3. Coefficients of the Nutation Sine and Cosine Series (J2000.0) (Con't)

i	$\alpha_i + \beta_i T$	$\gamma_i + \delta_i T$
71.	-0.833333 (-07)	0.277777 (-07)
72.	-0.833333 (-07)	0.277777 (-07)
73.	0.555555 (-07)	-0.277777 (-07)
74.	-0.555555 (-07)	0.277777 (-07)
75.	0.555555 (-07)	-0.277777 (-07)
76.	-0.555555 (-07)	0.277777 (-07)
77.	0.555555 (-07)	
78.	0.555555 (-07)	-0.277777 (-07)
79.	0.277777 (-07)	-0.277777 (-07)
80.	-0.277777 (-07)	
81.	0.277777 (-07)	-0.277777 (-07)
82.	-0.555555 (-07)	0.277777 (-07)
83.	-0.277777 (-07)	
84.	0.277777 (-07)	-0.277777 (-07)
85.	-0.277777 (-07)	0.277777 (-07)
86.	-0.277777 (-07)	0.277777 (-07)
87.	0.277777 (-07)	
88.	0.277777 (-07)	
89.	0.277777 (-07)	-0.277777 (-07)
90.	-0.277777 (-07)	
91.	-0.277777 (-07)	
92.	0.277777 (-07)	
93.	0.277777 (-07)	
94.	-0.277777 (-07)	
95.	0.277777 (-07)	

Table 2-3. Coefficients of the Nutation Sine and Cosine Series (J2000.0) (Con't)

i	$\alpha_i + \beta_i T$	$\gamma_i + \delta_i T$
96.	0.277777 (-07)	
97.	-0.277777 (-07)	
98.	-0.277777 (-07)	
99.	-0.277777 (-07)	
100.	-0.277777 (-07)	
101.	-0.277777 (-07)	
102.	-0.277777 (-07)	
103.	-0.277777 (-07)	
104.	0.277777 (-07)	
105.	-0.277777 (-07)	
106.	0.277777 (-07)	
	T = (JED - 2451545.0) / 36525 The quantities in the parentheses are the exponents of 10.	

Table 2-4. Arguments of the Nutation Sine and Cosine Series (J2000.0)

i	a_i	b_i	c_i	d_i
1.	125.04452220	-0.0529537648	0.15522(-11)	0.4560(-19)
2.	250.08904440	-0.1059075296	0.31044(-11)	0.9120(-19)
3.	41.66237996	0.2757608151	-0.17006(-10)	-0.5586(-18)
4.	83.38214224	-0.3287145800	0.18559(-10)	0.6042(-18)
5.	166.70690216	0.2228070503	-0.15454(-10)	-0.5130(-18)
6.	-160.41505000	-0.1113564531	0.80742(-11)	0.3249(-18)
7.	-279.16783004	0.05304790896	-0.85852(-12)	0.9120(-19)
8.	208.42666444	-0.3816683448	0.20111(-10)	-0.6498(-18)
9.	-159.06786124	1.9712947103	0.45340(-12)	0.0
10.	357.527723330	0.9856002831	-0.12014(-12)	-0.6840(-19)
11.	198.45986206	2.9568949934	0.33326(-12)	-0.6840(-19)
12.	-156.59558454	0.9856944272	0.57354(-12)	0.6840(-19)
13.	-284.11238344	2.0242484751	-0.10988(-10)	-0.4560(-19)
14.	-325.77476340	1.7484876600	0.15908(-10)	0.5130(-18)
15.	-63.54522384	26.5646080096	-0.86250(-11)	-0.3420(-19)
16.	355.05544660	1.9712005662	-0.24028(-12)	-0.1368(-18)
17.	122.57224550	0.9326465182	0.14320(-11)	-0.2288(-19)
18.	195.98758536	3.9424952765	0.21312(-12)	-0.1368(-18)
19.	-232.48320110	-1.0385540479	0.16723(-11)	0.1140(-18)
20.	90.81928560	-1.8014414248	-0.14355(-10)	-0.4674(-18)
21.	-281.64010674	1.0386481920	-0.97866(-12)	0.2280(-19)
22.	-200.73024120	1.6955338951	0.17460(-10)	0.5586(-18)
23.	73.41533986	3.0098487582	-0.12189(-11)	-0.1140(-18)
24.	-162.88738170	0.8742438300	0.79540(-11)	0.2565(-18)
25.	31.75295990	2.7340879431	0.15788(-10)	0.4446(-18)

The quantities in the parentheses are the exponents of 10.

Table 2-4. Arguments of the Nutation Sine and Cosine Series (J2000.0) (Con't)

i	a_i	b_i	c_i	d_i
26.	309.16440924	10.9348369451	0.10722(-10)	0.5016(-18)
27.	-119.35472040	22.4102976738	-0.26293(-11)	0.3534(-18)
28.	247.61676770	0.8796927534	0.29842(-11)	0.2280(-19)
29.	287.93190390	-0.9271975948	-0.64018(-11)	-0.2109(-18)
30.	-51.62918234	3.0628025231	-0.27711(-11)	-0.1596(-18)
31.	76.63286496	26.3527929503	-0.24162(-11)	0.2166(-18)
32.	134.96298140	13.0649929500	0.65192(-11)	0.3648(-18)
33.	311.58834276	26.4057467151	-0.39684(-11)	0.1710(-19)
34.	211.59584636	39.4177859003	0.41030(-11)	0.5814(-18)
35.	-100.73774480	-11.3165052900	0.93883(-11)	0.1482(-18)
36.	301.66988356	13.2878000003	-0.89354(-11)	-0.1482(-18)
37.	235.70072620	24.3814982400	-0.28696(-11)	0.2166(-18)
38.	260.00750360	13.0120391851	+0.80714(-11)	0.4104(-19)
39.	- 9.91839580	-13.1179467148	-0.49670(-11)	-0.3192(-18)
40.	177.37060976	37.6692982403	-0.11805(-10)	0.6840(-19)
41.	86.55132416	39.4707396651	0.25508(-11)	0.5358(-18)
42.	312.33359116	50.7342911903	-0.52885(-11)	0.4332(-18)
43.	269.925962801	26.1299859000	+0.13038(-10)	0.7296(-18)
44.	-24.10487984	15.0362876603	0.69726(-11)	0.3648(-18)
45.	346.55882776	52.4827788503	0.10622(-10)	0.9462(-18)
46.	186.54382056	26.4587004800	-0.55206(-11)	0.1254(-18)
47.	176.62536136	13.3407537651	-0.10487(-10)	-0.1938(-18)
48.	225.78226700	11.2635515251	-0.78366(-11)	-0.1026(-18)
49.	-335.69322260	-11.3694590548	0.10941(-10)	0.1938(-18)
50.	322.25205036	63.8522379051	-0.31872(-12)	0.7524(-18)

Table 2-4. Arguments of the Nutation Sine and Cosine Series (J2000.0) (Con't)

i	a_i	b_i	c_i	d_i
51.	-103.21002150	-10.3309050069	0.92687(-11)	0.7980(-19)
52.	74.16058826	27.3383932334	-0.25363(-11)	0.1482(-18)
53.	79.10514166	25.3671926672	-0.22960(-11)	0.2580(-18)
54.	87.29657256	63.7992841403	0.12334(-11)	0.7980(-18)
55.	10.66370760	37.4464911900	0.36496(-11)	0.5814(-18)
56.	110.85810156	28.1012806103	0.13491(-10)	0.7296(-18)
57.	0.74524840	24.3285444751	-0.13174(-11)	0.2622(-18)
58.	187.28906896	50.7872449551	-0.68380(-11)	0.3876(-18)
59.	-149.14940204	15.0892414251	0.54204(-11)	0.3192(-18)
60.	-110.65620400	-24.4344520048	0.44218(-11)	-0.1710(-18)
61.	-222.56474190	12.0793926669	0.66394(-11)	0.4332(-18)
62.	221.51430556	52.5357326151	0.90701(-11)	0.9006(-18)
63.	-238.17300290	-23.3458979569	0.27494(-11)	-0.2850(-18)
64.	-51.58083916	-13.3937075530	0.12039(-11)	0.2394(-18)
65.	297.85036310	12.1907491200	-0.14348(-11)	0.1083(-18)
66.	132.49070470	14.0505932331	0.63991(-11)	0.2964(-18)
67.	321.50680196	39.5236934300	0.99868(-11)	0.4902(-18)
68.	214.06812306	38.4321856172	0.42232(-11)	0.6498(-18)
69.	179.84288646	36.6836979512	-0.11684(-10)	0.1368(-18)
70.	-144.88144060	-26.1829396648	-0.11486(-11)	-0.6840(-18)
71.	121.52180916	65.5477718003	0.17141(-10)	0.1311(-17)
72.	314.80586786	49.7486909072	-0.51656(-11)	0.5016(-18)
73.	209.12356966	40.4033861834	0.39829(-11)	0.5130(-18)
74.	-59.07536484	-11.0407444748	-0.76180(-11)	-0.4104(-18)
75.	34.97048500	26.0770321351	0.14590(-10)	0.7752(-18)

Table 2-4. Arguments of the Nutation Sine and Cosine Series (J2000.0) (Con't)

i	a_i	b_i	c_i	d_i
76.	25.05202580	12.9590854203	0.96236(-11)	0.4560(-18)
77.	44.88894420	39.1949788500	+0.19557(-10)	0.1094(-17)
78.	14.48322806	38.5435420703	-0.38510(-11)	0.3249(-18)
79.	115.12606300	-13.1709004796	-0.34148(-11)	-0.2736(-18)
80.	-336.4384710	-35.6980035300	0.12258(-10)	-0.6840(-19)
81.	42.40762836	24.6043052903	-0.18324(-10)	-0.2964(-18)
82.	53.07133596	62.0507964803	-0.14674(-10)	0.2850(-18)
83.	-201.47548960	-22.6330105800	0.18777(-10)	0.2964(-18)
84.	333.42284346	16.0218879434	0.68525(-11)	0.2964(-18)
85.	322.25205036	63.8522379051	-0.31872(-12)	0.7524(-18)
86.	278.10835456	48.9855374251	-0.21193(-10)	-0.7980(-19)
87.	128.21370412	39.7465004803	-0.44456(-10)	-0.2280(-19)
88.	-98.26546810	-12.3021055731	0.95090(-11)	0.2166(-18)
89.	-14.18642064	28.1542343751	0.11939(-10)	0.6840(-18)
90.	222.25955396	76.8642770903	0.77527(-11)	0.1162(-17)
91.	135.70822980	37.3935374251	0.52018(-11)	0.6270(-18)
92.	27.47595932	28.4299951903	-0.50672(-11)	0.1254(-18)
93.	245.82108296	41.1662735603	0.20011(-10)	0.1094(-17)
94.	-274.19392424	15.1421951900	0.38682(-11)	0.2736(-18)
95.	309.11606606	27.3913469982	-0.40885(-11)	0.1026(-18)
96.	228.25454370	10.2779512420	-0.77165(-11)	-0.3420(-19)
97.	-61.49929836	-26.5116542448	0.70728(-11)	-0.7980(-19)
98.	138.78250186	14.1620438303	-0.98140(-12)	0.1083(-18)
99.	233.22844950	25.3670985231	-0.29897(-11)	0.1482(-18)
100.	-287.28156536	-37.7752057700	0.14909(-10)	0.2280(-19)

Table 2-4. Arguments of the Nutation Sine and Cosine Series (J2000.0) (Con't)

i	a_i	b_i	c_i	d_i
101.	-45.93938054	25.4201464320	-0.38482(-11)	0.2394(-18)
102.	21.83450070	-10.3838587717	0.10820(-10)	0.1254(-18)
103.	184.11988704	10.9877907100	0.91702(-11)	0.4560(-18)
104.	145.62668900	50.5114841400	0.10168(-10)	0.9462(-18)
105.	188.03431736	75.1157894303	-0.81554(-11)	0.6498(-18)
106.	295.37808640	13.1763494031	-0.15549(-11)	0.3990(-19)

4 THE TRUE OF DATE INERTIAL REFERENCE SYSTEM AND THE $\underset{\sim}{C}$ TRANSFORMATION (con't)

e $\vec{X}''$ is the vector in the true of date system. Due to the orthogonality , one may write for the inverse transformation:

$$\vec{X}' = \underset{\sim}{C}^T \vec{X}'' \tag{13}$$

$$\vec{X} = \underset{\sim}{D}^T \underset{\sim}{C}^T \vec{X}'' \quad . \tag{14}$$

EQUATORIAL EARTH-FIXED COORDINATE SYSTEMS

erence systems (iv), (v), and (vi) above are called equatorial earth-ed systems. Their origins lie within the earth and they utilize the restrial poles and equator as fundamental components. These coordinate tems are not inertial, since they are fixed and rotate with the earth. h of these three reference systems and associated transformation is cribed in the following subsections.

.1 THE INSTANTANEOUS EARTH-FIXED REFERENCE SYSTEM AND THE $\underset{\sim}{B}$ TRANSFORMATION

instantaneous earth-fixed system is an earth centered coordinate set ch has its (e', f', g') axes defined as follows:

$\hat{e}'$ is the unit vector in the true equatorial plane in the direction of the Greenwich meridian;

$\hat{g}'$ is the unit vector along the earth's true axis of rotation and is positive in the northern hemisphere; and

f' is the unit vector which completes the right-handed orthogonal system with $\hat{e}'$ and $\hat{g}'$.

geometry of Figure 2-5 depicts the relationship between the true of e inertial system and the instantaneous earth-fixed system.

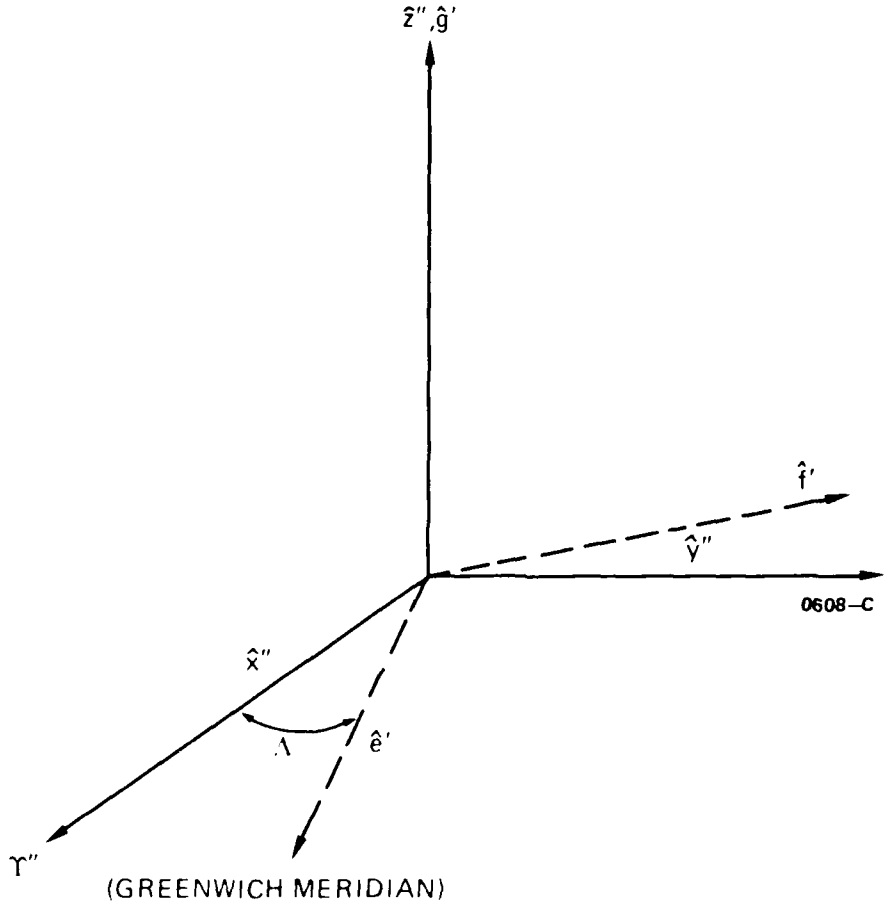

FIGURE 2-5. Relation Between True of Date System and Instantaneous Earth-Fixed System

3.2 SMTP STATION CALIBRATION (con't)

ρ/c = transmission delay, found as described in 3.1,

t_{d_j} = receiver equipment delay,

t_{rec} = station clock time at receipt of NAVSAT time mark, and

t_{scj} = clock error of j^{th} station clock.

The linear fit is made between $\Delta t_{sta_{jk}}$ and $t_{sta_{jk}}$ for all values of k for each station j for some epoch t_{o_j}. If the station clock is reset during the fit interval, it must be treated the same way as described for a NAVSAT clock reset for purposes of obtaining a fit and computing the time error afterward.

$$\Delta t_{sta_j} = \Delta t_{sta_{oj}} + \Delta t_{s_j} + b_{sta_j}(t-t_{oj}) + t_{scj}, \quad (4)$$

where

Δt_{sta_j} = station clock error in seconds at time t,

$\Delta t_{sta_{oj}}$ = constant term from linear fit for station clock j,

Δt_{s_j} = { 0 before station clock reset
reset adjustment after clock reset
(cumulative if more than one reset),

b_{sta_j} = first power term from linear fit, and

t_{oj} = epoch for linear fit for station j.

The above calibration permits correction of the station clock time at the end of each doppler observation interval, i.e.

NAVSAT CLOCK CALIBRATION (con't)

Δt_{so_i} = constant term from fit for $NAVSAT_i$,

Δt_{c_i} = { 0 before $NAVSAT_i$ reset,

= { reset adjustment after reset (cumulative if more than one reset),

b_{s_i} = first power term from linear fit, and

t_{o_i} = epoch for linear fit.

SMTP STATION CALIBRATION

r each NAVSAT clock has been calibrated, each station clock is calibrated g a similar procedure. The difference in the two procedures is that Δt_{sc_i} sed to correct for errors in NAVSAT time.

ation clock offset is found for each NAVSAT time mark for each station

$$\Delta t_{sta_{jk}} = t_{sta_{jk}} - t_{NAVSAT_i} + \Delta t_{sc_{ik}}, \quad (3)$$

e

$\Delta t_{sta_{jk}}$ = station clock error for k^{th} observation at station j,

$t_{sta_{jk}}$ = station clock time at NAVSAT transmission time for k^{th} observation,

= $t_{rec} - \rho/c - t_{d_j} - t_{scj}$,

t_{NAVSAT_i} = time of nearest multiple of 120 seconds,

$\Delta t_{sc_{ik}}$ = correction computed from (2) for $NAVSAT_i$ at t_{NAVSAT_i},

3.1 NAVSAT CLOCK CALIBRATION (con't)

$$\Delta t_{sc_{ik}} = t_{NAVSAT_i} - t_{sta_k} \quad (1)$$

where

$\Delta t_{sc_{ik}}$ = NAVSAT clock error for k^{th} observation of NAVSAT i,

$t_{sta_k} = t_{rec} - \rho/c - t_{d_j} - t_{scj}$,

= reference station clock time when signal k transmitted,

t_{NAVSAT_i} = time of nearest multiple of 120 seconds,

ρ/c = transmission time,

t_{d_j} = receiver equipment delay for j^{th} reference station receiver,

t_{rec} = reference station clock time of receipt of time mark , and

t_{scj} = clock error of j^{th} station clock.

An array is created for each NAVSAT satellite which contains all observations of (1) transmit time (NAVSAT clock) and (2) the NAVSAT time error.

If a satellite (NAVSAT) clock is reset during the interval of collection of data, the NAVSAT errors following reset are shifted by the negative of the reset (Δt_c) to conform to the earlier data for purposes of the linear fit.

A linear fit is made to the data set for each NAVSAT satellite. This linear fit provides the ability to compute the NAVSAT clock error at any time during the fit interval. The value derived from the computation is

$$\Delta t_{sc_i} = \Delta t_{so_i} + \Delta t_{c_i} + b_{s_i} (t - t_{o_i}) \quad , \quad (2)$$

where

Δt_{sc_i} = error in seconds of $NAVSAT_i$ clock at any time t,

SECTION 3

TIME CALIBRATION AND CORRECTION

ange difference data comes from the tracking stations tagged with station lock time at the end of the doppler count. However, because of errors which ay exist in station clocks, it is necessary to have a means of calibration f each station clock such that the time tags may be adjusted before any valuation of the range difference data can be made.

he calibration is accomplished through use of accurate reference clocks n a subset of the tracking stations and the NAVSAT clocks. The NAVSAT clocks ill first be calibrated by use of the reference station clocks. Then the tation clocks will be calibrated from the adjusted NAVSAT clock times. A inear fit is used to calibrate each NAVSAT clock such that fit coefficients letermine the error at any time during the fit span. Similarly, a linear fit is used to calibrate each station clock for all useable NAVSAT time marks. Before each fit, a check is made to evaluate the self-consistency of the data. Points not within reasonable bounds are deleted from the fit process.

3.1 NAVSAT CLOCK CALIBRATION

Each NAVSAT clock is calibrated approximately once per day. Since NAVSAT clocks emit time signals at two minute intervals, the calibration of the NAVSAT clock must be made with time corrected from receipt to transmit. This adjustment is accomplished by subtracting the propagation delay and the receiver equipment delay from the calibrated station's received time. The propagation delay is found by using SPASUR elements to obtain the NAVSAT position using the Brouwer-Lyddane prediction method. Then the range (ρ) is found by calculating the distance from the satellite to the calibrated station. The equipment delay is a function of the station and is kept in the station table.

The NAVSAT clock error is computed for each NAVSAT time mark for each reference observation station as follows:

---

e transformation of the station position from the earth-fixed to the inertial frame for pcomputation is performed using equations (29)-(30) of Section 2 when λ is replaced by $t-t_{ve}) + \lambda\}$, where $\tilde{\omega}$ is the earth rotation rate, t the time from the beginning of the , and t_{ve} the time from the beginning of the day of the first transit of the vernal inox. The e_s, f_s, and g_s components are now inertial station components.

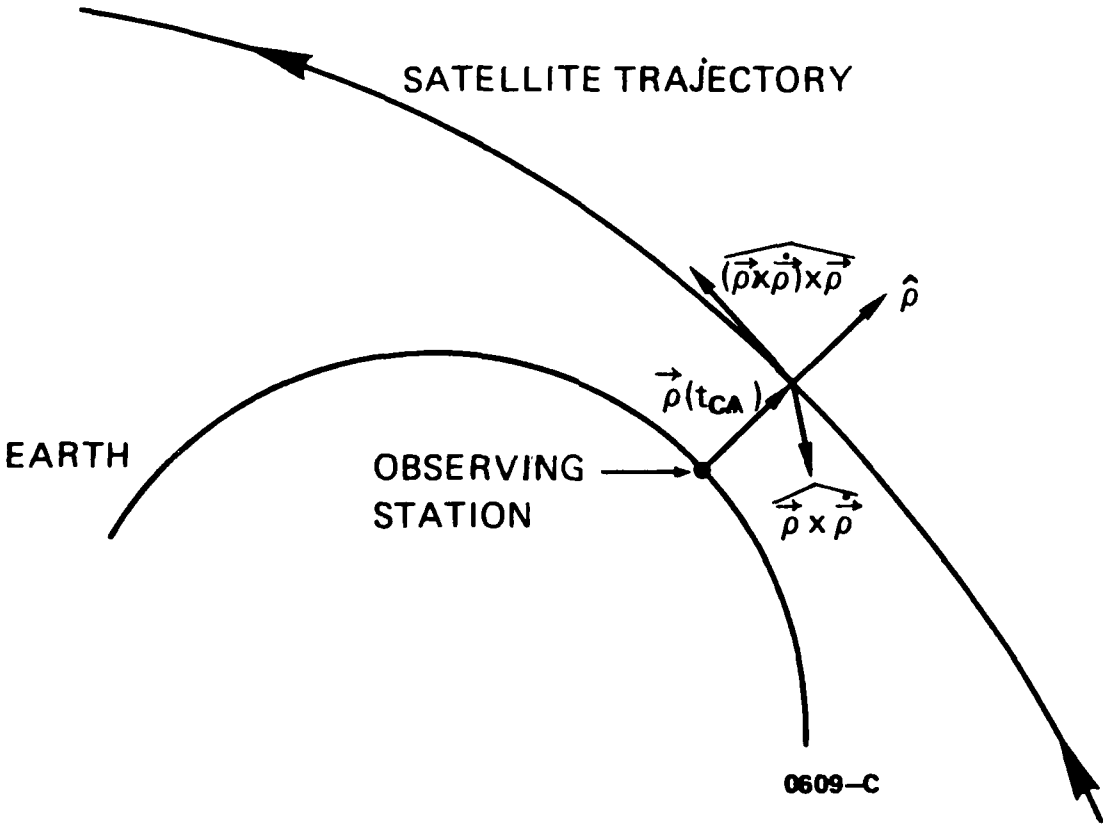

FIGURE 2-8. t_{ca} Reference Frame Geometry

2.3 TIME OF CLOSEST APPROACH (t_{CA}) COORDINATE SYSTEM (con't)

where $\vec{\rho}(t_{CA})$ and $\dot{\vec{\rho}}(t_{CA})$ are the position and velocity of the satellite relative to the observing station at the time of closest approach. The geometry of the t_{CA} system is shown in Figure 2-8.

A similarity transformation is used in the point and cross pass editors to transform the normal equations to the t_{CA} reference frame (see Section 7). The matrix used in this transformation is:

$$\underset{\sim}{T} = \begin{pmatrix} \underset{\sim}{T}' & \underset{\sim}{0} \\ \underset{\sim}{0} & \underset{\sim}{T}' \end{pmatrix}, \tag{32}$$

where $\underset{\sim}{0}$ is a 3 x 3 null submatrix and

$$\underset{\sim}{T}' = \begin{pmatrix} \hat{x} \cdot \hat{\rho} & \hat{x} \cdot \vec{\rho} \times \dot{\vec{\rho}} & \hat{x} \cdot (\vec{\rho} \times \dot{\vec{\rho}}) \times \vec{\rho} \\ \hat{y} \cdot \hat{\rho} & \hat{y} \cdot \vec{\rho} \times \dot{\vec{\rho}} & \hat{y} \cdot (\vec{\rho} \times \dot{\vec{\rho}}) \times \vec{\rho} \\ \hat{z} \cdot \hat{\rho} & \hat{z} \cdot \vec{\rho} \times \dot{\vec{\rho}} & \hat{z} \cdot (\vec{\rho} \times \dot{\vec{\rho}}) \times \vec{\rho} \end{pmatrix}. \tag{33}$$

In the above expression $\hat{x}$, $\hat{y}$, and $\hat{z}$ are unit vectors directed along the respective axes of the inertial reference system.

2.2.4 THE GEOGRAPHICAL REFERENCE SYSTEM

Cartesian coordinates for a station in the earth-fixed reference ellipsoid system are:

$$\begin{pmatrix} e_s \\ f_s \\ g_s \end{pmatrix} = (r_c + h) \begin{pmatrix} \cos\phi \cos\lambda \\ \cos\phi \sin\lambda \\ \sin\phi \end{pmatrix} - \varepsilon^2 r_c \begin{pmatrix} 0 \\ 0 \\ \sin\phi \end{pmatrix}, \qquad (29)$$

where

$$r_c = \frac{a_e}{(1 - \varepsilon^2 \sin^2\phi)^{\frac{1}{2}}} , \qquad (30)$$

and a_e and ε are the semi-major axis and eccentricity of the reference ellipsoid, respectively. The station's coordinates in the instantaneous earth-fixed or any of the inertial systems can be obtained by the proper application of the $\underset{\sim}{A}$, $\underset{\sim}{B}$, $\underset{\sim}{C}$, and $\underset{\sim}{D}$ transformations as discussed in the preceeding sections.

2.3 TIME OF CLOSEST APPROACH (t_{CA}) COORDINATE SYSTEM

The t_{CA} reference system is used extensively in the point and cross pass editors (see Section 7). This coordinate system is formed using the position and velocity vectors of the satellite relative to the observing station at the time of closest approach, the computation of which is described in Section 9. The axes of this time dependent reference frame are defined as follows:

$$\hat{\rho} = \vec{\rho}(t_{CA}) \Big/ \left| \vec{\rho}(t_{CA}) \right| ,$$

$$\overset{\frown}{\vec{\rho} \times \dot{\vec{\rho}}} = \vec{\rho}(t_{CA}) \times \dot{\vec{\rho}}(t_{CA}) \Big/ \left| \vec{\rho}(t_{CA}) \times \dot{\vec{\rho}}(t_{CA}) \right| , \qquad (31)$$

and

$$\overset{\frown}{(\vec{\rho} \times \dot{\vec{\rho}}) \times \vec{\rho}} = \left(\left[\vec{\rho}(t_{CA}) \times \dot{\vec{\rho}}(t_{CA}) \right] \times \vec{\rho}(t_{CA}) \right) \Big/ \left| \left[\vec{\rho}(t_{CA}) \times \dot{\vec{\rho}}(t_{CA}) \right] \times \vec{\rho}(t_{CA}) \right| ,$$

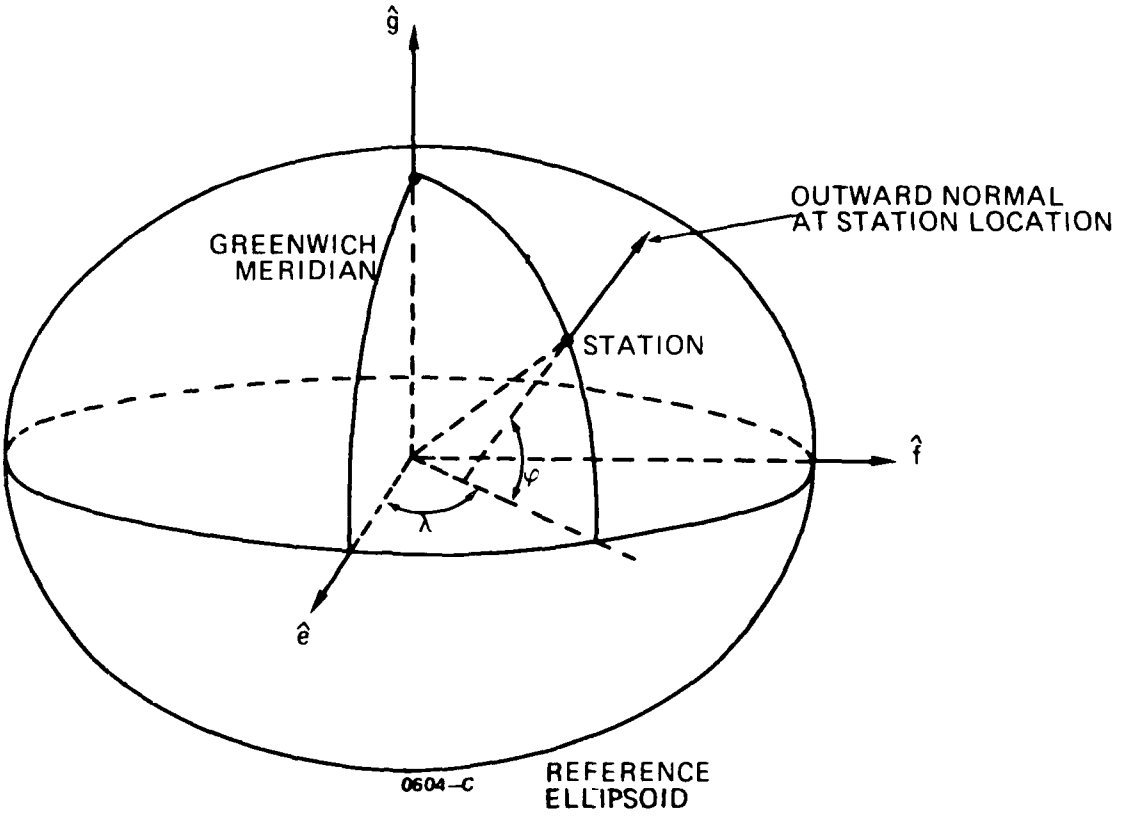

FIGURE 2-7. The Geographical Coordinate System

2.2.3 UT1 - UTC AND POLE WANDER PREDICTION (con't)

$$\Delta X_i = A'_i + B'_i t + \sum_{\ell=1}^{m} \left[C'_{i_\ell} \sin\left(\frac{2\pi t}{P_\ell}\right) + D'_{i_\ell} \cos\left(\frac{2\pi t}{P_\ell}\right) \right], \qquad (28)$$

where t is the time in days and A'_i, B'_i, C'_{i_ℓ}, and D'_{i_ℓ}, are externally supplied expansion coefficients, and P_ℓ are periods in days. The ΔX_i in equation (28) represents the pole positions, i.e. Δp when $i = 1$ and Δq when $i = 2$.

2.2.4 THE GEOGRAPHICAL REFERENCE SYSTEM

The geographical reference system uses two angular measures (one from the Greenwich meridian and one from the equatorial plane of the earth-fixed reference ellipsoid system) and a linear measure (of height above the reference ellipsoid) to specify the location of an observing station on the surface of the earth. These elements of location are defined as:

ϕ = geodetic latitude (the angular measure between the equator and the normal to the tangent surface at the station location);

λ = longitude (the angular measure between the Greenwich meridian and the station meridian as measured in the equatorial plane); and

h = geodetic height of observing station above the reference ellipsoid.

The geometry of this reference system is depicted in Figure 2-7.

2.2.2 THE EARTH-FIXED REFERENCE ELLIPSOID COORDINATE SYSTEM AND THE $\underset{\sim}{A}$ TRANSFORMATION (con't)

$$\vec{X}_e = \underset{\sim}{A}\vec{X}_{e'} = \underset{\sim}{A}\,\underset{\sim}{B}\,\vec{X}'' = \underset{\sim}{A}\,\underset{\sim}{B}\,\underset{\sim}{C}\,\vec{X}' = \underset{\sim}{A}\,\underset{\sim}{B}\,\underset{\sim}{C}\,\underset{\sim}{D}\,\vec{X}, \tag{24}$$

where $\vec{X}_e$ is the vector in the earth-fixed reference ellipsoid system. The inverse transformation may be written as:

$$\vec{X}_{e'} = \underset{\sim}{A}^T\vec{X}_e \tag{25}$$

or

$$\vec{X} = \underset{\sim}{D}^T\,\underset{\sim}{C}^T\,\underset{\sim}{B}^T\,\underset{\sim}{A}^T\,\vec{X}_e \quad . \tag{26}$$

2.2.3 UT1 - UTC AND POLE WANDER PREDICTION

PULSAR uses externally computed expansion coefficients to generate and predict values for Δp, Δq, and Δt at one day intervals. Values for those quantities at intermediate times are obtained using the linear interpolation method discussed in Section 9.

The UT1 - UTC predictions are made using the expansion

$$\Delta t = A + Bt + \sum_{m=1}^{k}\left[C_m \sin\left(\frac{2\pi t}{P_m}\right) + D_m \cos\left(\frac{2\pi t}{P_m}\right)\right] \tag{27}$$

where t is the time in days and A, B, C_m, and D_m are externally supplied expansion coefficients.

Pole position predictions are made using the expansion

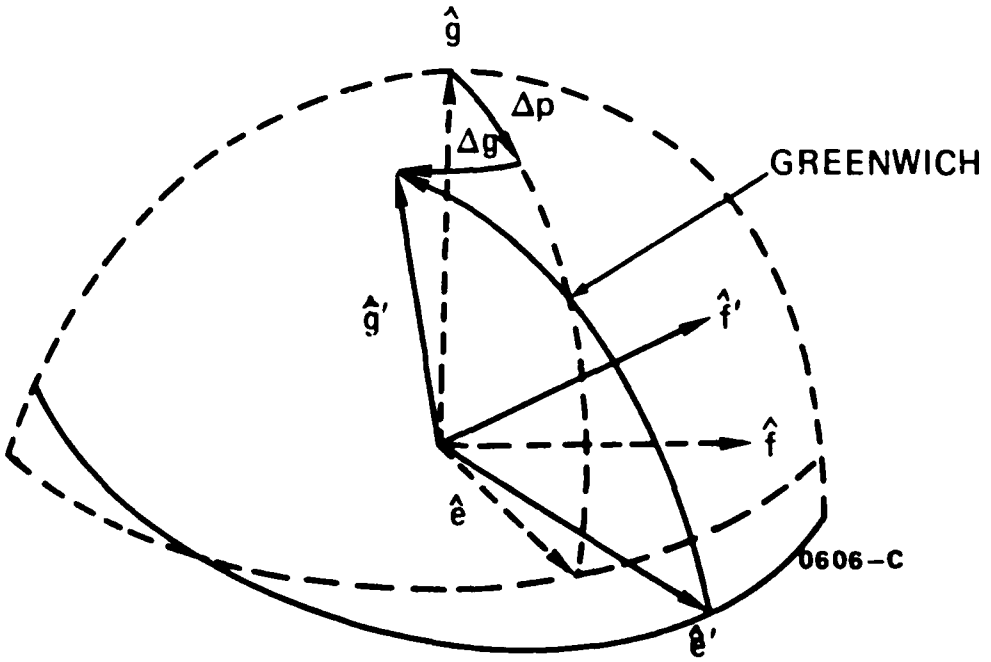

FIGURE 2-6. Polar Wander Geometry

2.2.2 THE EARTH-FIXED REFERENCE ELLIPSOID COORDINATE SYSTEM AND THE $\underset{\sim}{A}$ TRANSFORMATION

For reasons not completely understood, the crust of the earth slips slightly about the earth's axis of rotation. This produces an effect called polar wander, which is the displacement of the true pole of the $(\hat{e}', \hat{f}', \hat{g}')$ system from the pole of the earth-fixed reference ellipsoid system. This is a geocentric coordinate space which has its (e, f, g) axes defined as follows:

$\hat{e}$ is the unit vector in the plane of the equator at the date of observation and is in the direction of the Greenwich meridian;

$\hat{g}$ is the unit vector along the semiminor axis of the reference ellipsoid and is positive in the northern hemisphere; and

$\hat{f}$ is the unit vector which completes the right-handed orthogonal system with $\hat{e}$ and $\hat{g}$.

The geometry of polar wander is shown in Figure 2-6. The displacements Δp and Δq are angular quantities measured from the pole in the direction of Greenwich and perpendicular to this direction (positive towards the west), respectively.

The $\underset{\sim}{A}$ matrix corrects for polar wander by transforming from the instantaneous earth-fixed system to the reference ellipsoid system. This matrix is given by:

$$\underset{\sim}{A} = \begin{pmatrix} 1 & 0 & \Delta p \\ 0 & 1 & -\Delta q \\ -\Delta p & \Delta q & 1 \end{pmatrix} . \qquad (23)$$

An arbitrary vector $\vec{x}$ may be transformed as follows using the $\underset{\sim}{A}$ matrix:

2.2.1 THE INSTANTANEOUS EARTH-FIXED REFERENCE SYSTEM AND THE $\underset{\sim}{B}$ TRANSFORMATION (con't)

where ε and $\Delta\psi$ are given by equations (7), (8), (9) and (10). H_o is the mean hour angle of Greenwich at the beginning of the day of observation $(0^h\ UT)^2$. It is computed from

$$H_o = \text{mod}(GMS, 360°), \tag{18}$$

where GMS is the observed Greenwich mean sidereal angle:

$$GMS(°) = \begin{cases} 100.000100269 + 0.9856473459844(t-t_o) + 0.29015 \times 10^{-12}(t-t_o)^2, \\ \quad B1950.0 \\ \qquad\qquad \underline{\text{or}} \\ 100.460618333 + 0.9856473662902(t-t_o) + 0.29077 \times 10^{-12}(t-t_o)^2 . \\ \quad J2000.0 \end{cases} \tag{19}$$

Using the $\underset{\sim}{B}$ matrix one may write for an arbitrary vector $\vec{V}$:

$$\vec{V}_{e'} = \underset{\sim}{B}\,\vec{V}'' = \underset{\sim\sim}{BC}\vec{V}' = \underset{\sim\sim\sim}{BCD}\,\vec{V} \quad , \tag{20}$$

where $\vec{V}_{e'}$ is the vector in the instantaneous earth-fixed reference system. From the orthogonality property of the $\underset{\sim}{B}$ matrix one may also write:

$$\vec{V}'' = \underset{\sim}{B}^T\,\vec{V}_{e'} \tag{21}$$

or

$$\vec{V} = \underset{\sim}{D}^T\,\underset{\sim}{C}^T\,\underset{\sim}{B}^T\,\vec{V}_{e'} \tag{22}$$

2.2.1 THE INSTANTANEOUS EARTH-FIXED REFERENCE SYSTEM AND THE $\underset{\sim}{B}$ TRANSFORMATION (con't)

Transformation from the true of date system to the instantaneous earth fixed system is accomplished through application of the $\underset{\sim}{B}$ matrix given by:

$$\underset{\sim}{B} = \begin{pmatrix} \cos\Lambda & \sin\Lambda & 0 \\ -\sin\Lambda & \cos\Lambda & 0 \\ 0 & 0 & 1 \end{pmatrix} , \tag{15}$$

where Λ is the longitude of the Greenwich Meridian from the true vernal equinox of date and is given by:

$$\Lambda = H_o + \Delta H + \tilde{\omega}(t_f - \Delta t), \tag{16}$$

where $\tilde{\omega}$ is the earth's mean sidereal rotation rate determined by the time lapse between successive transits of the mean equinox and t_f is time of observation from the beginning of the day.

Δt is the UTC - UT1 correction [2,3,4,5,6] for irregular rotation of the earth. Values for this are published by the Bureau International de l'Heure. The ΔH in the last expression is the equation of the equinoxes shown on Figure 2-4 and is defined as:

$$\Delta H = \tan^{-1}\left[\tan\Delta\psi\cos\varepsilon\right], \tag{17}$$

---

[2] Universal Time (UT) is the local mean solar time of the Greenwich meridian.

[3] UTØ is Universal Time as determined from observations.

[4] UT1 is Universal Time obtained by correcting UTØ for polar motion.

[5] UT2 is Universal Time obtained by correcting UT1 for seasonal variations in the Earth's rotational speed.

[6] UTC is coordinated Universal Time which is an approximation to UT2 and is based upon the atomic standard. This time is broadcast by government agencies.

3.2 SMTP STATION CALIBRATION (con't)

$$T_{obs} = t_{sta_j} - \Delta t_{sta_j},$$

where

t_{sta_j} = time on input observation file for observation from station j

$_j$ = station clock time at end of doppler observation interval.

The station clock calibration is done on all SMTP stations, including the reference stations. All geodetic satellite doppler data from all stations are adjusted using the above procedures.

SECTION 4

OBSERVATION CORRECTIONS

4.1 TROPOSPHERIC CORRECTION

The method used for tropospheric correction in PULSAR is a version of the Hopfield model which has been modified for the purpose of simplifying numerical computation. The associated integral is evaluated in closed form, thus precluding integration of each data point. The basic modification made is in the expression for the refraction term N. The expression used is:

$$N = n - 1 = N_0 \left(\frac{r^2 - r_T^2}{r_0^2 - r_T^2} \right)^4 , \qquad (1)$$

where

n = index of refraction,

r_T = upper bound of integration,

r_0 = station distance from center of earth, and

r = variable distance from center of earth along line of sight from the station to the satellite.

The above expression applies both to the dry term and the wet term. The N_0 and r_T will be different for the two cases.

The integral to be evaluated is

$$\Delta R = \int_{r_{sta}}^{r_{sat}} (n-1) \frac{\underline{r} * d\underline{r}}{(\underline{r} * \underline{r} - k^2)^{\frac{1}{2}}} \quad \text{(earth-fixed parameters)}, \qquad (2)$$

$$= \frac{N_0}{(r_0^2 - r_T^2)^4} \int_{r_0}^{r_T} (r^2 - r_T^2)^4 \frac{r\,dr}{(r^2 - k^2)^{\frac{1}{2}}} , \qquad (3)$$

4.1 TROPOSPHERIC CORRECTION (con't)

where

$$r_o = r_{sta},$$

$$k = r_o \sin(Z_r), \text{ and}$$

$$Z_r = \text{zenith angle.}$$

Setting $$\mu = (r^2 - k^2)^{\frac{1}{2}} \tag{4}$$

$$\alpha = (r_o^2 - k^2)^{\frac{1}{2}} = r_o \cos(Z_r) \tag{5}$$

$$\beta = (r_T^2 - k^2)^{\frac{1}{2}} = [r_T^2 - r_o^2 \sin^2(Z_r)]^{\frac{1}{2}} \tag{6}$$

gives

$$\Delta R = \frac{N_o}{(\alpha - \beta)^4 (\alpha + \beta)^4} \int_{\alpha}^{\beta} (\mu - \beta)^4 (\mu + \beta)^4 \, d\mu \tag{7}$$

Integrating by parts and evaluating at the limits (all terms vanish at $\mu = \beta$) yields

$$\Delta R = \frac{N_o (\beta - \alpha)}{630} (126 + 84\chi + 36\chi^2 + 9\chi^3 + \chi^4), \tag{8}$$

where

$$\chi = \frac{\beta - \alpha}{\beta + \alpha} . \tag{9}$$

For the dry term, $N_{o_d} = [.776 * 10^{-4}] \, P/T_K$ and r_{T_d}, the effective upper bound, is given by:

$$r_{T_d} = r_o + 40.1 + .149T \text{ (kilometers)}. \tag{10}$$

4.1 TROPOSPHERIC CORRECTION (con't)

For the wet term, $N_{0_w} = (.373 * 10^{-2})^{E/T_K^2}$ and r_{T_w}, the effective upper bound, is given by:

$$r_{T_w} = r_o + 12.0 \text{ (kilometers)}. \tag{11}$$

In the above expressions

$$E = H\, e^{(-37.2465 + .213166T_K - .000256908T_K^2)}, \tag{12}$$

H = relative humidity, percent (default = 50),

P = pressure, millibars (default = 980),

T_K = T + 273 , and

T = temperature, °celcius (default = 15).

The total correction to range is the sum of the two terms

$$\Delta f_R = \Delta R_d + \Delta R_w \quad . \tag{13}$$

The actual range is always less than that computed from signal transit time; so, Δf_R represents the amount by which the measured range is excessive. For range difference data, this correction term is computed at both ends of the observation period and differenced to find the correction to range difference.

4.2 ANTENNA OFFSET CORRECTION

Since satellite transmitting antennae locations are normally displaced from the center of mass, quaternions relating body axes to inertial coordinates can be used to make the corrections that result from such displacements to the computed range values.

For purposes of these computations, it has been found adequate to interpolate over a set of eight four element quaternion arrays to find the elements of the array at any desired time. However, the interpolated array must be normalized such that it has an absolute value of unity. The normalization may be done by dividing each element by the square root of the sum of the squares of the four elements.

A quaternion set may be converted to a direction cosine matrix. The elements of the direction cosine matrix are

$$
\begin{aligned}
q_{11} &= Q_1^2 - Q_2^2 - Q_3^2 + Q_4^2 \\
q_{12} &= 2\,(Q_1\,Q_2 + Q_3\,Q_4) \\
q_{13} &= 2\,(Q_1\,Q_3 - Q_2\,Q_4) \\
q_{21} &= 2\,(Q_1\,Q_2 - Q_3\,Q_4) \\
q_{22} &= -Q_1^2 + Q_2^2 - Q_3^2 + Q_4^2 \\
q_{23} &= 2\,(Q_2\,Q_3 + Q_1\,Q_4) \\
q_{31} &= 2\,(Q_1\,Q_3 + Q_2\,Q_4) \\
q_{32} &= 2\,(Q_2\,Q_3 - Q_1\,Q_4) \\
q_{33} &= -Q_1^2 - Q_2^2 + Q_3^2 + Q_4^2
\end{aligned}
\qquad (14)
$$

As a quaternion, Q has the structure $Q_1 i + Q_2 j + Q_3 k + Q_4$.

4.2 ANTENNA OFFSET CORRECTION (con't)

The $\underset{\sim}{Q}$ matrix defines the orientation of a set of orthonormal vehicle fixed axes $[\hat{b}]$ relative to an inertial reference frame $[\hat{i}]$:

$$\begin{bmatrix} b_1 \\ b_2 \\ b_3 \end{bmatrix} = [\underset{\sim}{Q}] \begin{bmatrix} i_1 \\ i_2 \\ i_3 \end{bmatrix}_{iner} \tag{15}$$

The $\underset{\sim}{Q}$ matrix is used to convert the vector originating at the spacecraft center of mass and pointing to a transmitting antenna to a vector in inertial coordinates, $\Delta\vec{r}_A$. Thus,

$$\Delta\vec{r}_A = [\underset{\sim}{Q}]^T [V]_{bc} \quad , \tag{16}$$

where $[V]_{bc}$ is the body centered vector from the center of mass of the spacecraft to the phase center of the antenna.

$$[V]_{bc} = \begin{bmatrix} X \\ Y \\ Z \end{bmatrix} - \begin{bmatrix} X \\ Y \\ Z \end{bmatrix}_{cm} \quad \text{(all coordinates body centered).} \tag{17}$$

4.2 ANTENNA OFFSET CORRECTION (con't)

The coordinates of the antenna phase centers will be constant for a particular spacecraft.

The computed vector

$$\begin{bmatrix} \rho_x \\ \rho_y \\ \rho_z \end{bmatrix} = \begin{bmatrix} X \\ Y \\ Z \end{bmatrix}_{\substack{\text{sat.} \\ \text{CM}}} - \begin{bmatrix} X \\ Y \\ Z \end{bmatrix}_{\text{sta}} \tag{18}$$

must be adjusted by addition of $\Delta\vec{r}_A$ to compute the range from the station to the antenna (see Section 7).

4.3 RELATIVISTIC CORRECTIONS

Range measurements and range difference measurements computed classically from signal transit times are in error because of relativistic effects. The expression for the range corrected for relativistic effects is[1]

$$\rho = \rho_u - \Delta\rho_{GR}$$

or

$$\rho = \rho_u + \frac{t_{R_e}}{c}\left[\frac{\mu}{r_R} - \frac{3\mu}{2a_T} + \frac{V_R^2}{2}\right] - \frac{2}{c}\,\vec{r}(t_{R_e})\cdot\vec{V}(t_{R_e}), \tag{19}$$

[1] Gibson, L. R., Periodic Relativistic Effects in Satellite Tracking, NSWC/DL TR (In preparation), Dahlgren, Virginia, 1981.

4.3 RELATIVISTIC CORRECTIONS (con't)

where

ρ_u = Uncorrected range computed classically,

t_{Re} = station clock time when pulse was emitted by beacon,

μ = Earth's gravitational constant,

r_R = Station distance from earth center of mass,

a_T = Semi-major axis of satellite orbit,

V_R = Velocity of station in ECI frame,

C = Velocity of light in vacuo,

$\vec{r}(t_{Re})$ = Satellite position vector at time t_{Re}, and

$\vec{V}(t_{Re})$ = Satellite velocity vector at time t_{Re}.

The corresponding relationship for range difference is

$$\Delta\rho_i = \Delta\rho_{u_i} + \frac{\Delta t_{Re}}{C}\left[\frac{\mu}{r_R} - \frac{3\mu}{2a_T} + \frac{V_R^2}{2}\right] - \left(\frac{2\left[(\vec{r}\cdot\vec{V})_i - (\vec{r}\cdot\vec{V})_{i-1}\right]}{C}\right) \quad (20)$$

where

$\Delta t_{R_e} = t_{R_{e_i}} - t_{R_{e_{i-1}}}$, the i^{th} and $i-1$ observation, respectively,

$\vec{r}_i$ = position vector at observation time $t_{R_{e_i}}$, and

$\vec{V}_i$ = velocity vector at observation time $t_{R_{e_i}}$.

4.3 RELATIVISTIC CORRECTIONS (con't)

The first term is the uncorrected range difference, the second term varies only with Δt_{R_e} for a given orbit, and hence would be very nearly constant for a constant Δt_{R_e}. The third term is cyclic, varying with the eccentric anomaly of the satellite. It would, of course, be zero for a circular orbit and would be small enough to be negligible for many near-circular orbit satellites. However, PULSAR cannot ignore this term. So, corrections for both the second and third terms are made.

In the above expression the uncorrected range difference is

$$\Delta\rho_u = \frac{C}{f_T}\left[-N - \Delta f \Delta t_R\right] \quad , \tag{21}$$

where

N = Number of doppler counts within Δt_R,

$\Delta f = f_R - f_T$,

f_R = frequency of receiving station,

f_T = frequency of transmitting station, and

Δt_R = receiver clock interval for the N counts.

Tests have been made to determine the magnitude of the correction terms. Computations were made using satellite orbital elements typical of those supported by PULSAR for range difference with an observation time of twenty seconds. The Δt_{Re} term was of the order of two meters range difference correction. The last term, involving $\vec{r} \cdot \vec{V}$, varied in range difference correction over a fourteen minute interval (approximately a station pass) from a $\Delta\rho$ correction of -.14 meters to .23 meters.

4.4 CORRECTION FOR ROTATION OF CIRCULARLY POLARIZED ANTENNA

As is the case with many missions, e.g., space shuttle and LANDSAT, periodic adjustment of vehicle attitude provides the possibility that rotation about the antenna can produce erroneous results in the range difference computations. A procedure to compensate for the induced error has been devised and involves calculating the angular rotation of the satellite about the antenna boresight and computing the apparent doppler shift produced by that rotation.

Blanton[2] has shown that the angular rotation can be computed from the orientation quaternions by

$$\begin{bmatrix} \cos\frac{\omega\Delta t}{2} \\ \frac{\omega_1}{\omega}\sin\frac{\omega\Delta t}{2} \\ \frac{\omega_2}{\omega}\sin\frac{\omega\Delta t}{2} \\ \frac{\omega_3}{\omega}\sin\frac{\omega\Delta t}{2} \end{bmatrix} = \begin{bmatrix} Q_1(t) & Q_2(t) & Q_3(t) & Q_4(t) \\ Q_4(t) & Q_3(t) & -Q_2(t) & -Q_1(t) \\ -Q_3(t) & Q_4(t) & Q_1(t) & -Q_2(t) \\ Q_2(t) & -Q_1(t) & Q_4(t) & -Q_3(t) \end{bmatrix} \begin{bmatrix} Q_1(t+\Delta t) \\ Q_2(t+\Delta t) \\ Q_3(t+\Delta t) \\ Q_4(t+\Delta t) \end{bmatrix} \tag{22}$$

$$= [\underset{\sim}{QSQ}]\,[\underset{\sim}{Q}]$$

This formulation assumes that the components ω_i remain constant over the interval Δt. The accuracy of this method is insensitive to the size of the interval Δt. Thus, it is only necessary to use the quaternions at the beginning and end of an observation interval so that:

[2] Blanton, J. N., Memo to W.P.B., 9/2/81

4.4 CORRECTION FOR ROTATION OF CIRCULARLY POLARIZED ANTENNA (con't)

$$\begin{bmatrix} \cos\frac{\Omega}{2} \\ \frac{\Omega_1}{\Omega}\sin\frac{\Omega}{2} \\ \frac{\Omega_2}{\Omega}\sin\frac{\Omega}{2} \\ \frac{\Omega_3}{\Omega}\sin\frac{\Omega}{2} \end{bmatrix} = \begin{bmatrix} \cos\frac{\omega\Delta t}{2} \\ \frac{\omega_1}{\omega}\sin\frac{\omega\Delta t}{2} \\ \frac{\omega_2}{\omega}\sin\frac{\omega\Delta t}{2} \\ \frac{\omega_3}{\omega}\sin\frac{\omega\Delta t}{2} \end{bmatrix} = \begin{bmatrix} P_1 \\ P_2 \\ P_3 \\ P_4 \end{bmatrix} = [\underset{\sim}{QSQ}]\ [\underset{\sim}{Q}] \qquad (23)$$

Where

ω = angular rotation rate, and

Ω = angle of rotation in radians.

4.4 CORRECTION FOR ROTATION OF CIRCULARLY POLARIZED ANTENNA (con't)

Then

$$\Omega/2 = \cos^{-1} P_1 , \tag{24}$$

$$\Omega = 2 \cos^{-1} P_1 , \text{ and} \tag{25}$$

$$\Omega_i = P_{i+1} \quad \Omega/\sin(\frac{\Omega}{2}) . \tag{26}$$

The three components of the rotation make it possible to compute the rotation about the beacon boresight, Ω_{bbs}, which has body fixed direction cosines a_1, a_2, and a_3.

Then

$$\Omega_{bbs} = \sum_{i=1}^{3} \Omega_i a_i \quad . \tag{27}$$

Subsequent references to Ω will imply Ω_{bbs}.

The range difference error for a single frequency beacon is

$$\delta\Delta R = \frac{c}{f} \bullet \frac{\Omega}{2\pi} , \tag{28}$$

where f is the frequency and c is the speed of light.

The actual beacons, however, use frequency pairs to compensate for ionospheric effects (first order). The derivation which follows assumes a 400 mHz, 150 mHz pair. The results are the same whether processed by a TRANET receiver or by a GEOCEIVER. So, the development will be presented only once using notation which could be appropriate to either type processing. Let the associated offset frequencies be given by

CORRECTION FOR ROTATION OF CIRCULARLY POLARIZED ANTENNA (con't)

$$\Delta f_1 = \frac{-f_1}{c}\dot{\rho} + \frac{d_1}{f_1} + \frac{\omega}{2\pi} \quad , \tag{29}$$

$$\Delta f_2 = \frac{-f_2}{c}\dot{\rho} + \frac{d_1}{f_2} + \frac{\omega}{2\pi} \quad , \tag{30}$$

e ω = rate of rotation about the transmitting antenna. Combining the et frequencies to eliminate the ionospheric correction term involving ives

$$\Delta f' = \Delta f_1 - \lambda \Delta f_2 = \frac{-f_1}{c}(1-\lambda^2)\,\dot{\rho} + (1-\lambda)\,\frac{\omega}{2\pi} \quad , \tag{31}$$

e

$$\lambda = f_2/f_1 = 3/8.$$

ne sets

$$f' = f_1(1-\lambda^2) = \frac{55}{64} f_1 \quad ,$$

$$\Delta f' = -\frac{f'}{c}\,\dot{\rho} + (1-\lambda)\,\frac{\omega}{2\pi} \quad , \tag{32}$$

$$\dot{\rho} = \frac{c}{f'}\left[-\Delta f' + (1-\lambda)\,\frac{\omega}{2\pi}\right] \quad , \tag{33}$$

hat

$$\Delta R_i = \int_{t_{i-1}}^{t_i} \dot{\rho}\, dt = \frac{c}{f'}\int_{t_{i-1}}^{t_i} -\Delta f'\, dt + \frac{c}{f'}(1-\lambda)\,\frac{\Omega}{2\pi} \quad . \tag{34}$$

4.4 CORRECTION FOR ROTATION OF CIRCULARLY POLARIZED ANTENNA (con't)

Now

$$\Delta f_1 = f_{R_1} - f_{s_1} = f_{R_1} - f_{r_1} + f_{r_1} - f_{s_1} = \dot{N}_1 - (f_{s_1} - f_{r_1}), \qquad (35)$$

where

f_{R_1} = frequency of the signal received,

f_{r_1} = receiver reference frequency,

f_{s_1} = transmitter frequency,

also,

$$\Delta f_2 = \dot{N}_2 - (f_{s_2} - f_{r_2}),$$

and $\dot{N}_1$ and $\dot{N}_2$ are the doppler count rates for the upper and lower frequencies respectively.

The signs above are correct for the transmitter frequency being greater than the receiver local oscillator frequency. If $f_{r_i} > f_{s_i}$, then the sign of $\dot{N}_i$ is reversed.

Substituting the above into equation (31) gives

$$\Delta f' = \dot{N}_1 - \lambda \dot{N}_2 - (1 - \lambda^2)(f_{s_1} - f_{r_1}) \quad , \qquad (36)$$

so that

$$\Delta R_i = \frac{c}{(1-\lambda^2) f_{s_1}} \left[\int_{t_{i-1}}^{t_i} - (\dot{N}_1 - \lambda \dot{N}_2)\, dt + \int_{t_{i-1}}^{t_i} (1-\lambda^2)(f_{s_1} - f_{r_1})\, dt \right]$$

$$+ \frac{c}{(1-\lambda^2) f_{s_1}} (1 - \lambda) \frac{\Omega}{2\pi} \quad . \qquad (37)$$

5.2.1.1 The Canonical Equations of Motion (con't)

conjugate momentum p_ℓ is a constant, i.e. $p_\ell = \alpha_\ell$, and

$$H = H(p_1, p_2, \ldots, p_{\ell-1}, \alpha_\ell \; p_{\ell+1}, \ldots, p_{3n-k} \; ; \; q_1, q_2, \ldots, q_{\ell-1}, q_{\ell+1}, \ldots, q_{3n-k}; t) \quad . \tag{28}$$

Thus there are $2(3n - k) - 2$ equations to be solved and the problem has in fact been reduced in complexity. Consequently, the canonical formulation is particularly well suited for dealing with problems in which one or more of the coordinates is ignorable. It is clear that the simplest solution to a dynamical problem would result if the problem could be formulated in such a way that all coordinates were ignorable.

5.2.1.2 Hamilton-Jacobi Theory

Because of the simplification of the Hamiltonian by ignorable coordinates, it is desirable to seek coordinate transformations which would make all the coordinates ignorable thereby making the solution trivial. Thus given equations (27), one wishes to change from the $3n-k$ variables (q_j, p_j) to $3n-k$ new variables (Q_j, P_j) in such a way that it will be easy to determine the new equations of motion and at the same time preserve the canonical form of equations (27); i.e. one seeks a canonical transformation which produces a new Hamiltonian H' so that

$$\dot{Q}_j = \frac{\partial H'}{\partial P_j} \quad ; \quad \dot{P}_j = -\frac{\partial H'}{\partial Q_j} \quad (j = 1, 2, .., 3n-k), \tag{29}$$

where H' is easily related to H and is expressed as a function of Q_j and P_j .

According to a theorem devised by Carl Gustav Jacob Jacobi, the desired transformations between (q_j, p_j) and (Q_j, P_j) which give rise to the canonical equations (29) are

ROUWER METHOD (con't)

s in a more analytically tractable problem since two of the trans-
coordinates of position become constants of the motion.

f outline of the underlying theory is presented in section 5.2.1 and
sults of the Brouwer approach are summarized in section 5.2.2. It
be mentioned that the method used in PULSAR is that of a Lyddane
ed Brouwer orbit generator which has been modified to cope with small
l eccentricities.

UNDERLYING THEORY

onian dynamics and the application of perturbation theory are the
elements used in the development of the Brouwer theory. In the fol-
subsections the canonical equations of motion, Hamilton-Jacobi theory,
e Von Zeipel method of finding generating functions will be briefly
sed.

1 The Canonical Equations of Motion

ler the system of n particles subject to k constraints which limit the
l's freedom of motion. The Hamilton equations of motion which describe
'stem are given by

$$\dot{q}_j = \frac{\partial H}{\partial p_j} \quad ; \quad \dot{p}_j = -\frac{\partial H}{\partial q_j} \quad (j = 1, 2, \ldots, 3n - k), \tag{27}$$

$H = H(p_j; q_j; t)$ is the Hamiltonian for the system and q_j and p_j
le associated 3n - k generalized coordinates and momenta, respecti-
Because of the symmetrical appearance of equations (27), they are
nown as the canonical equations of motion.

uld be pointed out that in the canonical formulation, if q_ℓ is an
ble coordinate, i.e. it does not appear in the Hamiltonian, then its

5.1.1.3 Luni-Solar Gravitational Accelerations (con't)

Replacing each of $\ddot{\vec{r}}_s'$ and $\ddot{\vec{r}}_\oplus'$ by the accelerations exerted by the sun and moon, one finds that

$$\ddot{\vec{r}} = \ddot{\vec{r}}_{\text{sun s}} - \ddot{\vec{r}}_s + \ddot{\vec{r}}_{\text{moon s}} - \ddot{\vec{r}}_{\text{moon}} \quad . \tag{23}$$

Treating the sun and moon as point masses, one may write

$$\ddot{\vec{r}}_{is} = \frac{-\mu_i \vec{r}_{is}}{r_{is}^3} = -\mu \frac{\vec{r} - \vec{r}_i}{|\vec{r} - \vec{r}_i|^3} \quad , \tag{24}$$

and

$$\ddot{\vec{r}}_i = \mu_i \frac{\vec{r}_i}{|\vec{r}_i|^3} \quad , \tag{25}$$

where i = sun, moon and μ_i is the gravitational constant for the i^{th} celestial body. Substituting these into equation (23) gives the desired result

$$\vec{a}_{\text{sun}} + \vec{a}_{\text{moon}} = \ddot{\vec{r}} = -\mu_{\text{sun}} \left(\frac{\vec{r} - \vec{r}_{\text{sun}}}{|\vec{r} - \vec{r}_{\text{sun}}|^3} + \frac{\vec{r}_{\text{sun}}}{|\vec{r}_{\text{sun}}|^3} \right)$$

$$- \mu_{\text{moon}} \left(\frac{\vec{r} - \vec{r}_{\text{moon}}}{|\vec{r} - \vec{r}_{\text{moon}}|^3} + \frac{\vec{r}_{\text{moon}}}{|\vec{r}_{\text{moon}}|^3} \right) \quad . \tag{26}$$

5.2 BROUWER METHOD

The drag-free Brouwer method is an analytic technique which considers only geopotential acceleration for generating the orbit of an artificial earth satellite and makes use of the theory of generating functions in its development. This approach casts the Hamiltonian for the system into a form which

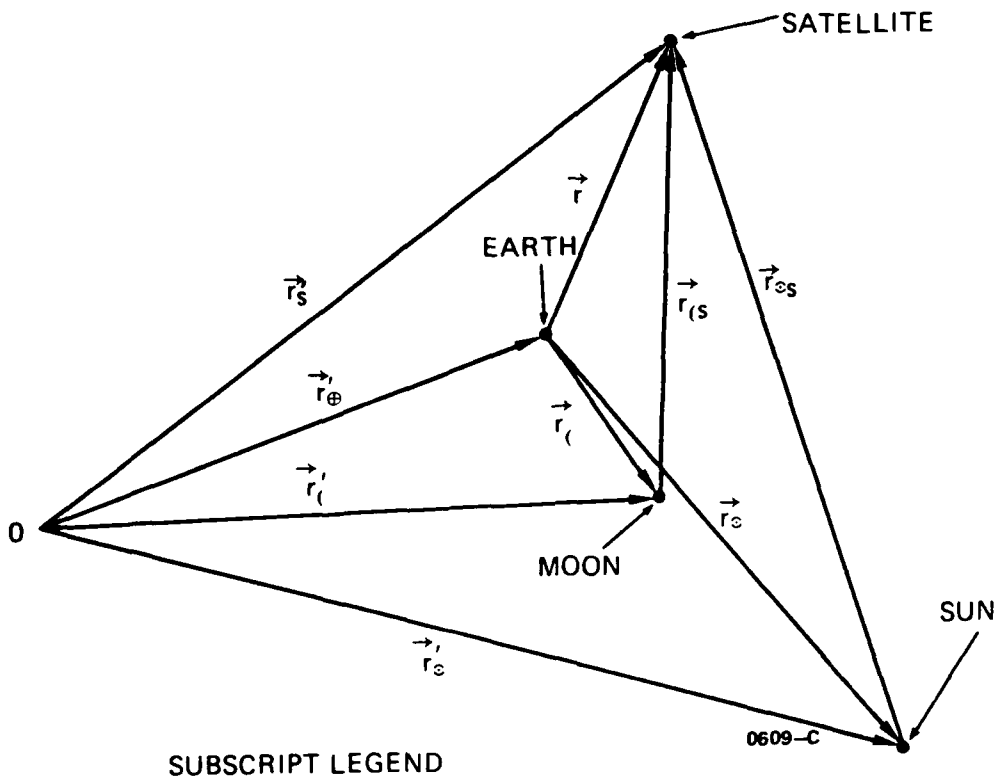

SUBSCRIPT LEGEND

s = SATELLITE
⊕ = EARTH
☉ = SUN
☾ = MOON

FIGURE 5-1. Luni-Solar Perturbation Geometry

5.1.1.2 Acceleration Due to Atmospheric Drag (con't)

where h is the geocentric altitude of the satellite given by:

$$h = r - \frac{a_e}{\left(1 + \frac{\varepsilon^2}{1 - \varepsilon^2} \sin^2\phi\right)^{\frac{1}{2}}} \quad . \tag{20}$$

In the last equation ϕ is the geocentric latitude and the quantities C_i (i = 1, 2, ..., 5) in equation (19) are data base constants.

A few comments are in order concerning the value of the satellite drag coefficient. In general this coefficient's value is dependent upon the physical properties of the satellite's surface, as well as the satellite's shape and angle of attack to the direction of motion, so that satellites which operate with continuously varying attitudes should exhibit time dependent values of C_D. However it has been shown that $C_D \sim 2.2$ for satellites with orbital parameters like those supported by PULSAR[2]. Thus PULSAR models C_D (or more precisely $C_D A/W$) as a constant over a trajectory segment.

5.1.1.3 Luni-Solar Gravitational Accelerations

To obtain expressions for the gravitational accelerations exerted by the sun and moon upon the satellite, consider the geometry depicted by Figure 5-1, where O is some fixed origin relative to the earth. Since

$$\vec{r} = \vec{r}_s' - \vec{r}_\oplus' \quad , \tag{21}$$

then

$$\ddot{\vec{r}} = \ddot{\vec{r}}_s' - \ddot{\vec{r}}_\oplus' \quad . \tag{22}$$

[2] King-Hele, D., Theory of Satellite Orbits in an Atmosphere, pp. 12-17, Butterworth & Co., 1964.

5.1.1.2 Acceleration Due to Atmospheric Drag (con't)

W = mg = weight of satellite;

m = mass of satellite;

g = gravitational acceleration at the surface of the earth;

ν = $|\vec{\nu}|$ = speed of the satellite relative to the atmosphere; and

ρ = local atmospheric density at the satellite's location.

The velocity of the satellite relative to the rotating atmosphere is:

$$\vec{\nu} = \dot{\vec{r}} - \vec{\omega} \times \vec{r} \quad , \tag{17}$$

where $\vec{r}$ and $\dot{\vec{r}}$ are the satellite's inertial position and velocity, respectively. The earth's angular velocity in the basic inertial reference frame, $\vec{\omega}$, is given by:

$$\vec{\omega} = (\underset{\sim\sim\sim}{BCD})^{-1} \begin{pmatrix} 0 \\ 0 \\ \tilde{\omega} \end{pmatrix} = (\underset{\sim\sim}{CD})^{-1} \underset{\sim}{B}^{-1} \begin{pmatrix} 0 \\ 0 \\ \tilde{\omega} \end{pmatrix} = (\underset{\sim\sim}{CD})^{-1} \begin{pmatrix} 0 \\ 0 \\ \tilde{\omega} \end{pmatrix} \quad , \tag{18}$$

where $\tilde{\omega}$ is the earth's mean sidereal rotation rate and $\underset{\sim\sim\sim}{BCD}$ are the transformation matrices of SECTION 2.

The atmospheric density used in equation (16) is computed using a simple density model which considers only the density variation with altitude above the earth's surface. Specifically the atmospheric density is computed from

$$\rho = e^{\left[c_1 h - c_2 - (c_3 h^2 + c_4 h - c_5)^{\frac{1}{2}}\right]} \quad , \tag{19}$$

5.1.1.1 Non-Central Geopotential Acceleration (con't)

To compute $\vec{a}_E$ PULSAR systematically evaluates the U_n^m and V_n^m functions by using the (n, m) = (0, 0), (1, 0) values of these functions as starting values and computing U_n^0 and V_n^0 for n = 2, 3, ..., n_{max} from the horizontal stepping recurrence relations. The diagonal stepping relations are then applied to compute U_1^1, V_1^1 and the U_n^1, V_n^1 for n = 2, 3, ..., n_{max} are calculated using again the horizontal stepping relations. This procedure is repeated until m = $m_{max} \leq n_{max}$. The acceleration $\vec{a}_E$ is then obtained by application of equations (8), (13), (14), and (15).

5.1.1.2 Acceleration Due to Atmospheric Drag

The acceleration arising from atmospheric drag as used by PULSAR's force model is assumed to be that of neutral particle drag opposite the direction of motion in an earth fixed, wind-free atmosphere. Aerodynamic lift forces are ignored. Drag acceleration is very difficult to determine accurately, due to gross uncertainties in the temporal behavior of the earth's atmosphere and the value of the satellite's drag coefficient. Additional inaccuracy is introduced if the satellite is nonspherical and its frontal area is continually changing.

The drag acceleration acting on a satellite due to the earth's atmosphere as modeled in PULSAR is given by:

$$\vec{a}_D = -\tfrac{1}{2} D g \rho v \vec{v} \quad , \tag{16}$$

where

$$D = C_D A / W$$

C_D = the dimensionless drag coefficient for the satellite;

A = cross-sectional area of the satellite normal to the direction of motion;

5.1.1.1 Non-Central Geopotential Acceleration (con't)

$$U_{n+1}^{n+1} = (2n+1)\left(\frac{a_e}{r}\right)\sin\theta\left[U_n^n\cos\lambda - V_n^n\sin\lambda\right] \tag{11}$$

$$V_{n+1}^{n+1} = (2n+1)\left(\frac{a_e}{r}\right)\sin\theta\left[U_n^n\sin\lambda + V_n^n\cos\lambda\right] \tag{12}$$

diagonal stepping,

$$\vec{\nabla}_e U_n^m = \frac{1}{2a_e}\begin{pmatrix} A_n^m\, U_{n+1}^{m-1} - U_{n+1}^{m+1} \\ -A_n^m\, V_{n+1}^{m-1} - V_{n+1}^{m+1} \\ -2(n-m+1)\, U_{n+1}^m \end{pmatrix}, \text{ and} \tag{13}$$

$$\vec{\nabla}_e V_n^m = \frac{1}{2a_e}\begin{pmatrix} A_n^m\, V_{n+1}^{m-1} - V_{n+1}^{m+1} \\ A_n^m\, U_{n+1}^{m-1} + U_{n+1}^{m+1} \\ -2(n-m+1)\, V_{n+1}^m \end{pmatrix}, \tag{14}$$

where

$$A_n^m = (n-m+1)\,(n-m+2). \tag{15}$$

5.1.1.1 Non-Central Geopotential Acceleration (con't)

Since the integration of the satellite equations of motion is performed in the basic inertial reference frame, the earth-fixed acceleration given by equation (6) must be transformed to the inertial acceleration by applying the $\underset{\sim\sim\sim}{BCD}$ transformations of SECTION 2 to equation (6). Thus

$$\vec{a}_E = (\underset{\sim\sim\sim}{BCD})^{-1} \vec{\nabla}_e V = (\underset{\sim\sim\sim}{BCD})^{-1} \sum_{\substack{n=0 \\ (n\neq 1)}}^{\infty} \sum_{m=0}^{n} \left[C_{nm} \vec{\nabla}_e U_n^m + S_{nm} \vec{\nabla}_e V_n^m \right] \quad . \quad (8)$$

It should be mentioned that summing the index n to infinity is not computationally realizible. In practice the summation must be truncated at $n = n_{max}$, where n_{max} is a user selectable integer less than or equal to 30 (of course, $\vec{a}_E$ is more accurately represented when large values of n_{max} are used).

For the sake of computational convenience, the well known recurrence relations for the associated Legendre functions and their derivatives[1] have been used to obtain recurrence relations for U_n^m, V_n^m, $\vec{\nabla}_e U_n^m$, and $\vec{\nabla}_e V_n^m$. In particular, it is found that:

$$U_{n+1}^m = \frac{a_e}{r(n-m+1)} \left[(2n+1)\cos\theta \, U_n^m - (n+m) \left(\frac{a_e}{r} \right) U_{n-1}^m \right] \quad (9)$$

$$V_{n+1}^m = \frac{a_e}{r(n-m+1)} \left[(2n+1)\cos\theta \, V_n^m - (n+m) \left(\frac{a_e}{r} \right) V_{n-1}^m \right] \quad (10)$$

} horizontal stepping,

[1] Arfken, G., Mathematical Methods for Physicists, p. 560, Academic Press, 1970.

5.1.1.1 Non-Central Geopotential Acceleration (con't)

$$V = \sum_{\substack{n=0 \\ (n\neq 1)}}^{\infty} \sum_{m=0}^{n} \left[C_{nm} U_n^m + S_{nm} V_n^m \right] \quad , \tag{3}$$

where

$$U_n^m = \frac{\mu a_e^n}{r^{n+1}} P_n^m (\cos\theta) \cos m\lambda \tag{4}$$

and

$$V_n^m = \frac{\mu a_e^n}{r^{n+1}} P_n^m (\cos\theta) \sin m\lambda \quad . \tag{5}$$

The acceleration in the earth-fixed reference frame is obtained by taking the corresponding gradient of the potential in equation (3). Since C_{nm} and S_{nm} are constants, one obtains

$$\vec{\nabla}_e V = \sum_{\substack{n=0 \\ (n\neq 1)}}^{\infty} \sum_{m=0}^{n} \left[C_{nm} \vec{\nabla}_e U_n^m + S_{nm} \vec{\nabla}_e V_n^m \right] \quad , \tag{6}$$

where $\vec{\nabla}_e$ is the gradient operator in the earth-fixed frame and is given by

$$\vec{\nabla}_e = \sum_{i=1}^{3} \hat{e}_i \frac{\partial}{\partial \chi_i} \quad . \tag{7}$$

In this expression, the $\hat{e}_i$ are unit vectors along the orthogonal Cartesian χ_i axes of the earth-fixed reference frame.

5.1.1 FORCE MODEL (con't)

$\vec{a}_{moon}$ = acceleration due to the lunar gravitational field; and

$\vec{a}_{sun}$ = acceleration due to the solar gravitational field.

The following sections describe the manner in which each of the terms on the right hand side of equation (1) is evaluated in PULSAR.

5.1.1.1 Non-Central Geopotential Acceleration

The earth's gravitational potential in an earth-fixed reference frame is given by the spherical harmonic expression

$$V = \mu \sum_{n=0}^{\infty} \sum_{m=0}^{n} \left[\frac{a_e^n}{r^{n+1}} P_n^m (\cos\Theta) \left\{ C_{nm} \cos m\lambda + S_{nm} \sin m\lambda \right\} \right] , \qquad (2)$$

where

μ = earth's gravitational constant;

a_e = earth's semi-major axis;

r = magnitude of the geocentric radius vector to the satellite;

$P_n^m(\cos\theta)$ = associated Legendre function;

θ = colatitude of sub-satellite point;

λ = east longitude of the sub-satellite point; and

C_{nm}, S_{nm} = gravitational harmonic expansion coefficients.

It should be noted that with the geopotential expressed in this form $C_{oo} = 1$; and $C_{10} = C_{11} = S_{11} = 0$, i.e. $n \neq 1$. For computational convenience, equation (2) may be recast into the form

5.1 COWELL METHOD (con't)

significant perturbations) and their step-by-step numerical integration to obtain $\vec{r}(t)$ and $\dot{\vec{r}}(t)$. In general the method consists of the following basic steps:

(i) given $\vec{r}$ and $\dot{\vec{r}}$ at some time t_i;

(ii) calculate the total acceleration acting upon the satellite at t_i;

(iii) numerically integrate to get $\dot{\vec{r}}$ at the next time point t_{i+1};

(iv) numerically integrate again to get the position at t_{i+1};

(v) with the new $\vec{r}$ and $\dot{\vec{r}}$, repeat the above steps for the next time point, t_{i+2}.

The procedure for initializing the numerical integration and the computational techniques employed in the numerical integration process are developed in Section 9. A discussion of the satellite equations of motion as applied to the orbital force environment of satellites serviced by the PULSAR system is given below.

5.1.1 FORCE MODEL

The force environment for the satellites serviced by the PULSAR system can be adequately represented by the acceleration function

$$\ddot{\vec{r}}(\vec{r},\dot{\vec{r}},t) = \vec{a}_E + \vec{a}_D + \vec{a}_{moon} + \vec{a}_{sun} \quad , \tag{1}$$

where

$\vec{a}_E$ = acceleration due to the gravitational field of the earth;

$\vec{a}_D$ = acceleration due to atmospheric drag;

SECTION 5

EPHEMERIS GENERATION

In the context of the PULSAR data editing system, ephemeris generation is the process of calculating positions and velocities for earth satellites at specified times. Although this ephemeris data need not be of superior geodetic quality, it provides for the editing process with sufficient accuracy:

(i) computed satellite observations used for state estimation and dynamic parameter improvement (section 7);

(ii) time histories of satellite positions and velocities; and

(iii) predicted values of future satellite positions and velocities.

Two techniques are used to generate earth satellite ephemerides in the PULSAR system, the well known Cowell and Brouwer methods. The Cowell method is a special perturbation theory requiring the numerical integration of the satellite's equations of motion to obtain time-dependent values of position and velocity. It is used to generate the satellite trajectory which initiates the point editing process. The Brouwer method is a general perturbation theory which provides the earth satellite's ephemeris through an analytic integration of a modified (and analytically tractable) formulation of the satellite equations of motion. This technique is used in time correction computations of the time calibration procedure. Both of these basic methods are discussed in the following subsections.

5.1 COWELL METHOD

The Cowell method is the most straightforward for determining the position $\vec{r}(t)$ and velocity $\dot{\vec{r}}(t)$ for the perturbed satellite trajectory. Its application involves the development of the satellite's equations of motion which is consistent with its force environment (taking care to include all

4.4 CORRECTION FOR ROTATION OF CIRCULARLY POLARIZED ANTENNA (con't)

Rearranging and integrating yields

$$\Delta R_i = -\frac{c}{f_{s_1}} \frac{N_1 - \lambda N_2}{(1 - \lambda^2)} + \frac{c}{f_1}(f_{s_1} - f_{r_1})\,(t_i - t_{i-1}) + \frac{c}{(1+\lambda)f_1}\,\frac{\Omega}{2\pi} \quad . \tag{38}$$

The contribution due to rotation is the last term, i.e.

$$\delta\Delta R_i = \frac{\delta}{11}\,\frac{c}{f_{s_1}}\,\frac{\Omega}{2\pi} \quad . \tag{39}$$

However, the expression for Ω assumes right hand circular polarization. With left hand circular polarization the sign is reversed giving

$$\delta\Delta R_i = -\frac{\delta}{11}\,\frac{c}{f_{s_1}}\,\frac{\Omega}{2\pi} \quad . \tag{40}$$

5.2.1.2 Hamilton-Jacobi Theory (con't)

$$p_j = \frac{\partial S(P_j;\ q_j;\ t)}{\partial q_j} \quad ; \quad Q_j = \frac{\partial S(P_j;\ q_j;\ t)}{\partial P_j} \quad (j = 1,\ 2,\ \ldots 3n\text{-}k), \qquad (30)$$

where $S(P_j;\ q_j;\ t)$ is called the generating function. The new Hamiltonian is related to the old through the transformation

$$H' = H\left(\frac{\partial S}{\partial q_j};\ q_j;\ t\right) + \frac{\partial S}{\partial t} \quad . \qquad (31)$$

5.2.1.3 Von Zeipel's Method

In this and the remaining subsections of section 5, the analytical development will be performed in terms of the six Delaunay variables defined within the context of PULSAR by:

$$\begin{aligned} L &= \sqrt{\mu a} & \ell &= \text{mean anomaly} \\ G &= L\sqrt{1 - e^2} & g &= \text{argument of perigee} \\ H &= G\cos i & h &= \text{right ascension of the ascending node,} \end{aligned} \qquad (32)$$

where μ is the earth's gravitational constant, and a, e, i are the orbital semi-major axis, eccentricity and inclination, respectively. The Delaunay variables provide the following system of canonical equations of motion:

$$\begin{aligned} \dot{L} &= \frac{\partial H}{\partial \ell} \quad ; & \dot{G} &= \frac{\partial H}{\partial g} \quad ; & \dot{H} &= \frac{\partial H}{\partial h} \quad ; \\ \dot{\ell} &= -\frac{\partial H}{\partial L} \quad ; & \dot{g} &= -\frac{\partial H}{\partial G} \quad ; & \dot{h} &= -\frac{\partial H}{\partial H} \end{aligned} \qquad , \qquad (33)$$

5.2.1.3 Von Zeipel's Method (con't)

where H is a function of the six Delaunay variables (note that in this context the variables L, G, H are the three variables of momenta and ℓ, g, h are the three variables of position).

The Von Zeipel method involves solving equations (33) by obtaining a series of variable transformations with the aid of a generating function. In particular, it is seen from the previous section that if one considers a new set of variables L', G', H', ℓ', g', h' and a generating function S(L', G', H', ℓ , g , h) such that

$$L = \frac{\partial S}{\partial \ell} ; \quad G = \frac{\partial S}{\partial g} ; \quad H = \frac{\partial S}{\partial h} ; \quad \ell' = \frac{\partial S}{\partial L'} ; \quad g' = \frac{\partial S}{\partial G'} ;$$

$$h' = \frac{\partial S}{\partial H'} ; \quad \text{and} \quad \frac{\partial S}{\partial t} = 0; \tag{34}$$

then the new system of equations is also canonical and

$$H(L, G, H, \ell, g, h) = H'(L', G', H', \ell', g', h'). \tag{35}$$

The transformation is selected such that H' is independent of one of the position variables on which H depends. If this operation is repeated several times, all position variables will be eliminated from H one by one, and the final Hamiltonian H'' will be a function only of L", G", and H". Thus in the equations

$$\dot{L}'' = \frac{\partial H''}{\partial \ell''} ; \quad \dot{G}'' = \frac{\partial H''}{\partial g''} ; \quad \dot{H}'' = \frac{\partial H''}{\partial h''} ; \tag{36}$$

the right hand sides will vanish and L", G", H" will be constants. Placing those values into the right hand sides of the canonical equations for the position coordinates, one finds that $\dot{\ell}''$, $\dot{g}''$, and $\dot{h}''$ are constants, so that

5.2.1.3 Von Zeipel's Method (con't)

ℓ'', g'', h'' are linear functions of time. Relations of the type given by equations (34) are then used to return to expressions for the original (unprimed) Delaunay variables.

In order to solve the problem in this fashion, one must be able to determine the generating function S. To do this using the Von Zeipel method, one expands the generating function and Hamiltonians in powers of some small parameter ε. Then

$$H = H_0 + H_1 + \ldots \; ; \; S = S_0 + S_1 + S_2 + \ldots;$$
$$H' = H_0' + H_1' + H_2' + \ldots; \tag{37}$$

and if one selects

$$S_0 = L'\ell + G'g + H'h \, , \tag{38}$$

the application of the second of equations (37) to equations (34) gives

$$L = L' + \frac{\partial S_1}{\partial \ell} + \frac{\partial S_2}{\partial \ell} + \ldots \, , \tag{39}$$

and similarly for G and H; and

$$\ell' = \ell + \frac{\partial S_1}{\partial L'} + \frac{\partial S_2}{\partial L'} + \ldots \, , \tag{40}$$

and similarly for g and h. If one performs a Taylor expansion of

$H\left(\frac{\partial S}{\partial \ell}, \frac{\partial S}{\partial g}, \frac{\partial S}{\partial h}; \ell, g, h\right)$ about $\frac{\partial S_0}{\partial \ell}$, $\frac{\partial S_0}{\partial g}$, and $\frac{\partial S_0}{\partial h}$ and

equates terms of equal orders, it is found to second order that:

5.2.1.3 Von Zeipel's Method (con't)

$$H_0 = H_0' \qquad \text{(zeroth order)}$$

$$\sum_{i=1}^{3} \left(\frac{\partial H_0}{\partial \alpha_i}\right)\left(\frac{\partial S_1}{\partial \beta_i}\right) + H_1 = H_1' \qquad \text{(first order)} \qquad (41)$$

$$\sum_{i=1}^{3} \left[\left(\frac{\partial H_0}{\partial \alpha_i}\right)\left(\frac{\partial S_2}{\partial \beta_i}\right) + \frac{1}{2}\left(\frac{\partial^2 H_0}{\partial \alpha_i^2}\right)\left(\frac{\partial S_1}{\partial \beta_i}\right)^2 + \left(\frac{\partial H_1}{\partial \alpha_i}\right)\left(\frac{\partial S_1}{\partial \beta_i}\right)\right]$$

$$+ H_2 = H_2' \qquad \text{(second order)},$$

where H_1 and H_2 are functions of the primed coordinates and $(\alpha_1, \alpha_2, \alpha_3) = (L', G', H')$ and $(\beta_1, \beta_2, \beta_3) = (\ell, g, h)$. It should be noted that this expansion can be continued indefinitely to higher orders of accuracy. These equations are then solved for S_1, S_2, etc., depending upon the accuracy required, and the desired solutions follow from equations (39) - (40). This procedure is repeated to eliminate the remaining position coordinates.

5.2.2 RESULTS OF THE BROUWER-LYDDANE THEORY

To illustrate the theory outlined in section 5.2.1, consider its application to the main problem of the artificial satellite theory, i.e. the geopotential is assumed to be of the form

$$V = \frac{\mu}{r} + \frac{\mu k_2}{r^3}\left(1 - 3\sin^2\Psi\right) \quad . \qquad (42)$$

where $k_2 = \frac{1}{2} J_2 a_e^2 = \frac{1}{2} C_{20} a_e^2$. For the sake of brevity, only the first order theory through the elimination of ℓ will be discussed.

The Hamiltonian for the system is given by

5.2.2 RESULTS OF THE BROUWER-LYDDANE THEORY (con't)

$$H = \frac{\mu}{2a} + \frac{\mu k_2}{r^3}(1 - 3\sin^2\psi). \tag{43}$$

Using spherical trigonometry and equations (32), one may rewrite the last equation as

$$H = H_0 + H_1 \ , \tag{44}$$

where

$$H_0 = \frac{\mu^2}{2L^2} \ , \tag{45}$$

and

$$H_1 = \frac{\mu^4 k_2}{L^6}\left[\left(-\frac{1}{2} + \frac{3}{2}\frac{H^2}{G^2}\right)\frac{a^3}{r^3} + \left(\frac{3}{2} - \frac{3}{2}\frac{H^2}{G^2}\right)\frac{a^3}{r^3}\cos(2g + 2f)\right] . \tag{46}$$

In the last expression f is the true anomaly. It may also be shown that

$$\frac{a^3}{r^3} = \frac{L^3}{G^3} + \sum_{j=1}^{\infty} 2P_j \cos j\ell = \frac{L^3}{G^3} + \delta_1 \tag{47}$$

and

$$\frac{a^3}{r^3}\cos(2g + 2f) = \sum_{\substack{j=-\infty \\ j\neq 0}}^{\infty} Q_j \cos(2g + j\ell) = \delta_2 \ , \tag{48}$$

5.2.2 RESULTS OF THE BROUWER-LYDDANE THEORY (con't)

where P_j and Q_j are power series in e. It is seen that H_0 is a function of L only and that H_1 is independent of h. The notational convention adopted for ignorable coordinates is that they will be replaced by a dash in the Hamiltonian's functional statement. Thus in this case one may write

$$H = H_0 (L) + H_1 (L, G, H, \ell, g, -) \quad . \tag{49}$$

To eliminate ℓ and obtain first order results, one applies the first two of equations (41) to obtain:

$$H_0 = H_0(L') = \frac{\mu^2}{2L'^2} \tag{50}$$

$$H_1' (L', G', H', -, g, -) = \left(\frac{\partial H_0}{\partial L'}\right)\left(\frac{\partial S_1}{\partial \ell}\right) + H_1 (L', G', H', \ell, g, -)$$

$$= -\left(\frac{\mu^2}{L'^3}\right)\left(\frac{\partial S_1}{\partial \ell}\right) + \frac{\mu^4 k_2}{L'^6}\left[\left(-\frac{1}{2} + \frac{3}{2}\frac{H'^2}{G'^2}\right)\left(\frac{L'^3}{G'^3} + \delta_1\right)\right.$$

$$\left. + \left(\frac{3}{2} - \frac{3}{2}\frac{H'^2}{G'^2}\right)\delta_2\right] \quad . \tag{51}$$

In order to obtain S_1 one notes that H_1 may be separated into a secular part independent of ℓ (H_{1_S}) and a periodic part dependent upon ℓ (H_{1_P}), i.e.

$$H_{1_S} (L', G', H', -, g, -) = \frac{\mu^4 k_2}{L'^6}\left[\left(-\frac{1}{2} + \frac{3}{2}\frac{H'^2}{G'^2}\right)\frac{L'^3}{G'^3}\right] \tag{52}$$

and

5.2.2 RESULTS OF THE BROUWER-LYDDANE THEORY (con't)

$$H_{1_p}(L', G', H', \ell, g, -) = \frac{\mu^4 k_2}{L'^6}\left[\left(-\frac{1}{2}+\frac{3}{2}\frac{H'^2}{G'^2}\right)\delta_1 + \left(\frac{3}{2}-\frac{3}{2}\frac{H'^2}{G'^2}\right)\delta_2\right]. \tag{53}$$

Thus one may write

$$H_1'(L', G', H', -, g, -) = H_{1_S}(L', G', H', -, g, -) = \frac{\mu^4 k_2}{L'^6}\left[\left(-\frac{1}{2}+\frac{3}{2}\frac{H'^2}{G'^2}\right)\frac{L'^3}{G'^3}\right] \tag{54}$$

and

$$\frac{\partial S_1}{\partial \ell} = \frac{\mu^2 k_2}{L'^3}\left[\left(-\frac{1}{2}+\frac{3}{2}\frac{H'^2}{G'^2}\right)\delta_1 + \left(\frac{3}{2}-\frac{3}{2}\frac{H'^2}{G'^2}\right)\delta_2\right], \tag{55}$$

or

$$S_1 = \frac{\mu^2 k_2}{L'^3}\left[\left(-\frac{1}{2}+\frac{3}{2}\frac{H'^2}{G'^2}\right)\int \delta_1\, d\ell + \left(\frac{3}{2}-\frac{3}{2}\frac{H'^2}{G'^2}\right)\int \delta_2\, d\ell\right]. \tag{56}$$

Using equations (47) - (48), the last expression becomes

$$S_1 = \frac{\mu^2 k_2}{L'^3}\left[\left(-\frac{1}{2}+\frac{3}{2}\frac{H'^2}{G'^2}\right)\sum_{j=1}^{\infty}\frac{2}{j}P_j \sin j\ell + \left(\frac{3}{2}-\frac{3}{2}\frac{H'^2}{G'^2}\right)\sum_{\substack{j=-\infty \\ j\neq 0}}^{\infty}\frac{Q_j}{j}\sin(2g + j\ell)\right]. \tag{57}$$

5.2.2 RESULTS OF THE BROUWER-LYDDANE THEORY (con't)

Equations (39) - (40) may be used to obtain expressions for L, G, H, ℓ, g, h through first order from equation (57). The last of equations (41) can then be applied to obtain second order expressions and the entire process repeated to eliminate g and obtain the final results.

This is essentially the procedure followed in the complete development of the Brouwer-Lyddane theory [3,4] except that there the significant effects of the third, fourth, and fifth zonal harmonic terms of the geopotential are also included. The results of the Brouwer-Lyddane theory as used in PULSAR are summarized below. Define:

$$
\left.
\begin{aligned}
a'' &= \text{semi-major axis constant (input)} \\
e'' &= \text{eccentricity constant (input)} \\
i'' &= \text{inclination constant (input)} \\
t &= \text{time from epoch} \\
n_0 &= (\mu/a''^3)^{\frac{1}{2}} \\
\eta &= (1 - e''^2)^{\frac{1}{2}} \\
\theta &= \cos i'' \\
\gamma_2 &= \frac{1}{2} C_{20} a_e^2 / a''^2 \\
\gamma_2' &= \gamma_2 \eta^{-4} \\
\gamma_3' &= -C_{30} a_e^3 a''^{-3} \eta^{-6} \\
\gamma_4' &= -\frac{3}{8} C_{40} a_e^4 a''^{-4} \eta^{-8} \\
\gamma_5' &= -C_{50} a_e^5 a''^{-5} \eta^{-10} \\
\alpha &= 1 - 5\theta^2
\end{aligned}
\right\} \qquad (58)
$$

[3] Brouwer, D., "Solution of the Problem of Artificial Satellite Theory Without Drag", The Astronomical Journal, Vol. 64, No. 1274, 1959, pp. 378-397.

[4] Lyddane, R. H., "Small Eccentricities or Inclinations in the Brouwer Theory of Artificial Satellites", The Astronomical Journal, Vol. 68, No. 8, 1963, pp. 555 - 558.

2.2 RESULTS OF THE BROUWER-LYDDANE THEORY (con't)

$$\left.\begin{aligned} \beta &= 1 - 11\theta^2 - 40\theta^4\,\alpha^{-1} \\ \gamma &= 1 - 3\theta^2 - 8\theta^4\,\alpha^{-1} \\ \delta &= 1 - 9\theta^2 - 24\theta^4\,\alpha^{-1} \\ \lambda &= 1 - 5\theta^2 - 16\theta^4\,\alpha^{-1} \quad . \end{aligned}\right\} \qquad \begin{matrix}(58)\\(\text{con't})\end{matrix}$$

en the secular terms are computed from:

$$\begin{aligned} \ell'' = n_o t \Bigg\{ & 1 + \frac{3}{2}\gamma_2'\,\eta(3\theta^2 - 1) + \frac{3}{32}\gamma_2'^{\,2}\,\eta\Big[-15 + 16\eta \\ & + 25\eta^2 + (30 - 96\eta - 90\eta^2)\theta^2 + (105 + 144\eta + 25\eta^2)\,\theta^4\Big] \\ & + \frac{15}{16}\gamma_4'\,\eta e''^2\Big[3 - 30\theta^2 + 35\theta^4\Big]\Bigg\} + \ell_o'' \quad , \end{aligned} \qquad (59)$$

$$\begin{aligned} g'' = n_o t \Bigg\{ & -\frac{3}{2}\gamma_2'\,\alpha + \frac{3}{32}\gamma_2'^{\,2}\Big[-35 + 24\eta + 25\eta^2 + (90 - 192\eta \\ & - 126\eta^2)\theta^2 + (385 + 360\eta + 45\eta^2)\theta^4\Big] + \frac{5}{16}\gamma_4'\Big[21 - 9\eta^2 \\ & + (-270 + 126\eta^2)\theta^2 + (385 - 189\eta^2)\theta^4\Big]\Bigg\} + g_o'' \quad , \end{aligned} \qquad (60)$$

ıd

$$\begin{aligned} h'' = n_o t \Bigg\{ & -3\gamma_2'\,\theta + \frac{3}{8}\gamma_2'^{\,2}\Big[(-5 + 12\eta + 9\eta^2)\theta + (-35 - 36\eta - 5\eta^2)\theta^3\Big] \\ & + \frac{5}{4}\gamma_4'\,(5 - 3\eta^2)\,\theta\,(3 - 7\theta^2)\Bigg\} + h_o'' \quad . \end{aligned} \qquad (61)$$

ıe long period (dependent upon g'') terms are computed from:

5.2.2 RESULTS OF THE BROUWER-LYDDANE THEORY (con't)

$$\delta_1 e = \frac{35}{96}\frac{\gamma_5'}{\gamma_2'} e''^2\eta^2 \lambda \sin i'' \sin^3 g'' - \frac{1}{12}\frac{e''\eta^2}{\gamma_2'}\left(3\gamma_2'^2\beta - 10\gamma_4'\gamma\right)$$

$$\sin^2 g'' - \frac{35}{128}\frac{\gamma_5'}{\gamma_2'} e''^2 \eta^2 \lambda \sin i'' \sin g'' + \frac{1}{4}\frac{\eta^2}{\gamma_2'} \qquad (62)$$

$$\left[\gamma_3' + \frac{5}{16}\gamma_5'(4 + 3e''^2)\delta\right]\sin i'' \sin g'' + \frac{e''\eta^2}{24\gamma_2'}\left[3\gamma_2'^2\beta - 10\gamma_4'\gamma\right]$$

$$\ell'+g' = g'' + \ell'' + \frac{1}{2}\left\{\frac{1}{24\gamma_2'}\left[-3\gamma_2'^2\left\{2 + e''^2 - 11(2 + 3e''^2)\theta^2 - 40(2 + 5e''^2)\right.\right.\right.$$

$$\left.\theta^4\alpha^{-1} - 400\, e''^2\theta^6\alpha^{-2}\right\} + 10\gamma_4'\left\{2 + e''^2 - 3(2 + 3e''^2)\theta^2\right.$$

$$\left.\left.\left. - 8(2 + 5e''^2)\theta^4\alpha^{-1} - 80e''^2\theta^6\alpha^{-2}\right\}\right] + \frac{\eta^3}{\gamma_2'}\left[\frac{\gamma_2'^2}{4}\beta - \frac{5}{6}\gamma_4'\gamma\right]\right\}$$

$$\sin 2g'' + \left\{\frac{35}{384}\frac{\gamma_5'}{\gamma_2'}\eta^3 e'' \lambda \sin i'' + \frac{35}{1152}\frac{\gamma_5'}{\gamma_2'}\right.$$

$$\left[\lambda\left\{-e''(3 + e''^2)\sin i'' + \frac{e''^3\theta^2}{\sin i''}\right\} + 2e''^3\theta^2 \sin i'' \right. \qquad (63)$$

$$\left.\left.\left\{5 + 32\theta^2\alpha^{-1} + 80\theta^4\alpha^{-2}\right\}\right]\right\}\cos 3g'' + \left\{-\frac{\gamma_3' e''\theta^2}{4\gamma_2' \sin i''} + \frac{5}{64}\frac{\gamma_5'}{\gamma_2'}\right.$$

$$\left[-e''\frac{\theta^2}{\sin i''}(4 + 3e''^2) + e'' \sin i''(26 + 9e''^2)\right]\delta - \frac{15}{32}\frac{\gamma_5'}{\gamma_2'}$$

$$e''\theta^2 \sin i''(4 + 3e''^2)(3 + 16\theta^2\alpha^{-1} + 40\theta^4\alpha^{-2}) + \frac{1}{4}\frac{\gamma_3'}{\gamma_2'}\sin i''.$$

.2.2 RESULTS OF THE BROUWER-LYDDANE THEORY (con't)

$$\left(\frac{e''}{1+\eta^3}\right)\left[3-e''^2(3-e''^2)\right]+\frac{5}{64}\frac{\gamma_5'}{\gamma_2'}\eta^2\delta\left[\frac{e''(-32+81e''^4)}{4+3e''^2+\eta(4+9e''^2)}\right]\sin i''\Bigg\}\cos g'' \tag{63 (con't)}$$

nd

$$h' = h'' + \frac{35\gamma_5' e''^3\theta}{144\,\gamma_2'}\left\{\tfrac{1}{2}\lambda\sin^{-1}i'' + \sin i''\left[5+32\theta^2\alpha^{-1}+80\theta^4\alpha^{-2}\right]\right\}$$

$$\sin^2 g''\cos g'' + \frac{e''^2\theta}{12\gamma_2'}\left\{-3\gamma_2'^2\left[11+80\theta^2\alpha^{-1}+200\theta^4\alpha^{-2}\right]+10\gamma_4'\right.$$

$$\left.\left[3+16\theta^2\alpha^{-1}+40\theta^4\alpha^{-2}\right]\right\}\sin g''\cos g'' + \left\{-\frac{35\gamma_5'}{576\gamma_2'}e''^3\theta\right. \tag{64}$$

$$\left[\tfrac{1}{2}\lambda\sin^{-1}i''+\sin i''(5+32\theta^2\alpha^{-1}+80\theta^4\alpha^{-2})\right]+\frac{e''\theta}{4\gamma_2'\sin i''}\left[\gamma_3'+\right.$$

$$\frac{5}{16}\gamma_5'(4+3e''^2)\delta+\frac{15}{8}\gamma_5'(4+3e''^2)(3+16\theta^2\alpha^{-1}+40\theta^4\alpha^{-2})$$

$$\left.\sin^2 i''\right]\Bigg\}\cos g'' \quad .$$

he short periodics (dependent upon E', f', ℓ'') are computed from:

$$a = a'' - a''\frac{\gamma_2}{\eta^3}(3\theta^2-1)+\left[\frac{a''\gamma_2}{(1-e''\cos E')^3}\right]\left[3\theta^2-1+3\sin^2 i''\right. \tag{65}$$

$$\left.\cos(2g''+2f')\right]$$

5.2.2 RESULTS OF THE BROUWER-LYDDANE THEORY (con't)

$$e = e'' + \delta_1 e + \frac{\eta^2\gamma_2}{2}\left\{\frac{3\eta^2-1}{\eta^6}\left[\frac{e''}{1+\eta^3}\left\{3 - e''^2(3 - e''^2)\right\} + \left\{3 + e''\cos f'.\right.\right.\right.$$

$$\left.\left.\left.(3 + e''\cos f')\right\}\cos f'\right] + \frac{3(1-\theta^2)}{\eta^6}\left[e'' + \left\{3 + e''\cos f'\ (3+e''\cos f')\right\}\cos f'\right]$$

$$\left.\cos(2f' + 2g'')\right\} - \frac{\eta^2\gamma_2'}{2}(1-\theta^2)\left[3\cos(2g'' + f') + \cos(2g'' + 3f')\right] \quad (66)$$

$$i = i'' - \frac{e''\theta}{\eta^2 \sin i''}\delta_1 e + e''\gamma_2'\,\theta\sin i''\sin f'\sin(2f' + 2g'') + 2e''\gamma_2'\theta\sin i''.$$

$$\cos f'\cos(2f' + 2g'') + \frac{3}{2}\gamma_2'\,\theta\sin i''\cos(2f' + 2g'') \quad (67)$$

$$g + \ell = g' + \ell' + \frac{\gamma_2'}{4}\left\{-6\alpha(f' - \ell'' + e''\sin f') + (3 - 5\theta^2)\left[3\sin(2f'\right.\right.$$

$$\left.\left. + 2g'') + 3e''\sin(2g'' + f') + e''\sin(2g'' + 3f')\right]\right\}$$

$$+ \frac{e''\eta^2\gamma_2'}{4(1+\eta)}\left\{2(3\theta^2 - 1)(\sigma+1)\sin f'\right.$$

$$\left. + 3(1-\theta^2)\left[(1-\sigma)\sin(2g'' + f') + (\sigma + 1/3)\sin(2g'' + 3f')\right]\right\} \quad (68)$$

$$h = h' + \left[2e''\gamma_2'\,\theta\cos f' + \frac{3}{2}\gamma_2'\theta\right]\sin(2g'' + 2f') - e''\gamma_2'\theta\sin f'\cos$$

$$(2f' + 2g'') - 3\gamma_2'\theta(f' - \ell'' + e''\sin f') \quad (69)$$

and

RESULTS OF THE BROUWER- LYDDANE THEORY (con't)

$$\delta i = \frac{1}{2}\frac{e''\eta^3}{\gamma_2'}\left\{\frac{1}{4}\gamma_2'\beta - \frac{5}{6}\gamma_4'\gamma\right\}\sin 2g'' - \left\{\frac{1}{4}\frac{\gamma_3'}{\gamma_2'}\eta^3\sin i'' + \frac{5}{64}\frac{\gamma_5'}{\gamma_2'}\eta^3\sin i''(4 + 9e^{2''})\delta\right\}\cdot\cos g'' + \frac{35}{384}\frac{\gamma_5'}{\gamma_2'}\eta^3 e''^2\lambda \sin i''\cos 3g'' - \frac{1}{4}\gamma_2'\eta^3\left\{2(3\theta^2 - 1)(\sigma + 1)\sin f' + 3(1 - \theta^2)(1 - \sigma)\sin(2g'' + f') + (\sigma + 1/3)\sin(2g'' + 3f')\right\} \quad , \tag{70}$$

$$r = \left(\frac{\eta}{1 - e''\cos E'}\right)^2 + \left(\frac{1}{1 - e''\cos E'}\right) \quad , \tag{71}$$

ccentric anomaly E' is obtained from a Newton-Raphson iteration upon epler equation (refer to SECTION 9)

$$E' - e''\sin E' = \ell'' \quad , \tag{72}$$

ne true anomaly f' is found from

$$\sin f' = \frac{\eta \sin E'}{1 - e''\cos E'} \quad ,$$

$$\cos f' = \frac{\cos E' - e''}{1 - e''\cos E'} \quad . \tag{73}$$

inal osculating values for a, i, and h are computed from equations (65), and (69), respectively. Equations (66), (68), (70) and (72) are used lculate final osculating values for ℓ, g, and e from the following ions:

5.2.2 RESULTS OF THE BROUWER-LYDDANE THEORY (con't)

$$A = e\cos\ell'' - e\delta\ell\sin\ell'' \quad , \tag{74}$$

$$B = e\sin\ell'' + e\delta\ell\cos\ell'' \quad , \tag{75}$$

$$\ell = \tan^{-1}(B/A) \quad , \tag{76}$$

$$g = (\ell + g) - \ell \quad , \tag{77}$$

and

$$e = (A^2 + B^2)^{\frac{1}{2}} \quad . \tag{78}$$

The inertial position and velocity are obtainable from the osculating Brouwer elements through the following relationships:

$$\vec{r} = a\underset{\sim}{Q} \begin{pmatrix} \cos E - e \\ \sqrt{1 - e^2}\sin E \end{pmatrix} \quad , \tag{79}$$

and

$$\dot{\vec{r}} = \frac{(\mu a)^{\frac{1}{2}}}{a(1 - e\cos E)} \underset{\sim}{Q} \begin{pmatrix} -\sin E \\ \sqrt{1 - e^2}\cos E \end{pmatrix} \quad , \tag{80}$$

where

$$\underset{\sim}{Q} = \begin{pmatrix} \cos h\cos g - \sin h\cos i\sin g & -\cos h\sin g - \sin h\cos i\cos g \\ \cos g\sin h + \cos h\cos i\sin g & \cos h\cos i\cos g - \sin h\sin g \\ \sin i\sin g & \sin i\cos g \end{pmatrix} \tag{81}$$

AD-A154 601 A MATHEMATICAL DESCRIPTION OF THE PULSAR DOPPLER SATELLITE TRACKING DATA EDITOR(U) NAVAL SURFACE WEAPONS CENTER DAHLGREN VA A D PARKS ET AL. SEP 82 2/3

UNCLASSIFIED NSWC/TR-82-391 F/G 17/3 NL

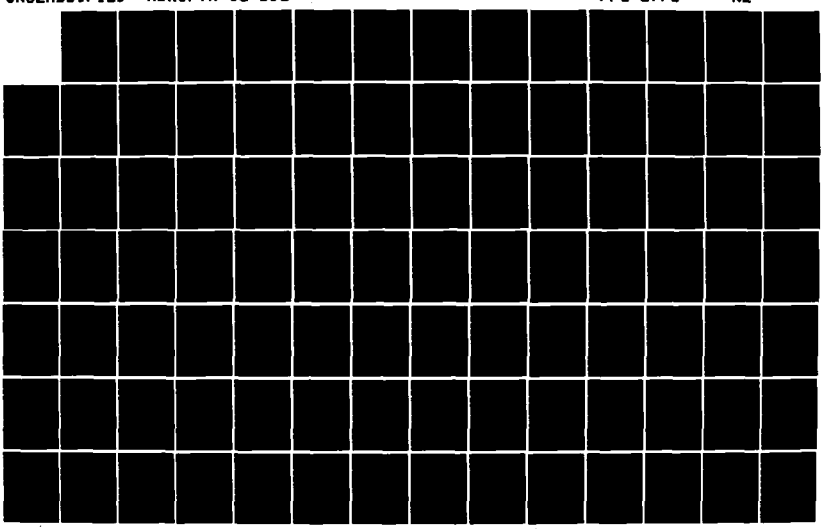

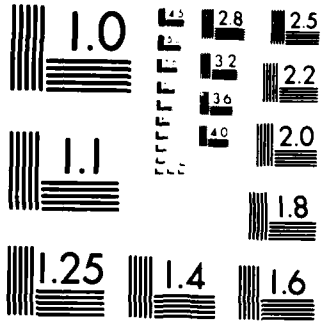

5.2.2 RESULTS OF THE BROUWER-LYDDANE THEORY (con't)

It should be mentioned in closing that the input Brouwer orbital elements are obtained from NAVSPASUR and that the semi-major axis thus provided is the Kaula semi-major axis expressed in earth radii. The Kaula semi-major axis must be converted from units of earth radii to linear units using the following relation:

$$a'' = a_K a_e \left(\frac{1 + 2\mathbb{X}}{1 - \mathbb{X}} \right)^{2/3} , \tag{82}$$

where a_K is the Kaula semi-major axis obtained from NAVSPASUR and

$$\mathbb{X} = \frac{3\, C_{20}\, (1 - \frac{3}{2} \sin^2 i'')}{4\, a_K^2\, (1 - e''^2)^{3/2}} . \tag{83}$$

SECTION 6

VARIATIONAL EQUATIONS

If an approximate or initial orbit is available for a satellite, further orbit improvement involves the application of differential correction methods. Such methods are used to improve orbital parameters in the point editing and cross-pass editing processes and will be discussed in detail in SECTION 7. Fundamental to the parameter improvement process is the evaluation of partial derivatives of $\vec{r}$ and $\dot{\vec{r}}$ with respect to those dynamic parameters being improved, e.g. orbital elements, drag coefficient, etc. In PULSAR values for these partial derivatives are obtained from the numerical integration of the variational equations.

In the following subsections the form of the variational equations used by PULSAR is developed. Also included in the last subsection is a discussion of the state transition matrix which has important applications in the point editing process and in the propagation of the state improvements (SECTION 7).

6.1 DEVELOPMENT OF THE VARIATIONAL EQUATIONS AND ASSOCIATED ANALYTICS

A mathematically rigorous method of obtaining the partial derivatives of $\vec{r}$ and $\dot{\vec{r}}$ with respect to those dynamic parameters which are being improved in the differential correction process is through the use of the variational equations. In PULSAR these equations are integrated numerically along with the equations of motion and are stored along with the ephemeris on the trajectory file. The partial derivatives obtained in this way include all of the secular and periodic variations introduced by the satellite's force environment. The variational equations and closed form analytic expressions for coefficients appearing in the equations are developed below.

6.1.1 THE VARIATIONAL EQUATIONS

The variational equations are a system of differential equations which can in general be derived from the acceleration function for the satellite. If p_K is an orbital or dynamic model parameter which is to be improved via the

6.1.1 THE VARIATIONAL EQUATIONS (con't)

differential correction process and p_{k_0} is the parameter at epoch t_0, then the acceleration function can be differentiated with respect to p_{k_0} to obtain

$$\frac{\partial \ddot{\vec{r}}}{\partial p_{k_0}} = \frac{\partial \vec{a}}{\partial \vec{r}} \frac{\partial \vec{r}}{\partial p_{k_0}} + \frac{\partial \vec{a}}{\partial \dot{\vec{r}}} \frac{\partial \dot{\vec{r}}}{\partial p_{k_0}} + \frac{\partial \vec{a}}{\partial p_{k_0}} , \tag{1}$$

where

$$\frac{\partial \vec{a}}{\partial \vec{r}} = \begin{pmatrix} \frac{\partial \ddot{x}}{\partial x} & \frac{\partial \ddot{x}}{\partial y} & \frac{\partial \ddot{x}}{\partial z} \\ \frac{\partial \ddot{y}}{\partial x} & \frac{\partial \ddot{y}}{\partial y} & \frac{\partial \ddot{y}}{\partial z} \\ \frac{\partial \ddot{z}}{\partial x} & \frac{\partial \ddot{z}}{\partial y} & \frac{\partial \ddot{z}}{\partial z} \end{pmatrix} , \tag{2}$$

$$\frac{\partial \vec{a}}{\partial \dot{\vec{r}}} = \begin{pmatrix} \frac{\partial \ddot{x}}{\partial \dot{x}} & \frac{\partial \ddot{x}}{\partial \dot{y}} & \frac{\partial \ddot{x}}{\partial \dot{z}} \\ \frac{\partial \ddot{y}}{\partial \dot{x}} & \frac{\partial \ddot{y}}{\partial \dot{y}} & \frac{\partial \ddot{y}}{\partial \dot{z}} \\ \frac{\partial \ddot{z}}{\partial \dot{x}} & \frac{\partial \ddot{z}}{\partial \dot{y}} & \frac{\partial \ddot{z}}{\partial \dot{z}} \end{pmatrix} , \tag{3}$$

$$\frac{\partial \vec{r}}{\partial p_{k_0}} = \begin{pmatrix} \frac{\partial x}{\partial p_{k_0}} \\ \frac{\partial y}{\partial p_{k_0}} \\ \frac{\partial z}{\partial p_{k_0}} \end{pmatrix} , \qquad \frac{\partial \dot{\vec{r}}}{\partial p_{k_0}} = \begin{pmatrix} \frac{\partial \dot{x}}{\partial p_{k_0}} \\ \frac{\partial \dot{y}}{\partial p_{k_0}} \\ \frac{\partial \dot{z}}{\partial p_{k_0}} \end{pmatrix} , \tag{4}$$

and

6.1.1 THE VARIATIONAL EQUATIONS (con't)

$$\frac{\partial \vec{a}}{\partial p_{k_0}} = \begin{pmatrix} \frac{\partial \ddot{x}}{\partial p_{k_0}} \\ \frac{\partial \ddot{y}}{\partial p_{k_0}} \\ \frac{\partial \ddot{z}}{\partial p_{k_0}} \end{pmatrix} \quad . \tag{5}$$

In the above expressions $\vec{a}$ represents the sum of accelerations acting upon the satellite. For the PULSAR system $\vec{a}$ is given by the right hand side of equation (1) of SECTION 5.

If one lets

$$\vec{\psi}_{p_k} = \frac{\partial \vec{r}}{\partial p_{k_0}} \tag{6}$$

represent the solution to equation (1), then it may be recast into the form of a system of inhomogeneous second order linear differential equations:

$$\ddot{\vec{\psi}}_{p_k} = \underset{\sim}{G}_1 \vec{\psi}_{p_k} + \underset{\sim}{G}_2 \dot{\vec{\psi}}_{p_k} + \underset{\sim}{G}_3 \quad , \tag{7}$$

where

$$\underset{\sim}{G}_1 = \frac{\partial \vec{a}}{\partial \vec{r}} \quad , \quad \underset{\sim}{G}_2 = \frac{\partial \vec{a}}{\partial \dot{\vec{r}}} \quad , \text{ and } \underset{\sim}{G}_3 = \frac{\partial \vec{a}}{\partial p_{k_0}} \quad . \tag{8}$$

Note that if the acceleration function does not depend explicitly upon the parameter p_k, then equation (7) reduces to a system of linear homogeneous second order equations since $\underset{\sim}{G}_3 = \underset{\sim}{0}$.

6.1.1 THE VARIATIONAL EQUATIONS (con't)

The only dynamic parameters improved by the differential correction process in PULSAR are the set of osculating orbital elements (or the associated inertial position and velocity components) and the drag factor $D = C_D A/W$, i.e.

$$p_k = \begin{cases} a \\ e \sin \omega \\ e \cos \omega \\ i \\ M + \omega \\ \Omega \\ D \end{cases} \quad \text{or} \quad \begin{cases} x \\ y \\ z \\ \dot{x} \\ \dot{y} \\ \dot{z} \\ D \end{cases} , \tag{9}$$

where a, e, i, ω, M, and Ω are the Keplerian orbital elements. Consideration of the force model used by PULSAR (SECTION 5) provides the following general expressions for the coefficient matrices $\underset{\sim}{G}_1$ and $\underset{\sim}{G}_2$, as well as the forcing term $\underset{\sim}{G}_3$:

$$\underset{\sim}{G}_1 = \frac{\partial \vec{a}}{\partial \vec{r}} E + \frac{\partial \vec{a}}{\partial \vec{r}} D + \frac{\partial \vec{a}}{\partial \vec{r}} \text{moon} + \frac{\partial \vec{a}}{\partial \vec{r}} \text{sun} , \tag{10}$$

$$\underset{\sim}{G}_2 = \frac{\partial \vec{a}}{\partial \dot{\vec{r}}} D , \tag{11}$$

and

$$\underset{\sim}{G}_3 = \begin{cases} \dfrac{\partial \vec{a}}{\partial D} D & \text{for } p_k = D = C_D A/W \\ \underset{\sim}{0} & \text{for } p_k = \text{element set.} \end{cases} \tag{12}$$

6.1.2 CLOSED FORM EXPRESSIONS FOR $\underset{\sim}{G}_1$, $\underset{\sim}{G}_2$, and $\underset{\sim}{G}_3$

The coefficient matrices $\underset{\sim}{G}_1$ and $\underset{\sim}{G}_2$, as well as the forcing term $\underset{\sim}{G}_3$, can be expressed in closed form from consideration of the explicit representations of the accelerations contributing to the force model (SECTION 5). In the subsections below, closed form expressions are obtained for each of the terms on the right hand sides of equations (10) - (12) above. These results can be summed to give closed form expressions for the $\underset{\sim}{G}$ matrices.

6.1.2.1 Position Derivatives of the Geopotential Acceleration: $\frac{\partial \vec{a}}{\partial \vec{r}} E$

Let $\vec{\nabla}_I$ and $\vec{\nabla}_e$ be gradient operators in the inertial and earth-fixed reference frames, respectively. These operators are related by the following transformation:

$$\vec{\nabla}_I = (\underset{\sim}{B}\,\underset{\sim}{C}\,\underset{\sim}{D})^{-1}\,\vec{\nabla}_e \tag{13}$$

where $\underset{\sim}{B}\ \underset{\sim}{C}\ \underset{\sim}{D}$ are the transformations described in SECTION 2 and the gradient operators expressed in matrix notation have the form

$$\vec{\nabla}_j = \begin{pmatrix} \frac{\partial}{\partial x_j} \\ \frac{\partial}{\partial y_j} \\ \frac{\partial}{\partial z_j} \end{pmatrix}, \quad (j = I, e). \tag{14}$$

From equation (2) one sees that

$$\frac{\partial \vec{a}}{\partial \vec{r}} E = \begin{pmatrix} \vec{\nabla}_I^T a_{E_x} \\ \vec{\nabla}_I^T a_{E_y} \\ \vec{\nabla}_I^T a_{E_z} \end{pmatrix} = \begin{pmatrix} \vec{\nabla}_e^T a_{E_x} \\ \vec{\nabla}_e^T a_{E_y} \\ \vec{\nabla}_e^T a_{E_z} \end{pmatrix} \left[(\underset{\sim}{B}\,\underset{\sim}{C}\,\underset{\sim}{D})^{-1}\right]^T, \tag{15}$$

6.1.2.1 Position Derivatives of the Geopotential Acceleration: $\frac{\partial \vec{a}}{\partial \vec{r}} E$ (con't)

where the superscript T means matrix transposition. Applying equation (8) of SECTION 5 to the last expression gives

$$\frac{\partial \vec{a}}{\partial \vec{r}} E = (\underset{\sim}{B}\,\underset{\sim}{C}\,\underset{\sim}{D})^{-1} \sum_{\substack{n=0 \\ n\neq 1}}^{\infty} \sum_{m=0}^{n} \left[C_{nm} \begin{pmatrix} \vec{\nabla}_e^{\,T} (\vec{\nabla}_e U_n^m)_x \\ \vec{\nabla}_e^{\,T} (\vec{\nabla}_e U_n^m)_y \\ \vec{\nabla}_e^{\,T} (\vec{\nabla}_e U_n^m)_z \end{pmatrix} + S_{nm} \begin{pmatrix} \vec{\nabla}_e^{\,T} (\vec{\nabla}_e V_n^m)_x \\ \vec{\nabla}_e^{\,T} (\vec{\nabla}_e V_n^m)_y \\ \vec{\nabla}_e^{\,T} (\vec{\nabla}_e V_n^m)_z \end{pmatrix} \right] \left[(\underset{\sim}{B}\,\underset{\sim}{C}\,\underset{\sim}{D})^{-1} \right]^T . \tag{16}$$

Using equations (13) - (14) from SECTION 5, it is seen that

$$\begin{pmatrix} \vec{\nabla}_e^{\,T} (\vec{\nabla}_e U_n^m)_x \\ \vec{\nabla}_e^{\,T} (\vec{\nabla}_e U_n^m)_y \\ \vec{\nabla}_e^{\,T} (\vec{\nabla}_e U_n^m)_z \end{pmatrix} = \frac{1}{2a_e} \begin{pmatrix} A_n^m \, \vec{\nabla}_e^{\,T} U_{n+1}^{m-1} - \vec{\nabla}_e^{\,T} U_{n+1}^{m+1} \\ -A_n^m \, \vec{\nabla}_e^{\,T} V_{n+1}^{m-1} - \vec{\nabla}_e^{\,T} V_{n+1}^{m+1} \\ -2(n-m+1)\, \vec{\nabla}_e^{\,T} U_{n+1}^m \end{pmatrix}, \tag{17}$$

and

6.1.2.1 Position Derivatives of the Geopotential Acceleration: $\frac{\partial \vec{a}_E}{\partial \vec{r}}$ (con't)

$$\begin{pmatrix} \vec{\nabla}_e^T (\vec{\nabla}_e V_n^m)_x \\ \vec{\nabla}_e^T (\vec{\nabla}_e V_n^m)_y \\ \vec{\nabla}_e^T (\vec{\nabla}_e V_n^m)_z \end{pmatrix} = \frac{1}{2a_e} \begin{pmatrix} A_n^m \vec{\nabla}_e^T V_{n+1}^{m-1} - \vec{\nabla}_e^T V_{n+1}^{m+1} \\ A_n^m \vec{\nabla}_e^T U_{n+1}^{m-1} + \vec{\nabla}_e^T U_{n+1}^{m+1} \\ -2(n-m+1) \vec{\nabla}_e^T V_{n+1}^m \end{pmatrix}, \qquad (18)$$

where

$$A_n^m = (n - m + 1)(n - m + 2) \quad . \qquad (19)$$

The gradients of the U_i^j and V_i^j terms in the right hand sides of equation (17) - (18) above are themselves computed from equations (13) - (14) of SECTION 5.

6.1.2.2 Position Derivatives of the Atmospheric Drag Acceleration: $\frac{\partial \vec{a}_D}{\partial \vec{r}}$

From equation (16) SECTION 5, it is seen that

$$\frac{\partial \vec{a}_D}{\partial \vec{r}} = -\frac{1}{2} D_g \left[\frac{\partial \rho}{\partial \vec{r}} v v + \rho \frac{\partial v}{\partial \vec{r}} v + \rho v \frac{\partial \vec{v}}{\partial \vec{r}} \right] \quad . \qquad (20)$$

Consider the first partial derivative on the right hand side of the last equation:

$$\frac{\partial \rho}{\partial \vec{r}} = \frac{\partial \rho}{\partial h} \frac{\partial h}{\partial \vec{r}} \quad . \qquad (21)$$

From equation (19) of SECTION 5, one finds that

6.1.2.2 Position Derivatives of the Atmospheric Drag Acceleration: $\frac{\partial \vec{a}_D}{\partial \vec{r}}$ (con't)

$$\frac{\partial \rho}{\partial h} = \rho \left[C_1 - \frac{1}{2} \frac{2C_3 h + C_4}{(C_3 h^2 + C_4 h - C_5)^{1/2}} \right] . \qquad (22)$$

Equation (20) of SECTION 5 may be rewritten as

$$h = r \left\{ 1 - \frac{a_e}{\left[r^2 + \left(\frac{\varepsilon^2}{1 - \varepsilon^2} \right) x_3^2 \right]^{1/2}} \right\} , \qquad (23)$$

where a_e is the semi major axis of the reference ellipsoid, ε is the earth's eccentricity and r is the magnitude of the satellite inertial position vector. Note that the notation $(x_1, x_2, x_3) = (x, y, z)$ has been adopted.

Taking the partial derivative of h with respect to the i^{th} position component and rearranging results gives

$$\frac{\partial h}{\partial X_i} = \frac{X_i}{r^2} \left[h + \frac{(r - h)^3}{a_e^2} + \frac{(r - h)^3 e^2}{a_e^2 (1 - e^2)} \delta_{i3} \right] , \qquad (24)$$

where δ_{i3} is the Kronecker delta. This result may be expressed more generally as

$$\frac{\partial h}{\partial \vec{r}} = \frac{1}{r^2} \left\{ \left[h + \frac{(r - h)^3}{a^2_e} \right] \vec{r}^T + \frac{(r - h)^3 e^2}{a_e^2 (1 - e^2)} \left(\vec{r}^T \hat{e}_3 \right) \hat{e}_3^T \right\} , \qquad (25)$$

6.1.2.2 Position Derivatives of the Atmospheric Drag Acceleration: $\frac{\partial \vec{a}_D}{\partial \vec{r}}$ (con't)

where $\hat{e}_3$ is the unit vector along the inertial x_3 axis.

Consider now the second partial derivative on the right hand side of equation (20). Since

$$v = |\vec{v}| = (\vec{v}^{\,T}\,\vec{v})^{\frac{1}{2}} \quad , \tag{26}$$

then by taking the partial derivative of equation (26) with respect to the i^{th} position component, one obtains

$$\frac{\partial v}{\partial x_i} = \frac{\vec{v}^T}{v}\,\frac{\partial \vec{v}}{\partial x_i} \quad , \tag{27}$$

or more generally

$$\frac{\partial v}{\partial \vec{r}} = \frac{\vec{v}^{\,T}}{v}\,\frac{\partial \vec{v}}{\partial \vec{r}} \quad . \tag{28}$$

An expression for $\frac{\partial \vec{v}}{\partial \vec{r}}$ is now needed. Once this is obtained, both equation (28) and the third partial derivative on the right hand side of equation (20) will be known in closed form.

The velocity of the satellite relative to the rotating atmosphere is given in Section 5 by equations (17) - (18). Thus the relative velocity's i^{th} component is given by

.2.2 Position Derivatives of the Atmospheric Drag Acceleration: $\frac{\partial \vec{a}_D}{\partial \vec{r}}$ (con't)

$$v_i = \dot{x}_i - (\vec{\omega} \times \vec{r})_i = \dot{x}_i - \sum_{\substack{j=1 \\ k=1}}^{3} \varepsilon_{ijk}\ \omega_j\ x_k \quad (i = 1,2,3)\ , \tag{29}$$

re ε_{ijk} is the Levi-Civita density defined by

$$\varepsilon_{ijk} = \begin{cases} 0 \text{ if any index is equal to any other index} \\ +1 \text{ if } i, j, k \text{ form an even permutation of } 1, 2, 3 \\ -1 \text{ if } i, j, k \text{ form an odd permutation of } 1, 2, 3\ . \end{cases} \tag{30}$$

ing the partial derivative of equation (29) with respect to the ℓ^{th}
ition component gives

$$\frac{\partial v_i}{\partial x_\ell} = \frac{\partial \dot{x}_i}{\partial x_\ell} - \sum_{\substack{j=1 \\ k=1}}^{3} \varepsilon_{ijk}\ \omega_j\ \frac{\partial x_k}{\partial x_\ell} = - \sum_{\substack{j=1 \\ k=1}}^{3} \varepsilon_{ijk}\ \omega_j\ \delta_{k\ell}\ , \tag{31}$$

$$\frac{\partial v_i}{\partial x_\ell} = - \sum_{j=1}^{3} \varepsilon_{ij\ell}\ \omega_j\ . \tag{32}$$

ese results may be collected to give the desired closed form result:

6.1.2.2 Position Derivatives of the Atmospheric Drag Acceleration: $\frac{\partial \vec{a}_D}{\partial \vec{r}}$ (con't)

$$\left(\frac{\partial \vec{a}_D}{\partial \vec{r}}\right)_{ij} = \frac{\partial (\vec{a}_D)_i}{\partial X_j} = -\frac{1}{2} Dg \left\{ \left(\frac{\partial \rho}{\partial h}\right) \frac{v}{r^2} v_i X_j \left[h + \frac{(r-h)^3}{a_e^2} + \frac{(r-h)^3 \varepsilon^2}{a_e^2 (1-\varepsilon^2)} \delta_{j3} \right] + \frac{\rho}{v} v_i \sum_k v_k \frac{\partial v_k}{\partial X_j} + \rho v \frac{\partial v_i}{\partial X_j} \right\}, \quad (33)$$

where the position derivatives of velocity are given by equation (32).

6.1.2.3 Position Derivatives of the Luni-Solar Gravitational Accelerations: $\frac{\partial \vec{a}_\ell}{\partial \vec{r}}$, ($\ell$ = sun, moon)

The luni-solar gravitational acceleration is given by equation (26) in SECTION 5. Taking the partial derivative if the i^{th} acceleration component with respect to the j^{th} position component gives

$$\frac{\partial (\vec{a}_\ell)_i}{\partial X_j} = -\mu_\ell \frac{\partial}{\partial X_j} \left\{ \frac{(X_i - X_{\ell_i})}{\left[\sum_{k=1}^{3} (X_k - X_{\ell_k})^2\right]^{3/2}} + \frac{X_{\ell_i}}{\left[\sum_k X_{\ell_k}^2\right]^{3/2}} \right\}, \quad (\ell = \text{sun, moon}). \quad (34)$$

i.e.

$$r_\ell = \left[\sum_{k=1}^{3} (X_k - X_{\ell_k})^2\right]^{1/2} \quad (35)$$

7.1.1 APPLICATION TO THE POINT EDITING PROCESS (con't)

pass normal equations for the parameter corrections are outined in SECTION 9.

7.1.1.1 Computed Observations and Observation Partial Derivatives

It can be seen from equations (14) - (15) that in order to form the $\underset{\sim}{B}$ and $\underset{\sim}{E}$ matrices, one must not only be able to provide computed values for the observations to be processed, but one must also be able to form the matrix of data partial derivatives with respect to the parameters to be improved. Furthermore, it may be necessary to correct the computed observations for effects introduced by variable attitude and displacement of the transmitting antennae from the center of mass. The computed observations must also be corrected for tropospheric refraction, antenna rotation and general relativistic effects. Details concerning the observation corrections can be found in SECTION 4. The time associated with each observation has previously been corrected for transmission delay and clock errors before the observations are edited by the point editor.

The data processed by the point editor are range difference observations. A computed value for the i^{th} range difference point is obtained from

$$C_i = \mathcal{D}(p_j, t_i) - \mathcal{D}(p_j, t_{i-1}) + \delta\Delta R_i, \tag{16}$$

where

$$\mathcal{D}(p_j, t) = |\vec{\rho}| - \frac{C}{f_0} f_b (t - t_1) - \frac{C}{2f_0} \dot{f}_b (t - t_1)^2 + (1 + C_R)\Delta f_R , \tag{17}$$

and $\delta\Delta R_i$ is the correction for antenna rotation which is discussed in SECTION 4. It is considered here as a correction to the observed range difference, but has been added to the computed range difference for convenience. Consequently, its partial derivatives will vanish when forming the $\underset{\sim}{a}$ matrix [equation (19)].

Since $|\Delta\vec{r}_A|$ is small, one may Taylor expand the exact expression for $|\vec{\rho}|$ given by

$$|\vec{\rho}| = \left\{ 1 + \frac{\Delta\rho_{GR}}{|\vec{r}(t_e) - \vec{r}_s(t_R) + \Delta\vec{r}_A(t_e)|} \right\} \left| \vec{r}(t_e) - \vec{r}_s(t_R) + \Delta\vec{r}_A(t_e) \right|$$

THE METHOD OF WEIGHTED LEAST SQUARES (con't)

$$\underset{\sim}{B} = \underset{\sim}{a}^T \underset{\sim}{W} \underset{\sim}{a} \quad , \text{ and} \tag{14}$$

$$\underset{\sim}{E} = \underset{\sim}{a}^T \underset{\sim}{W} (\underset{\sim}{O} - \underset{\sim}{C}) \quad . \tag{15}$$

.1 APPLICATION TO THE POINT EDITING PROCESS

PULSAR applications a pass of tracking data for a given satellite is ined to be the set of observations made by a single tracking station during of its satellite-station inview periods for the satellite. Since all ob- vations in a given pass are not necessarily of equivalent accuracy, it is essary to identify observations which are inconsistent with other observa- ons in the same pass so they will not corrupt results obtained by any post- SAR processing of the observation data. This identification procedure is formed by PULSAR's point editing process.

e point editor processes observations on a pass-by-pass basis by fitting e satellite's orbit to a pass of data using the method of weighted least uares. The resulting fitting parameter improvements Δp are used to adjust e observation residuals $O - C$. The quality of the adjusted residuals is sessed and if the quality of certain of them is not acceptable, those servations are tagged as outliersand they are not used in the formation the normal equations for the next iteration of the associated differential rrection process. However, the quality of the residuals associated with e tagged observations are assessed during each iteration of the correction ocess and if their quality is found to be acceptable during these iterations e data points are untagged and used in the formation of the normal equations subsequent iterations of the differential correction process.

this subsection only the underlying mathematics used in forming the pass rmal equations and the associated differential correction process are dis- ssed. The statistical methods used to assess the quality of the observations d the criteria used to define the iterative convergence conditions are dressed in SECTION 8. The numerical techniques used in the solution of the

7.1 THE METHOD OF WEIGHTED LEAST SQUARES (con't)

confidence levels between the various observations, as well as possible inter-relationships between the observation errors). This statement is equivalent to a weighted least squares minimization procedure, i.e. find the value of $\langle \underset{\sim}{\Delta p} \rangle$ which will minimize the functional J given by

$$J(\langle \underset{\sim}{\Delta p} \rangle) = \left[(\underset{\sim}{O} - \underset{\sim}{C}) - \underset{\sim}{a} \langle \underset{\sim}{\Delta p} \rangle \right]^T \underset{\sim}{W} \left[(\underset{\sim}{O} - \underset{\sim}{C}) - \underset{\sim}{a} \langle \underset{\sim}{\Delta p} \rangle \right], \tag{9}$$

where $\underset{\sim}{W}$ is an M X M symmetric, positive definite weighting matrix which is assumed to be known. Taking the variation of J with respect to $\langle \underset{\sim}{\Delta p} \rangle$ gives

$$\begin{aligned} \delta J &= -\delta \langle \underset{\sim}{\Delta p} \rangle^T \underset{\sim}{a}^T \underset{\sim}{W} \left[(\underset{\sim}{O} - \underset{\sim}{C}) - \underset{\sim}{a} \langle \underset{\sim}{\Delta p} \rangle \right] - \left[(\underset{\sim}{O} - \underset{\sim}{C}) - \underset{\sim}{a} \langle \underset{\sim}{\Delta p} \rangle \right]^T \underset{\sim}{W} \underset{\sim}{a} \delta \langle \underset{\sim}{\Delta p} \rangle \\ &= 2\delta \langle \underset{\sim}{\Delta p} \rangle^T \underset{\sim}{a}^T \underset{\sim}{W} \left[(\underset{\sim}{O} - \underset{\sim}{C}) - \underset{\sim}{a} \langle \underset{\sim}{\Delta p} \rangle \right] , \end{aligned} \tag{10}$$

provided that $\underset{\sim}{W} = \underset{\sim}{W}^T$. If the above equation is to be an extremum, it must be zero. Since the variation $\delta \langle \underset{\sim}{\Delta p} \rangle$ is completely arbitrary, one has

$$\underset{\sim}{a}^T \underset{\sim}{W} \left[(\underset{\sim}{O} - \underset{\sim}{C}) - \underset{\sim}{a} \langle \underset{\sim}{\Delta p} \rangle \right] = \underset{\sim}{\emptyset} , \tag{11}$$

or

$$(\underset{\sim}{a}^T \underset{\sim}{W} \underset{\sim}{a}) \langle \underset{\sim}{\Delta p} \rangle = \underset{\sim}{a}^T \underset{\sim}{W} (\underset{\sim}{O} - \underset{\sim}{C}). \tag{12}$$

This equation is referred to as the normal equation for the weighted least squares problem. In subsequent sections the best estimate notation will be suppressed and the normal equations will be written as

$$\underset{\sim}{B} \underset{\sim}{\Delta p} = \underset{\sim}{E} , \tag{13}$$

where it is understood that $\underset{\sim}{\Delta p}$ is the "best estimate" in the weighted least squares sense and $\underset{\sim}{B}$ and $\underset{\sim}{E}$ are given by

7.1 THE METHOD OF WEIGHTED LEAST SQUARES (con't)

Retaining only the linear terms, one then has for the i^{th} observation

$$(O - C)_i \cong \sum_{j=1}^{N} \frac{\partial D(p_j, t_i)}{\partial p_j} \Bigg|_{p_j = p^\circ_j} (p_j - p^\circ_j) + \varepsilon_i \quad . \tag{6}$$

For all M observations the following matrix equation may be written:

$$\underset{\sim}{(O - C)} = \underset{\sim}{a}\,\underset{\sim}{\Delta p} + \underset{\sim}{\varepsilon} \quad , \tag{7}$$

where $\underset{\sim}{(O - C)}$ is the M X 1 residual matrix, $\underset{\sim}{a}$ is the M X N matrix of partial derivatives of the observations with respect to the unknown parameters p_j, $\underset{\sim}{\Delta p}$ is the N X 1 matrix of parameter corrections, and $\underset{\sim}{\varepsilon}$ is the M X 1 matrix of random errors.

As a result of the last expression, the orbit estimation problem may be restated as: given the matrix of observation residuals $\underset{\sim}{(O - C)}$ and the matrix $\underset{\sim}{a}$, find the "best estimate" of $\underset{\sim}{\Delta p}$, i.e. $\langle \underset{\sim}{\Delta p} \rangle$. Once $\langle \underset{\sim}{\Delta p} \rangle$ is known, the "best estimate" of the unknown parameters p_j, i.e. $\langle p_j \rangle$ is obtained from

$$\langle p_j \rangle = p^\circ_j + \langle \Delta p_j \rangle \quad , \quad j = 1, 2, \ldots, N. \tag{8}$$

It should be noted that since the estimation problem has been linearized (i.e. only the n = 1 term retained in equation (5)), equation (7) may have to be solved many times (in the iterative sense) to obtain a solution to the nonlinear problem. The method of nonlinear least square curve fitting is called differential correction.

The "best estimate" in the least squares sense will be that particular set of values $\langle \underset{\sim}{\Delta p} \rangle$ which minimizes the weighted sum of squares of the elements of the residual matrix (weighting is used to account for the difference in

7.1 THE METHOD OF WEIGHTED LEAST SQUARES (con't)

$$O_i = y(t_i) + \varepsilon_i \quad , \tag{2}$$

where the quantity ε_i represents the error associated with the i^{th} observation. It should be noted that it is assumed that no errors exist in the time t_i at which a particular observation is being made.

In general $\mathcal{D}(pj, t)$ is nonlinear in the parameters pj. Even though particular nonlinear functional forms could be applied to specific cases, it is desirable to obtain a method which is applicable in the general case. To facilitate this suppose it is known that the true values of the pj lie close to some prescribed set $p\overset{\circ}{j}$. Then the values

$$C_i = \mathcal{D}(p\overset{\circ}{j}, t_i) \tag{3}$$

can be computed. The observation residual for the i^{th} observation can be formed by differencing equations (2) - (3) to give the observation residual

$$(O - C)_i = O_i - C_i = \mathcal{D}(pj, t_i) - \mathcal{D}(p\overset{\circ}{j}, t_i) + \varepsilon_i \quad . \tag{4}$$

It should be noted that the observation residual is still corrupted by the errors arising from the observation technique.

Expanding the right hand side of the last equation in a Taylor series about $p\overset{\circ}{j}$ gives

$$(O - C)_i = \mathcal{D}(p\overset{\circ}{j}, t_i) + \sum_{n=1}^{\infty} \left(\frac{1}{n!}\right) \sum_{j=1}^{N} \frac{\partial^n \mathcal{D}(pj, t_i)}{\partial pj^n} \Bigg|_{pj = p\overset{\circ}{j}} \cdot$$

$$(pj - p\overset{\circ}{j})^n + \varepsilon_i - \mathcal{D}(p\overset{\circ}{j}, t_i). \tag{5}$$

SECTION 7

STATE ESTIMATION AND PARAMETER IMPROVEMENT

Since a very large number of observational measurements of an earth satellite's position and velocity are usually available, the satellite orbital state estimation problem is generally highly over-determined. This remains true even when various modeling parameters (e.g. drag coefficient, station parameters, etc.) are introduced into the problem. As a result, the state estimation process is very effective, since it can be supported by least squares estimation methods which also permit a statistical interpretation of the orbit.

In the following subsections the method of weighted least squares is discussed and the associated normal equations are developed. These results are then applied in a description of the processing which is utilized by both the point editor and cross pass editor of PULSAR. Also included is a brief discussion concerning the state improvement propagation technique used in PULSAR.

7.1 THE METHOD OF WEIGHTED LEAST SQUARES

The fundamental orbit estimation process is that of solving for a set of observation model parameters Xj in such a manner that the constrained, weighted sum of the squares of the differences between the observation model and the observed trajectory is minimized. To initiate the development of the mathematics related to the orbit estimation problem consider an arbitrary curve in space which is described by

$$y(t) = \mathcal{D}(p_1, p_2, \ldots, p_N, t) = \mathcal{D}(pj, t) \qquad (1)$$

where the pj ($j = 1, 2, \ldots, N$) are as yet unspecified parameters. Assume at the times t_i ($i = 1, 2, \ldots, M$; $M > N$) observations are made of $y(t_i)$. In general the true value of $y(t_i)$ will be corrupted by errors arising from the observation techniques, so that the observation at time t_i and denoted by O_i is

6.2 THE STATE TRANSITION MATRIX (con't)

The matrix $\underset{\sim}{\Phi}^{-1}_{t_0}(t_1)\ \underset{\sim}{\Phi}_{t_1}(t_1)$ is referred to as the state transition matrix, since it enables the variational equation solutions referenced to one epoch, say t_0, to be transformed to another reference epoch t_1.

6.2 THE STATE TRANSITION MATRIX (con't)

$p_k(t_0)$ refers to the orbit elements at epoch t_0. Thus one may write for the general solution

$$\underset{\sim}{\Psi}_{p_k(t_1)}(t) = \underset{\sim}{\Phi}_{t_0}(t)\,\underset{\sim}{K} \quad , \tag{61}$$

where

$$\underset{\sim}{\Phi}_{t_0}(t) = \left(\underset{\sim}{\Psi}_{p_1(t_0)}(t) \quad \underset{\sim}{\Psi}_{p_2(t_0)}(t) \quad \underset{\sim}{\Psi}_{p_3(t_0)}(t) \quad \underset{\sim}{\Psi}_{p_4(t_0)}(t) \quad \underset{\sim}{\Psi}_{p_5(t_0)}(t) \quad \underset{\sim}{\Psi}_{p_6(t_0)}(t)\right). \tag{62}$$

Solving for $\underset{\sim}{K}$ at $t = t_1$ gives

$$\underset{\sim}{K} = \underset{\sim}{\Phi}^{-1}_{t_0}(t_1)\;\underset{\sim}{\Psi}_{p_k(t_1)}(t_1) \quad , \tag{63}$$

so that equation (61) becomes

$$\underset{\sim}{\Psi}_{p_k(t_1)}(t) = \underset{\sim}{\Phi}_{t_0}(t)\;\underset{\sim}{\Phi}^{-1}_{t_0}(t_1)\;\underset{\sim}{\Psi}_{p_k(t_1)}(t_1) \quad . \tag{64}$$

This expression may be generalized so that the solutions for all orbit parameters p_k can be transformed simultaneously by using the form of equation (62) in the last expression to obtain

$$\underset{\sim}{\Phi}_{t_1}(t) = \underset{\sim}{\Phi}_{t_0}(t)\;\underset{\sim}{\Phi}^{-1}_{t_0}(t_1)\;\underset{\sim}{\Phi}_{t_1}(t_1) \quad . \tag{65}$$

Equations (43) - (54) are used to evaluate $\underset{\sim}{\Psi}_{p_k(t_1)}(t_1)$ and $\underset{\sim}{\Phi}_{t_1}(t_1)$.

6.1.3 INITIAL CONDITION PARTIAL DERIVATIVES: $\vec{\psi}_{p_k}$, $\dot{\vec{\psi}}_{p_k}$ (con't)

$$\vec{\psi}_D = \vec{0}$$

and (57)

$$\dot{\vec{\psi}}_D = \vec{0} \quad .$$

6.2 THE STATE TRANSITION MATRIX

It is necessary to develop a set of orbit parameter transformations which can be used to change the epoch of the p_{k_0} of the variational equation solutions from the trajectory epoch t_0 to the new epoch t_1. To facilitate this one can write equation (7) in a more convenient form. If one lets

$$\underset{\sim}{\Psi}_{p_k}(t) = \begin{pmatrix} \vec{\psi}_{p_k}(t) \\ \dot{\vec{\psi}}_{p_k}(t) \end{pmatrix} \quad , \tag{58}$$

then equation (7) becomes

$$\dot{\underset{\sim}{\Psi}}_{p_k}(t) = \underset{\sim}{\Gamma}(t) \; \underset{\sim}{\Psi}_{p_k}(t) + \underset{\sim}{\Lambda}(t) \quad , \tag{59}$$

where

$$\underset{\sim}{\Gamma}(t) = \begin{pmatrix} \underset{\sim}{0} & \underset{\sim}{I} \\ \underset{\sim}{G}_1 & \underset{\sim}{G}_2 \end{pmatrix} \quad \text{and} \quad \underset{\sim}{\Lambda}(t) = \begin{pmatrix} \underset{\sim}{0} \\ \underset{\sim}{G}_3 \end{pmatrix} \quad . \tag{60}$$

When p_k is an orbit parameter, the variational equation is homogeneous in form and its general solution in terms of orbit elements at some epoch t_1, denoted by $\underset{\sim}{\Psi}_{p_k(t_1)}(t)$, is a linear combination of the $\underset{\sim}{\Psi}_{p_k(t_0)}(t)$, where the subscript

6.1.3 INITIAL CONDITION PARTIAL DERIVATIVES: $\vec{\psi}_{p_k}$, $\dot{\vec{\psi}}_{p_k}$ (con't)

$$\dot{\vec{\psi}}_{M+\omega} = -n\left(\frac{a}{r}\right)^3 \vec{r} \quad , \tag{53}$$

and

$$\dot{\vec{\psi}}_{\Omega} = \begin{pmatrix} -\dot{y} \\ \dot{x} \\ 0 \end{pmatrix} \quad , \tag{54}$$

where E is the eccentric anomaly and

$$\begin{aligned} n &= \left(\frac{\mu}{a^3}\right)^{1/2} \\ \gamma &= (1 - e^2)^{1/2} \\ p &= a(1 - e^2) \quad . \end{aligned} \tag{55}$$

It should be noted that if position and velocity are used instead of orbital elements, then the initial conditions are given by

$$\vec{\psi}_i = \begin{pmatrix} \delta_{ix} \\ \delta_{iy} \\ \delta_{iz} \end{pmatrix} \quad \text{and} \quad \dot{\vec{\psi}}_j = \begin{pmatrix} \delta_{j\dot{x}} \\ \delta_{j\dot{y}} \\ \delta_{j\dot{z}} \end{pmatrix} \quad , \tag{56}$$

where $\delta_{i\alpha}$ is the Kronecker delta, i = x, y, z and j = $\dot{x}$, $\dot{y}$, $\dot{z}$.

To facilitate integration of the inhomogeneous form of the variational equations, the following conditions are imposed at the integration epoch for p_k = D:

6.1.3 INITIAL CONDITION PARTIAL DERIVATIVES: $\vec{\psi}_{p_k}$, $\dot{\vec{\psi}}_{p_k}$ (con't)

$$\vec{\psi}_{M+\omega} = \frac{1}{n}\dot{\vec{r}} \quad , \tag{47}$$

$$\vec{\psi}_{\Omega} = \begin{pmatrix} -y \\ X \\ 0 \end{pmatrix} \quad , \tag{48}$$

$$\dot{\vec{\psi}}_{a} = -\frac{1}{2}\frac{\dot{\vec{r}}}{a} \quad , \tag{49}$$

$$\dot{\vec{\psi}}_{e\sin\omega} = \frac{n}{\gamma^2}\left(\frac{a}{r}\right)^2\left[\left(\frac{p}{r} + e\cos E\right)\cos(\omega + E) - e\cos\omega\left(\frac{e^2\cos^2 E + \gamma}{1+\gamma}\right)\right]\vec{r} + \frac{1}{\gamma^2}\left[\sin(\omega+E) - e\cos\omega\left(\frac{e\sin E}{1+\gamma}\right)\right]\dot{\vec{r}} \quad , \tag{50}$$

$$\dot{\vec{\psi}}_{e\cos\omega} = \frac{n}{\gamma^2}\left(\frac{a}{r}\right)^2\left[-\left(\frac{p}{r} + e\cos E\right)\sin(\omega+E) + e\sin\omega\left(\frac{e^2\cos^2 E+\gamma}{1+\gamma}\right)\right]\cdot$$

$$\vec{r} + \frac{1}{\gamma^2}\left[\cos(\omega+E) + e\sin\omega\left(\frac{e\sin E}{1+\gamma}\right)\right]\dot{\vec{r}} \quad , \tag{51}$$

$$\dot{\vec{\psi}}_{i} = \begin{pmatrix} \dot{z}\sin\Omega \\ -\dot{z}\cos\Omega \\ \dot{y}\cos\Omega - \dot{x}\sin\Omega \end{pmatrix} \quad , \tag{52}$$

6.1.3 INITIAL CONDITION PARTIAL DERIVATIVES: $\vec{\psi}_{p_k}$, $\dot{\vec{\psi}}_{p_k}$.

In order to integrate the variational equations, one must have initial conditions for the $\vec{\psi}_{p_k}$ and $\dot{\vec{\psi}}_{p_k}$ vectors. These are obtained for the orbital elements by evaluating the following closed form expressions at the integration epoch. Since the derivatives of these relations have been developed elsewhere[1], only the results will be given here:

$$\vec{\psi}_a = \frac{\vec{r}}{a} \quad , \tag{43}$$

$$\vec{\psi}_{e\sin\omega} = -\frac{1}{\gamma^2}\left[\sin(\omega+E) + e\sin\omega - e\cos\omega\,\frac{e\sin E}{1+\gamma}\right]\vec{r} +$$

$$\frac{1}{n}\left[-\left(1+\frac{r}{p}\right)\cos(\omega+E) + \frac{r}{p}\,e\cos\omega\,\frac{(e\cos E+\gamma)}{1+\gamma}\right]\dot{\vec{r}}, \tag{44}$$

$$\vec{\psi}_{e\cos\omega} = -\frac{1}{\gamma^2}\left[\cos(\omega+E) + e\cos\omega + e\sin\omega\,\frac{e\sin E}{1+\gamma}\right]\vec{r} +$$

$$\frac{1}{n}\left[\left(1+\frac{r}{p}\right)\sin(\omega+E) - \frac{r}{p}\,e\sin\omega\,\frac{(e\cos E+\gamma)}{1+\gamma}\right]\dot{\vec{r}}\,, \tag{45}$$

$$\vec{\psi}_i = \begin{pmatrix} z\sin\Omega \\ -z\cos\Omega \\ y\cos\Omega - x\sin\Omega \end{pmatrix} . \tag{46}$$

---

[1] Hubbard, E. C., Orbit Elements Determinate At Zero Eccentricity, NWL Technical Memorandum No. K - 26/63, Dahlgren, Virginia, 1963.

6.1.2.3 Velocity Derivatives of the Atmospheric Drag Acceleration: $\frac{\partial \vec{a}}{\partial \dot{\vec{r}}} D$ (con't)

Using equation (26), one sees that

$$\frac{\partial v}{\partial \dot{\vec{r}}} = \frac{\vec{v}^{\,T}}{v} \frac{\partial \vec{v}}{\partial \dot{\vec{r}}} , \tag{39}$$

where $\vec{v}$ is given by equation (29). Taking the partial derivative of equation (29) with respect to the ℓ^{th} velocity component gives

$$\frac{\partial v_i}{\partial \dot{X}_\ell} = \frac{\partial \dot{X}_i}{\partial \dot{X}_\ell} - \sum_{jk} \varepsilon_{ijk} \omega_j \frac{\partial X_k}{\partial \dot{X}_\ell} = \delta_{i\ell} . \tag{40}$$

Collecting these results gives the desired closed form result:

$$\left(\frac{\partial \vec{a}}{\partial \dot{\vec{r}}} D\right)_{ij} = \frac{\partial (\vec{a}_D)_i}{\partial \dot{X}_j} = - \frac{1}{2} D g \left(\frac{\rho}{v}\right) \left[v_i v_j + v^2 \delta_{ij} \right] . \tag{41}$$

6.1.2.5 Partial Derivative of Atmospheric Drag Acceleration with Respect to the Drag Coefficient: $\frac{\partial \vec{a}}{\partial D} D$

To obtain an expression for this forcing term, one merely differentiates equation (16) of SECTION 5 with respect to the drag coefficient D to obtain

$$\frac{\partial \vec{a}}{\partial D} D = - \frac{1}{2} g \rho v \vec{v} , \tag{42}$$

where $\vec{v}$ is given in SECTION 5 by equations (17) - (18).

6.1.2.3 Position Derivatives of the Luni-Solar Gravitational Accelerations: $\frac{\partial \vec{a}_\ell}{\partial \vec{r}}$, ($\ell$ = sun, moon) (con't)

one finds that equation (34) becomes

$$\frac{\partial(\vec{a}_\ell)_i}{\partial X_j} = \frac{-\mu_\ell}{\eta_\ell^5}\left\{\eta_\ell^2\ \delta_{ij} - 3(X_i - X_{\ell_i})\ (X_j - X_{\ell_j})\right\}\ ,\quad (\ell=\text{sun, moon}) \qquad (36)$$

where δ_{ij} is the Kronecker delta and i, j = 1, 2, 3. Putting this result in the form of equation (2) gives:

$$\frac{\partial \vec{a}_\ell}{\partial \vec{r}} = \frac{-\mu_\ell}{\eta_\ell^5}\begin{pmatrix} \eta_\ell^2 - 3(X_1 - X_{\ell_1})^2 & -3(X_1 - X_{\ell_1})(X_2 - X_{\ell_2}) & -3(X_1 - X_{\ell_1})(X_3 - X_{\ell_3}) \\ -3(X_2 - X_{\ell_2})(X_1 - X_{\ell_1}) & \eta_\ell^2 - 3(X_2 - X_{\ell_2})^2 & -3(X_2 - X_{\ell_2})(X_3 - X_{\ell_3}) \\ -3(X_3 - X_{\ell_3})(X_1 - X_{\ell_1}) & -3(X_3 - X_{\ell_3})(X_2 - X_{\ell_2}) & \eta_\ell^2 - 3(X_3 - X_{\ell_3})^2 \end{pmatrix}, \qquad (37)$$

where ℓ = sun, moon.

6.1.2.4 Velocity Derivatives of the Atmospheric Drag Acceleration: $\frac{\partial \vec{a}_D}{\partial \dot{\vec{r}}}$

Since the atmospheric density is independent of velocity, the velocity derivatives of equation (16) SECTION 5 are

$$\frac{\partial \vec{a}_D}{\partial \dot{\vec{r}}} = -\frac{1}{2} D g \left[\rho \frac{\partial v}{\partial \dot{\vec{r}}}\ \vec{v} + \rho v \frac{\partial \vec{v}}{\partial \dot{\vec{r}}}\right] . \qquad (38)$$

7.1.1.1 Computed Observations and Observation Partial Derivatives (con't)

to obtain the nearly exact result used to form the computed observations:

$$|\vec{\rho}| \simeq |\vec{r}(t_e) - \vec{r}_s(t_R)| + \vec{\Delta r}_A(t_e) \cdot \left\{ \frac{\vec{r}(t_e) - \vec{r}_s(t_R)}{|\vec{r}(t_e) - \vec{r}_s(t_R)|} \right\} + \Delta\rho_{GR} \quad . \tag{18}$$

In equation (17),

f_0 = 10^6 ,

f_b = frequency bias,

$\dot{f}_b$ = frequency drift bias,

C_R = refraction bias,

Δf_R = tropospheric refraction correction (see SECTION 4),

t_1 = time of first observation of pass,

and

C = speed of light in vacuo,

where

t_e = time of signal emmission from satellite,

t_R = time of signal reception at observing station,

$\vec{r}_s(t)$ = inertial station position at time t,

$\vec{r}(t)$ = inertial position of satellite center of mass at time t,

7.1.1.1 Computed Observations and Observation Partial Derivatives (con't)

$\vec{\Delta r}_A(t)$ = inertial correction vector for antenna offset and satellite attitude at time t (see SECTION 4),

and

$\Delta\rho_{GR}$ = general relativistic correction to range (see SECTION 4).

For range difference observations the elements of the $\underset{\sim}{a}$ matrix are obtained by evaluating the expressions for the partial derivatives of the computed observations with respect to the parameters to be improved. Taking the partial derivative of equation (16) with respect to the parameter p_k gives

$$(\underset{\sim}{a})_{ik} = \frac{\partial C_i}{\partial p_k} = \frac{\partial \mathcal{D}(p_j, t_i)}{\partial p_k} - \frac{\partial \mathcal{D}(p_j, t_{i-1})}{\partial p_k} + \frac{\partial (\delta\Delta R_i)}{\partial p_k} \quad , \tag{19}$$

where $\mathcal{D}(p_j, t)$ is given by equation (17). If p_k is a dynamic parameter (i.e. an orbital element or drag parameter), one may write for the observation partial derivative at time t

$$\frac{\partial \mathcal{D}(p_j, t)}{\partial p_k} = \frac{\partial \mathcal{D}(p_j, t)}{\partial \vec{r}} \cdot \frac{\partial \vec{r}}{\partial p_k} + \frac{\partial \mathcal{D}(p_j, t)}{\partial \dot{\vec{r}}} \cdot \frac{\partial \dot{\vec{r}}}{\partial p_k} \quad , \tag{20}$$

or

$$\frac{\partial \mathcal{D}(p_j, t)}{\partial p_k} = \vec{\nabla}\mathcal{D}(p_j, t) \cdot \vec{\Psi}_{p_k}(t) + \dot{\vec{\nabla}}\mathcal{D}(p_j, t) \cdot \dot{\vec{\Psi}}_{p_k}(t) \quad , \tag{21}$$

where $\vec{\Psi}_{p_k}(t)$ and $\dot{\vec{\Psi}}_{p_k}(t)$ are the associated solutions to the variational equations (see SECTION 6). By inspection of equation (17) it is seen that $\mathcal{D}(p_j, t)$ is independent of velocity, so that one may write

7.1.1.1 Computed Observations and Observation Partial Derivatives (con't)

$$\dot{\vec{\nabla}}\mathcal{D}(p_j,\ t) \quad = \vec{0} \quad . \tag{22}$$

Also one finds that the position partial derivatives of the observation at time t reduces to

$$\vec{\nabla}\mathcal{D}(p_j,\ t) \quad = \frac{\partial |\vec{\rho}|}{\partial \vec{r}} \quad . \tag{23}$$

Since $\vec{\rho}$ is a vector in inertial space, its magnitude can be written as the square root of the sum of squares if its three inertial components X_i, i.e.

$$|\vec{\rho}| \quad = \quad (\vec{\rho} \cdot \vec{\rho})^{\frac{1}{2}} \quad = \left[\sum_{i=1}^{3} \quad X_i^2 \quad \right]^{\frac{1}{2}} \quad . \tag{24}$$

Then the k^{th} component of equation (23) becomes

$$\left[\vec{\nabla}\mathcal{D}(p_j,\ t)\right]_k \quad = \quad \frac{\partial}{\partial X_k} \left[\sum_{i=1}^{3} \quad X_i^{\ 2} \right]^{\frac{1}{2}}$$

$$= \quad \tfrac{1}{2} \left[\sum_{i=1}^{3} X_i^{\ 2} \right]^{-\frac{1}{2}} \quad (2X_i) \left(\frac{\partial X_i}{\partial X_k} \right)$$

$$= \quad \frac{X_k}{|\vec{\rho}|} \quad , \quad (k = 1,\ 2,\ 3). \tag{25}$$

Using this result and that of equation (22) allows one to write equation (21) as

7.1.1.1 Computed Observations and Observation Partial Derivatives (con't)

$$\frac{\partial \mathcal{D}(p_j,\ t)}{\partial p_k} = \frac{\vec{\rho}}{|\vec{\rho}|} \cdot \vec{\psi}_{p_k}(t) \quad (p_k = \text{orbit element or } \mathcal{D}). \tag{26}$$

Consider now the case when p_k is a component of the observing station's earth-fixed position vector $\vec{r}_{E_S}$. Then equation (17) reduces to

$$\left[\frac{\partial \mathcal{D}(p_j,\ t)}{\partial \vec{r}_{E_S}}\right]_k = \frac{\partial |\vec{\rho}|}{\partial \left(\vec{r}_{E_S}\right)_k}\ , \tag{27}$$

or

$$\left[\frac{\partial \mathcal{D}(p_j,\ t)}{\partial \vec{r}_{E_S}}\right]_k = \frac{\partial}{\partial \left(\vec{r}_{E_S}\right)_k} (\vec{\rho} \cdot \vec{\rho})^{\frac{1}{2}}\ . \tag{28}$$

Since

$$\vec{\rho}_E = (\underset{\sim\sim\sim\sim}{ABCD})\vec{\rho} \tag{29}$$

$$= \left[1 + \frac{\Delta\rho_{GR}}{|\vec{r}(t_e) - \vec{r}_s(t_R) + \Delta\vec{r}_A(t_e)|}\right] \underset{\sim\sim\sim\sim}{ABCD} \left[\vec{r}(t_e) - \vec{r}_s(t_R) + \Delta\vec{r}_A(t_e)\right],$$

or

$$\vec{\rho}_E = \left[1 + \frac{\Delta\rho_{GR}}{|\underset{\sim\sim\sim\sim}{ABCD}(\vec{r}(t_e) + \Delta\vec{r}_A(t_e)) - \vec{r}_{E_S}(t_R)|}\right] \cdot$$

$$\left[\underset{\sim\sim\sim\sim}{ABCD}\ (\vec{r}(t_e) + \Delta\vec{r}_A(t_e)) - \vec{r}_{E_S}(t_R)\right]\ , \tag{30}$$

7.1.1.1 Computed Observations and Observation Partial Derivatives (con't)

where the $\underset{\sim\sim\sim\sim}{ABCD}$ are those matrices discussed in SECTION 2 which transforms an inertial vector to the earth-fixed system of coordinates, then equation (28) may be written as

$$\left[\frac{\partial \mathcal{D}(p_j, t)}{\partial \vec{r}_{E_S}}\right]_k = \frac{\partial}{\partial(\vec{r}_{E_S})_k} \left(\vec{\rho}_E \cdot \vec{\rho}_E\right)^{\frac{1}{2}} , \tag{31}$$

or

$$\left[\frac{\partial \mathcal{D}(p_j, t)}{\partial \vec{r}_{E_S}}\right]_k = \frac{\partial}{\partial(\vec{r}_{E_S})_k} \left\{ \left[1 + \frac{\Delta\rho_{GR}}{|\underset{\sim\sim\sim\sim}{ABCD}(\vec{r}(t_e) + \Delta\vec{r}_A(t_e)) - \vec{r}_{E_S}(t_R)|}\right] \cdot \left[\left[\underset{\sim\sim\sim\sim}{ABCD}\,(\vec{r}(t_e) + \Delta\vec{r}_A(t_e)) - \vec{r}_{E_S}(t_R)\right] \cdot \left[\underset{\sim\sim\sim\sim}{ABCD}\,(\vec{r}(t_e) + \Delta\vec{r}_A(t_e)) - \vec{r}_{E_S}(t_R)\right]\right]^{\frac{1}{2}} \right\} . \tag{32}$$

Application of the chain rule to equation (32) gives

$$\frac{\partial \mathcal{D}(p_j, t)}{\partial(\vec{r}_{E_S})_k} = - \left[\frac{\vec{\rho}_E^{\,T}}{|\vec{\rho}_E|}\right]_k \tag{33}$$

or

$$\left[\frac{\partial \mathcal{D}(p_j, t)}{\partial \vec{r}_{E_S}}\right]_k = - \left[\frac{\vec{\rho}^{\,T}}{|\vec{\rho}|}\,(\underset{\sim\sim\sim\sim}{ABCD})^T\right]_k . \tag{34}$$

7.1.1.1 Computed Observations and Observation Partial Derivatives (con't)

Expressions for the observation partial derivatives with respect to the bias parameters are easily obtained. When $p_k = f_b$, $\dot{f}_b$, or C_R, one readily finds from equations (17) the following results:

$$\frac{\partial \mathcal{D}(p_j, t)}{\partial f_b} = - \frac{C}{f_o} (t - t_1) \tag{35}$$

$$\frac{\partial \mathcal{D}(p_j, t)}{\partial \dot{f}_b} = - \frac{1}{2} \frac{C}{f_o} (t - t_1)^2 \tag{36}$$

and

$$\frac{\partial \mathcal{D}(p_j, t)}{\partial C_R} = \Delta f_R \quad . \tag{37}$$

7.1.1.2 Pass Normal Equations and Parameter Improvement

The results of the previous subsections are used to form the pass normal equations. Initially this is done using all of the observations in a pass of sufficient elevation to form the residuals $(\underset{\sim}{O} - \underset{\sim}{C})$. As mentioned before, on subsequent iterations those observations which have been identified to be inconsistent with the other observations of the pass are not used in the formation of the normal equations. An overview of the point editor logic is presented in the flowchart of Figure 7-1.

The $\underset{\sim}{B}$ and $\underset{\sim}{E}$ matrices are formed using equations (14), (15), (19), (26), (34), (35), (36), and (37) where the weighting matrix is given by

$$W_{ij} = \left(\frac{1}{\lambda \sigma_i^2} \right) \delta_{ij} \quad . \tag{38}$$

Here σ_i^2 is the variance for the i^{th} observation; δ_{ij} is the Kronecker delta; and λ is a multiplier which is set equal to unity on the first iteration and recomputed for each subsequent iteration (see SECTION 8). For computational convenience the $\underset{\sim}{B}$ and $\underset{\sim}{E}$ matrices are partitioned in the following manner:

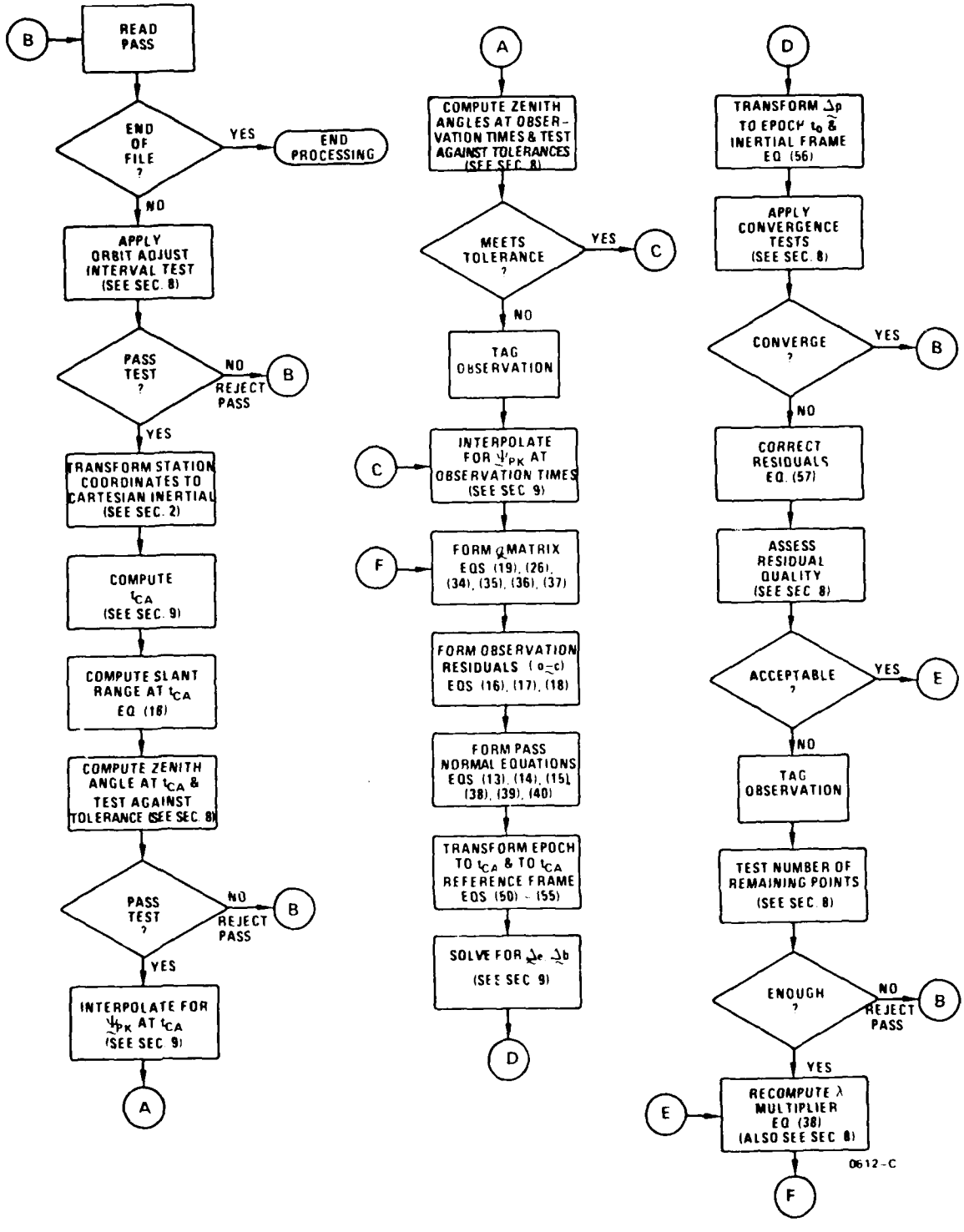

FIGURE 7-1. Point Editor Process Flow

7.1.1.2 Pass Normal Equations and Parameter Improvement (con't)

$$\underset{\sim}{B} = \begin{pmatrix} \underset{\sim}{B}_{e,e} & \underset{\sim}{B}_{e,D} & \underset{\sim}{B}_{e,s} & \underset{\sim}{B}_{e,b} \\ \underset{\sim}{B}_{D,e} & \underset{\sim}{B}_{D,D} & \underset{\sim}{B}_{D,s} & \underset{\sim}{B}_{D,b} \\ \underset{\sim}{B}_{s,e} & \underset{\sim}{B}_{s,D} & \underset{\sim}{B}_{s,s} & \underset{\sim}{B}_{s,b} \\ \underset{\sim}{B}_{b,e} & \underset{\sim}{B}_{b,D} & \underset{\sim}{B}_{b,s} & \underset{\sim}{B}_{b,b} \end{pmatrix} \tag{39}$$

and

$$\underset{\sim}{E} = \begin{pmatrix} \underset{\sim}{E}_{e} \\ \underset{\sim}{E}_{D} \\ \underset{\sim}{E}_{s} \\ \underset{\sim}{E}_{b} \end{pmatrix} , \tag{40}$$

where the subscripts "e", "D", "s", and "b" mean that the partitioned $\underset{\sim}{B}$ and $\underset{\sim}{E}$ matrices are formulated using the $\underset{\sim}{a}$ matrix of equation (19) with p_k being orbit elements, drag parameter, station coordinates, and bias parameters, respectively.

To perform editing on the observation residuals, the point editor first suppresses the submatrices of the $\underset{\sim}{B}$ and $\underset{\sim}{E}$ matrices which are related to the drag parameter and station coordinates. The remaining orbit element submatrices are then re-epoched from the initial trajectory epoch, t_o, to the time of closest approach for the pass, t_{CA} (details concerning the computation of t_{CA} are given in SECTION 9). Assuming that the $\underset{\sim}{a}$ matrix is epoched at t_{CA} (i.e. the partial derivatives of $\vec{r}$ and $\dot{\vec{r}}$ of the $\vec{\Psi}$ and $\dot{\vec{\Psi}}$ matrices are taken with respect to the orbit parameters at t_{CA}), one may use equation (65) of SECTION 6 to write for the i^{th} observation partials with respect to the orbit elements:

7.1.1.2 Pass Normal Equations and Parameter Improvement (con't)

$$\left(\underset{\sim}{a}_{t_{CA}}\right)_{i^{th}\ row} = \left(\vec{\nabla}^T C(t_i) \quad \dot{\vec{\nabla}}^T C(t_i)\right) \underset{\sim}{\Phi}_{t_{CA}}(t_i)$$

$$= \left(\vec{\nabla}^T C(t_i) \quad \dot{\vec{\nabla}}^T C(t_i)\right) \underset{\sim}{\Phi}(t_i) \quad \underset{\sim}{\Phi}^{-1}(t_{CA}) \quad \underset{\sim}{\Phi}_{t_{CA}}(t_{CA})$$

$$= \left(\underset{\sim}{a}_{t_o}\right)_{i^{th}\ row} \quad \underset{\sim}{\Phi}^{-1}(t_{CA}) \quad \underset{\sim}{\Phi}_{t_{CA}}(t_{CA}) \quad , \qquad (41)$$

where

$$\vec{\nabla} = \begin{pmatrix} \frac{\partial}{\partial x} \\ \frac{\partial}{\partial y} \\ \frac{\partial}{\partial z} \end{pmatrix} \quad \text{and} \quad \dot{\vec{\nabla}} = \begin{pmatrix} \frac{\partial}{\partial \dot{x}} \\ \frac{\partial}{\partial \dot{y}} \\ \frac{\partial}{\partial \dot{z}} \end{pmatrix} . \qquad (42)$$

Using this result in equation (14) gives the desired transformation from t_o:

$$\underset{\sim}{B}_{ee}(t_{CA}) = \left[\underset{\sim}{a}_{t_o} \quad \underset{\sim}{\Phi}^{-1}(t_{CA}) \quad \underset{\sim}{\Phi}_{t_{CA}}(t_{CA})\right]^T \quad \underset{\sim}{W} \quad \left[\underset{\sim}{a}_{t_o} \quad \underset{\sim}{\Phi}^{-1}(t_{CA}) \quad \underset{\sim}{\Phi}_{t_{CA}}(t_{CA})\right]$$

or

$$\underset{\sim}{B}_{ee}(t_{CA}) = \left[\underset{\sim}{\Phi}^{-1}(t_{CA}) \; \underset{\sim}{\Phi}_{t_{CA}}(t_{CA})\right]^T \quad \underset{\sim}{B}_{ee}(t_o) \quad \left[\underset{\sim}{\Phi}^{-1}(t_{CA}) \quad \underset{\sim}{\Phi}_{t_{CA}}(t_{CA})\right] . \qquad (43)$$

For the bias partials (i.e. when $p_k = f_b$, $\dot{f}_b$, or C_R) one finds that

$$\underset{\sim}{a}_{t_{CA}} = \underset{\sim}{a}_{t_o} \quad , \qquad (44)$$

7.1.1.2 Pass Normal Equations and Parameter Improvement (con't)

so that

$$\underset{\sim}{B}_{bb}(t_{CA}) = \underset{\sim}{B}_{bb}(t_o) \tag{45}$$

and that

$$\underset{\sim}{B}_{eb}(t_{CA}) = \left[\underset{\sim}{\Phi}^{-1}(t_{CA}) \quad \underset{\sim}{\Phi}_{t_{CA}}(t_{CA}) \right]^T \underset{\sim}{B}_{eb}(t_o) \tag{46}$$

and

$$\underset{\sim}{B}_{be}(t_{CA}) = \underset{\sim}{B}_{be}(t_o) \quad \underset{\sim}{\Phi}^{-1}(t_{CA}) \quad \underset{\sim}{\Phi}_{t_{CA}}(t_{CA}) \quad . \tag{47}$$

Similarly by applying equation (41) to equation (15), one finds

$$\underset{\sim}{E}_{e}(t_{CA}) = \left[\underset{\sim}{\Phi}^{-1}(t_{CA}) \quad \underset{\sim}{\Phi}_{t_{CA}}(t_{CA}) \right]^T \underset{\sim}{E}_{e}(t_o) \tag{48}$$

and

$$\underset{\sim}{E}_{b}(t_{CA}) = \underset{\sim}{E}_{b}(t_o) \quad . \tag{49}$$

These results can be used to write for the "drag parameter/station coordinates suppressed" matrices epoched at t_{CA}

$$\underset{\sim}{B}'(t_{CA}) = \begin{pmatrix} e_{11} & e_{12} \\ e_{21} & e_{22} \end{pmatrix} \tag{50}$$

(con't next page)

7.1.1.2 Pass Normal Equations and Parameter Improvement (con't)

$$
\left.
\begin{aligned}
e_{11} &= \left[\underset{\sim}{\Phi}^{-1}(t_{CA})\ \underset{\sim}{\Phi}_{t_{CA}}(t_{CA})\right]^T\ \underset{\sim}{B}_{ee}(t_o)\ \left[\underset{\sim}{\Phi}^{-1}(t_{CA})\ \underset{\sim}{\Phi}_{t_{CA}}(t_{CA})\right] \\
e_{12} &= \left[\underset{\sim}{\Phi}^{-1}(t_{CA})\ \underset{\sim}{\Phi}_{t_{CA}}(t_{CA})\right]^T\ \underset{\sim}{B}_{eb}(t_o) \\
e_{21} &= \underset{\sim}{B}_{be}(t_o)\left[\underset{\sim}{\Phi}^{-1}(t_{CA})\ \underset{\sim}{\Phi}_{t_{CA}}(t_{CA})\right] \\
e_{22} &= \underset{\sim}{B}_{bb}(t_o)
\end{aligned}
\right\} \quad (50)\ (\text{con't})
$$

and

$$
\underset{\sim}{E}'(t_{CA}) = \begin{pmatrix} \left[\underset{\sim}{\Phi}^{-1}(t_{CA})\ \underset{\sim}{\Phi}_{t_{CA}}(t_{CA})\right]^T\ \underset{\sim}{E}_e(t_o) \\ \\ \underset{\sim}{E}_b(t_o) \end{pmatrix} . \quad (51)
$$

7.1.1.2 Pass Normal Equations and Parameter Improvement (con't)

Prior to performing a solution for the orbit and bias parameter corrections the $\underset{\sim}{B}'(t_{CA})$ and $\underset{\sim}{E}'(t_{CA})$ matrices are transferred to the t_{CA} reference frame using the $\underset{\sim}{T}$ transformation defined in SECTION 2. The submatrix transformations are given by:

$$\left.\begin{aligned}
\underset{\sim}{\beta}_{ee}(t_{CA}) &= \underset{\sim}{T}^{T}\ \underset{\sim}{B}_{ee}(t_{CA})\ \underset{\sim}{T} \\
\underset{\sim}{\beta}_{eb}(t_{CA}) &= \underset{\sim}{T}^{T}\ \underset{\sim}{B}_{eb}(t_{CA}) \\
\underset{\sim}{\beta}_{be}(t_{CA}) &= \underset{\sim}{B}_{be}(t_{CA})\ \underset{\sim}{T} \\
\underset{\sim}{\beta}_{bb}(t_{CA}) &= \underset{\sim}{B}_{bb}(t_{CA}) \\
\underset{\sim}{\varepsilon}_{e}(t_{CA}) &= \underset{\sim}{T}^{T}\ \underset{\sim}{E}_{e}(t_{CA})
\end{aligned}\right\} \qquad (52)$$

and

$$\underset{\sim}{\varepsilon}_{b}(t_{CA}) = \underset{\sim}{E}_{b}(t_{CA}) \quad ,$$

so that one may write

$$\underset{\sim}{\beta}(t_{CA}) = \begin{pmatrix} \underset{\sim}{\beta}_{ee}(t_{CA}) & \underset{\sim}{\beta}_{eb}(t_{CA}) \\ \underset{\sim}{\beta}_{be}(t_{CA}) & \underset{\sim}{\beta}_{bb}(t_{CA}) \end{pmatrix} \quad , \qquad (53)$$

.1.1.2 Pass Normal Equations and Parameter Improvement (con't)

$$\underset{\sim}{\varepsilon}(t_{CA}) = \begin{pmatrix} \underset{\sim}{\varepsilon}_e(t_{CA}) \\ \\ \underset{\sim}{\varepsilon}_b(t_{CA}) \end{pmatrix} , \tag{54}$$

nd the associated pass normal equation in the t_{CA} reference frame:

$$\underset{\sim}{\beta}(t_{CA}) \begin{pmatrix} \underset{\sim}{\Delta e}'_{t_{CA}} \\ \\ \underset{\sim}{\Delta b}'_{t_{CA}} \end{pmatrix} = \underset{\sim}{\varepsilon}(t_{CA}). \tag{55}$$

n the last equation $\underset{\sim}{\Delta e}'_{t_{CA}}$ and $\underset{\sim}{\Delta b}'_{t_{CA}}$ represent the orbit element and ias parameter corrections at epoch t_{CA} in the t_{CA} reference frame.

Cholesky decomposition (see SECTION 9) is used to solve equation (55) or the parameter corrections. These corrections are transformed back to he initial frame at epoch t_o via the expression

$$\begin{pmatrix} \underset{\sim}{\Delta e} \\ \\ \underset{\sim}{\Delta b} \end{pmatrix}_{t_o} = \begin{pmatrix} \left[\underset{\sim}{\Phi}^{-1}(t_o) \;\; \underset{\sim}{\Phi}_{t_o}(t_o)\right] \;\; \underset{\sim}{T} \;\; \underset{\sim}{\Delta e}_{t_{CA}} \\ \\ \underset{\sim}{\Delta b}_{t_{CA}} \end{pmatrix} . \tag{56}$$

rocessing for the pass is tested against the convergence criteria of ECTION 8, and if they are met the updated pass matrices given by equaions (39) - (40), along with both tagged and untagged observations, are tored for processing by the cross pass editor. If processing has not onverged, the observation residuals are corrected using the linear relation

7.1.1.2 Pass Normal Equations and Parameter Improvement (con't)

$$(\underset{\sim}{O - C})_{\text{corrected}} = (\underset{\sim}{O - C})_{\text{current}} - \underset{\sim}{a} \begin{pmatrix} \underset{\sim}{\Delta e} \\ \Phi \\ \phi \\ \underset{\sim}{\Delta b} \end{pmatrix}_{t_o} , \qquad (57)$$

where zeroes have been inserted for drag parameter and station coordinate corrections, since none are computed in equation (55). The quality of the corrected observation residuals is then assessed and outlier observations are tagged as such. The differential correction process then repeats itself using only untagged observations and associated residuals in equations (38) - (57).

7.1.2 APPLICATION TO THE CROSS PASS EDITING PROCESS

The cross pass editor utilizes the pass matrices ($\underset{\sim}{B}$, $\underset{\sim}{E}$) generated by the point editor to determine the quality and useability of each pass of observations (for the arc of interest, i.e. editing span) in post-PULSAR applications. Those passes of observations which do not meet the quality criteria imposed by the cross pass editor are flagged as such during the editing process.

The basic processing of the cross pass editor involves first combining those pass matrices of sufficient quality in a particular manner to form the arc matrices $\underset{\sim}{B}_{ARC}$ and $\underset{\sim}{E}_{ARC}$ which are comprised only of elements related to the dynamic parameters (i.e. orbit elements and drag parameter). An arc solution for dynamic parameter corrections, $\underset{\sim}{\Delta P}_{ARC}$, is obtained and used to compute for each pass an estimate of the offsets in station location in the t_{CA} reference frame which minimizes the observation residuals of the pass while keeping the orbit fixed (hereafter, this will be referred to as a navigation solution). The quality of all navigation solutions is assessed and those of inadequate quality are tagged. This procedure is continued until the process converges with $\underset{\sim}{B}_{ARC}$ and $\underset{\sim}{E}_{ARC}$ being reformed each time using only the pass matrices

8.1.1 ZENITH ANGLE EDITING (con't)

quality. Furthermore, if the vehicle location at t_{CA} (see SECTION 9) for a given pass is too near the observing station's horizon, then it is assumed that all observations for that pass are too near the horizon and the entire pass is identified as being unusable by the cross pass editor and for any post-PULSAR processing.

In order to derive concise mathematical expressions for the zenith angle tests, consider the geometry of Figure 8-1 where

$\vec{N}$ = Outward directed vector normal to the reference ellipsoid at station location in inertial reference system,

$\vec{\rho}$ = position vector of satellite relative to the station in inertial reference system, and

z = zenith angle.

One readily sees that

$$\cos z = \frac{\vec{N}}{|\vec{N}|} \cdot \frac{\vec{\rho}}{|\vec{\rho}|} = \hat{N} \cdot \hat{\rho} \quad , \tag{1}$$

so that

$$\sin z = (1 - \cos^2 z)^{\frac{1}{2}} = [1 - (\hat{N} \cdot \hat{\rho})^2]^{\frac{1}{2}} \quad . \tag{2}$$

Since

$$\tan z = \frac{\sin z}{\cos z} \quad , \tag{3}$$

SECTION 8

DATA QUALITY ASSESSMENT METHODS AND ITERATIVE CONVERGENCE CRITERIA

: underlying mathematics associated with the point and cross pass data edi-
's are developed in detail in SECTION 7. However, little attention is
voted there to a discussion of the methods used to identify those observa-
ns which are of unacceptable quality for use in post-PULSAR processing. Also
itted from SECTION 7 is any discussion of the criteria used in PULSAR to
termine when the point and cross pass processors have adequately edited the
servation data and should terminate their processing, i.e. the iterative
nvergence criteria.

e observation quality assessment methods and the iterative convergence
iteria used in the point and cross pass editors are outlined in some detail
the following subsections. Also included below is a discussion of the
chnique used to determine whether or not the initial state vector (and suc-
eding day's initial conditions) need be corrected and the point and cross
ss editors recycled again using a new reference trajectory derived from the
rrected initial state vector.

1 POINT EDITOR METHODS AND CRITERIA

described in SECTION 7, the primary function of the point editor is to
entify observations on a pass by pass basis which are of inadequate quality.
en certain conditions are satisfied the point editor can also identify an
tire pass of observations as unusable by the cross pass editor, as well as
post-PULSAR processing. The methods used to perform these identifications
e generally straight forward and are described below. Also included are
scriptions of the simple iterative convergence criteria employed by the
int editor.

1.1 ZENITH ANGLE EDITING

nce reliable tropospheric refraction corrections (see SECTION 4) cannot
made for observations which lie too near an observing station's local
rizon, the point editor tags these observations as being of inadequate

$$(\underset{\sim}{W}_N)_{ij} = \left(\frac{1}{\sigma^2_{N_i}}\right) \delta_{ij}, \quad (i, j = 1, 2, 3; \; N_i = \Delta R, \Delta T, \Delta N), \tag{96}$$

and

$$(\underset{\sim}{W}_{ARC})_{ij} = \left(\frac{1}{\sigma^2_{P_i}}\right) \delta_{ij}, \quad (i, j = 1, 2, \ldots, 7; \; P_i = e_1, e_2, \ldots, e_6, D), \tag{97}$$

where the σ^2 are 'a priori' weighting variances and δ_{ij} is the Kronecker delta.

7.2 THE PROPAGATION OF STATE IMPROVEMENTS (con't)

Although not used in initiating the succeeding day's processing, the state covariance $\underset{\sim}{B}^{-1}_{ARC}$ is also propagated to the succeeding day's epoch for operational convenience. This propagation is performed in the following manner:

$$\underset{\sim}{B}^{-1}_{ARC_{t_s}} = \begin{bmatrix} \underset{\sim}{\Phi}(t_s) & \underset{\sim}{\Psi}(t_s) \\ t_o & D(t_o) \end{bmatrix} \underset{\sim}{B}^{-1}_{ARC} \begin{bmatrix} \underset{\sim}{\Phi}(t_s) & \underset{\sim}{\Psi}(t_s) \\ t_o & D(t_o) \end{bmatrix}^T . \qquad (93)$$

It should be mentioned that state improvements and associated covariance matrices cannot be propagated across the orbit adjust discontinuities which will exist in PULSAR generated trajectories (see SECTION 9). When such discontinuities occur, only the improvements and covariance associated with the state vector used to generate the post orbit adjust trajectory will be propagated forward to improve initial conditions for succeeding days.

7.3 'A PRIORI' ADDITIVE WEIGHTING

An 'a priori' additive weighting feature is generally used in the point and cross pass editors. The details of this feature have been suppressed for the sake of brevity in the preceeding development. They can, however, be made explicit by replacing: (i) $\underset{\sim}{B}_{bb}$ with $\underset{\sim}{B}_{bb} + \underset{\sim}{W}_b$ everywhere in equations (52), (58), (60)-(62), (64), (65), (86), and (88); (ii) each of the bias eliminated station pass matrices with itself plus $\underset{\sim}{W}_s$ in each summation term used to form $\underset{\sim}{B}_{\varepsilon_{s_i s_i}}$ in equations (66), (69)-(74), (76), and (77); (iii) $\underset{\sim}{T}'^T \underset{\sim}{B}_{\varepsilon_{s_i s_i}} \underset{\sim}{T}'$ with $\underset{\sim}{T}'^T(\underset{\sim}{B}_{\varepsilon_{s_i s_i}} + \underset{\sim}{W}_s)\underset{\sim}{T}' + \underset{\sim}{W}_N$, where $\underset{\sim}{B}_{\varepsilon_{s_i s_i}}$ is now the bias eliminated station pass matrix, everywhere in equations (85) and (88); and (iv) $\underset{\sim}{B}_{ARC}$ with $\underset{\sim}{B}_{ARC} + \underset{\sim}{W}_{ARC}$ in equations (75), (79), and (93). Here the $\underset{\sim}{W}$ matrices are the 'a priori' weighting matrices given by:

$$(\underset{\sim}{W}_b)_{ij} = \left(\frac{1}{\sigma^2_{b_i}}\right) \delta_{ij}, \quad (i, j = 1, 2, 3;\ b_i = f_b, \dot{f}_b, C_R), \qquad (94)$$

$$(\underset{\sim}{W}_s)_{ij} = \left(\frac{1}{\sigma^2_{x_i}}\right) \delta_{ij}, \quad (i, j = 1, 2, 3;\ x_i = \text{earth fixed coordinate}), \qquad (95)$$

7.2 THE PROPAGATION OF STATE IMPROVEMENTS

If it is determined that the initial state vector needs to be corrected using the arc solution $\Delta\underset{\sim}{p}_{ARC}$ and the point and cross pass editing procedure repeated using a newly integrated reference trajectory, then it is quite likely that the initial state vectors for succeeding days that were derived from the same initial reference trajectory should also be corrected using the final arc solution.

Propagating the state improvement of $\Delta\underset{\sim}{p}_{ARC}$ to a new epoch time can be handled quite easily by using the solutions to the variational equations that were discussed in SECTION 6. The improved state vector at time t is given by

$$\underset{\sim}{X}(t) = \underset{\sim}{X}_{old}(t) + \Delta\underset{\sim}{X}(t) \quad , \tag{89}$$

where $\Delta\underset{\sim}{X}(t)$ is the state correction propagated to the time t. Using equation (62) Section 6, one may write this correction as

$$\Delta\underset{\sim}{X}(t) = \begin{pmatrix} \vec{\Delta r}\,(t) \\ \\ \dot{\vec{\Delta r}}\,(t) \end{pmatrix} = \left(\underset{\sim}{\Phi}_{t_o}(t) \;\; \underset{\sim}{\Psi}_{D(t_o)}(t) \right) \Delta\underset{\sim}{p}_{ARC} \quad , \tag{90}$$

where the $\Delta\underset{\sim}{p}_{ARC}$ corrections are the dynamic parameter corrections referenced to epoch t_o. Thus if the succeeding day's epoch is $t = t_s$, then the improved initial vector for that day is given by

$$\underset{\sim}{X}(t_s) = \underset{\sim}{X}_{old}(t_s) + \left(\underset{\sim}{\Phi}_{t_o}(t_s) \;\; \underset{\sim}{\Psi}_{D(t_o)}(t_s) \right) \Delta\underset{\sim}{p}_{ARC} \quad . \tag{91}$$

In a similar fashion, the improved state vector at epoch t_o is

$$\underset{\sim}{X}(t_o) = \underset{\sim}{X}_{old}(t_o) + \left(\underset{\sim}{\Phi}_{t_o}(t_o) \;\; \underset{\sim}{\Psi}_{D(t_o)}(t_o) \right) \Delta\underset{\sim}{p}_{ARC} \quad . \tag{92}$$

7.1.2.2 Navigation and Bias Solutions (con't)

$$\Delta \underset{\sim}{p}_b \cong \underset{\sim}{B}_{bb}^{-1}(\underset{\sim}{p}_o)\left[\underset{\sim}{E}_b(\underset{\sim}{p}_o) - \underset{\sim}{B}_{be}(\underset{\sim}{p}_o)\,\Delta \underset{\sim}{p}_e - \underset{\sim}{B}_{bD}(\underset{\sim}{p}_o)\,\Delta \underset{\sim}{p}_D\right] . \tag{86}$$

The bias solution is computed from this expression only after the final arc solution iteration.

A great deal of computational convenience is introduced by using equations (85) - (86), since they can be written as

$$\Delta \underset{\sim}{p}_\gamma = \underset{\sim}{C}_1^{(\gamma)} - \underset{\sim}{C}_2^{(\gamma)}\Delta \underset{\sim}{p}_e - \underset{\sim}{C}_3^{(\gamma)}\Delta \underset{\sim}{p}_D \quad , (\gamma = s_i, b) \quad , \tag{87}$$

where the $\underset{\sim}{C}_i^{(\gamma)}$ are constant matrices which need only be computed once and are given by:

$$\left.\begin{aligned}
\underset{\sim}{C}_1^{(s_i)} &= \left[\underset{\sim}{T}'^{T}\underset{\sim}{B}_{\varepsilon_{s_i s_i}}(p_o)\underset{\sim}{T}'\right]^{-1}\underset{\sim}{T}'^{T}\underset{\sim}{E}_{\varepsilon_{s_i}}(\underset{\sim}{p}_o)\ ; \quad \underset{\sim}{C}_1^{(b)} = \underset{\sim}{B}_{bb}^{-1}(\underset{\sim}{p}_o)\,\underset{\sim}{E}_b(\underset{\sim}{p}_o)\\
\underset{\sim}{C}_2^{(s_i)} &= \left[\underset{\sim}{T}'^{T}\underset{\sim}{B}_{\varepsilon_{s_i s_i}}(\underset{\sim}{p}_o)\underset{\sim}{T}'\right]^{-1}\underset{\sim}{T}'^{T}\underset{\sim}{B}_{\varepsilon_{s_i e}}(\underset{\sim}{p}_o);\quad \underset{\sim}{C}_2^{(b)} = \underset{\sim}{B}_{bb}^{-1}(\underset{\sim}{p}_o)\,\underset{\sim}{B}_{be}(\underset{\sim}{p}_o)\\
\underset{\sim}{C}_3^{(s_i)} &= \left[\underset{\sim}{T}'^{T}\underset{\sim}{B}_{\varepsilon_{s_i s_i}}(\underset{\sim}{p}_o)\underset{\sim}{T}'\right]^{-1}\underset{\sim}{T}'^{T}\underset{\sim}{B}_{\varepsilon_{s_i D}}(\underset{\sim}{p}_o);\quad \underset{\sim}{C}_3^{(b)} = \underset{\sim}{B}_{bb}^{-1}(\underset{\sim}{p}_o)\,\underset{\sim}{B}_{bD}(\underset{\sim}{p}_o)
\end{aligned}\right\} \tag{88}$$

7.1.2.2 Navigation and Bias Solutions (con't)

then the desired result is

$$\Delta\underset{\sim}{p}_{\gamma} \simeq \underset{\sim}{B}^{-1}_{\gamma\gamma}(\underset{\sim}{p}_o)\left[\underset{\sim}{E}_{\gamma}(\underset{\sim}{p}_o) - \underset{\sim}{B}_{\gamma e}(\underset{\sim}{p}_o)\ \Delta\underset{\sim}{p}_e - \underset{\sim}{B}_{\gamma D}(\underset{\sim}{p}_o)\ \Delta\underset{\sim}{p}_D\right] \quad . \tag{84}$$

Equation (84) may be applied to obtain the navigation solution for the i^{th} observing station by letting $\gamma = s_i$. However, the cross pass editing process performs its pass data quality assessment using the tangential and radial station navigation components, ΔT_i and ΔR_i, respectively, in the t_{CA} reference system. Thus the above expression must be transformed to the t_{CA} system using the $\underset{\sim}{T}'$ transformation of SECTION 2. This gives

$$\Delta\underset{\sim}{p}_{s_i} = \begin{pmatrix} \Delta R_i \\ \Delta T_i \\ \Delta N_i \end{pmatrix} \simeq \left[\underset{\sim}{T}'^{T}\underset{\sim}{B}_{\varepsilon_{s_i s_i}}(p_o)\ \underset{\sim}{T}'\right]^{-1}\left[\underset{\sim}{T}'^{T}\underset{\sim}{E}_{\varepsilon_{s_i}}(\underset{\sim}{p}_o) - (\underset{\sim}{T}'^{T}\underset{\sim}{B}_{\varepsilon_{s_i e}}(\underset{\sim}{p}_o)\ \underset{\sim}{T}')\underset{\sim}{T}'^{-1}\Delta\underset{\sim}{p}_e\right.$$

$$\left. - (\underset{\sim}{T}'^{T}\underset{\sim}{B}_{\varepsilon_{s_i D}}(\underset{\sim}{p}_o)\ \underset{\sim}{T}')\underset{\sim}{T}'^{-1}\Delta\underset{\sim}{p}_D\right]$$

$$\simeq \left[\underset{\sim}{T}'^{T}\underset{\sim}{B}_{\varepsilon_{s_i s_i}}(\underset{\sim}{p}_o)\ \underset{\sim}{T}'\right]^{-1}\left[\underset{\sim}{T}'^{T}\underset{\sim}{E}_{\varepsilon_{s_i}}(\underset{\sim}{p}_o) - \underset{\sim}{T}'^{T}\underset{\sim}{B}_{\varepsilon_{s_i e}}(\underset{\sim}{p}_o)\ \Delta\underset{\sim}{p}_e\right.$$

$$\left. - \underset{\sim}{T}'^{T}\underset{\sim}{B}_{\varepsilon_{s_i D}}(\underset{\sim}{p}_o)\ \Delta\underset{\sim}{p}_D\right] \quad , \tag{85}$$

where the ΔN_i is the normal station navigation component and the subscript "ε" has been added since the station navigation solution is obtained using the bias eliminated station matrices. It should be noted that the station navigations are obtained for each iteration associated with the arc differential correction process.

Bias solutions are obtained directly from equation (84) by setting $\gamma = b$. The expression for the bias solution is then

7.1.2.2 Navigation and Bias Solutions

Navigation and bias solutions are obtained in the cross pass editor via a linear approximation using the results of the arc solution. To find this linear approximation, consider the normal equation given by

$$\underset{\sim}{B}_{\gamma\gamma}(\underset{\sim}{p})\Delta\underset{\sim}{p}_{\gamma} = \underset{\sim}{E}_{\gamma}(\underset{\sim}{p}) \quad . \tag{80}$$

Assume that

$$\underset{\sim}{p} = \underset{\sim}{p}_o + \Delta\underset{\sim}{p}_{ARC} \tag{81}$$

where $\underset{\sim}{p}_o$ is the initial value matrix for the parameters. One may expand equation (80) in a Taylor series about $\underset{\sim}{p}_o$ to obtain

$$\underset{\sim}{B}_{\gamma\gamma}(\underset{\sim}{p}_o)\ \Delta\underset{\sim}{p}_{\gamma} \cong \underset{\sim}{E}_{\gamma}(\underset{\sim}{p}_o) + \left.\frac{\partial \underset{\sim}{E}_{\gamma}}{\partial \underset{\sim}{p}}\right|_{\underset{\sim}{p}_o} \Delta\underset{\sim}{p}_{ARC} \quad , \tag{82}$$

where only linear terms have been retained. Since

$$\begin{aligned}
\left.\frac{\partial \underset{\sim}{E}_{\gamma}}{\partial \underset{\sim}{p}}\right|_{\underset{\sim}{p}_o} \Delta\underset{\sim}{p}_{ARC} &\simeq - \left[\underset{\sim}{a}_{\gamma}^{T}\ \underset{\sim}{W}\ \frac{\partial \underset{\sim}{C}}{\partial \underset{\sim}{p}}\right] \Delta\underset{\sim}{p}_{ARC} \\
&\simeq - \underset{\sim}{a}_{\gamma}^{T}(\underset{\sim}{p}_o)\ \underset{\sim}{W}\ \left.\frac{\partial \underset{\sim}{C}}{\partial \underset{\sim}{p}_e}\right|_{\underset{\sim}{p}_o} \Delta\underset{\sim}{p}_e - \underset{\sim}{a}_{\gamma}^{T}(\underset{\sim}{p}_o)\ \underset{\sim}{W}\ \left.\frac{\partial \underset{\sim}{C}}{\partial \underset{\sim}{p}_D}\right|_{\underset{\sim}{p}_o} \Delta\underset{\sim}{p}_D \\
&\simeq - \underset{\sim}{a}_{\gamma}^{T}(\underset{\sim}{p}_o)\ \underset{\sim}{W}\ \underset{\sim}{a}_e(\underset{\sim}{p}_o)\ \Delta\underset{\sim}{p}_e - \underset{\sim}{a}_{\gamma}^{T}(\underset{\sim}{p}_o)\ \underset{\sim}{W}\ \underset{\sim}{a}_D(\underset{\sim}{p}_o)\ \Delta\underset{\sim}{p}_D \\
&\simeq - \underset{\sim}{B}_{\gamma e}(\underset{\sim}{p}_o)\ \Delta\underset{\sim}{p}_e - \underset{\sim}{B}_{\gamma D}(\underset{\sim}{p}_o)\ \Delta\underset{\sim}{p}_D \quad ,
\end{aligned} \tag{83}$$

7.1.2.1 Arc Normal Equation and Parameter Improvement (con't)

These results provide the bias and station eliminated arc normal equation given by

$$\underset{\sim}{B}_{ARC} \quad \underset{\sim}{\Delta p}_{ARC} = \underset{\sim}{E}_{ARC} \quad , \tag{75}$$

where

$$\underset{\sim}{B}_{ARC} = \begin{pmatrix} \underset{\sim}{B}_{\varepsilon_{ee}} - \sum_{i=1}^{K} \underset{\sim}{B}_{\varepsilon_{es_i}} \underset{\sim}{B}^{-1}_{\varepsilon_{s_i s_i}} \underset{\sim}{B}_{\varepsilon_{s_i e}} & \underset{\sim}{B}_{\varepsilon_{eD}} - \sum_{i=1}^{K} \underset{\sim}{B}_{\varepsilon_{es_i}} \underset{\sim}{B}^{-1}_{\varepsilon_{s_i s_i}} \underset{\sim}{B}_{\varepsilon_{s_i D}} \\ \underset{\sim}{B}_{\varepsilon_{De}} - \sum_{i=1}^{K} \underset{\sim}{B}_{\varepsilon_{Ds_i}} \underset{\sim}{B}^{-1}_{\varepsilon_{s_i s_i}} \underset{\sim}{B}_{\varepsilon_{s_i e}} & \underset{\sim}{B}_{\varepsilon_{DD}} - \sum_{i=1}^{K} \underset{\sim}{B}_{\varepsilon_{Ds_i}} \underset{\sim}{B}^{-1}_{\varepsilon_{s_i s_i}} \underset{\sim}{B}_{\varepsilon_{s_i D}} \end{pmatrix} , \tag{76}$$

$$\underset{\sim}{E}_{ARC} = \begin{pmatrix} \underset{\sim}{E}_{\varepsilon_e} - \sum_{i=1}^{K} \underset{\sim}{B}_{\varepsilon_{es_i}} \underset{\sim}{B}^{-1}_{\varepsilon_{s_i s_i}} \underset{\sim}{E}_{\varepsilon_{s_i}} \\ \underset{\sim}{E}_{\varepsilon_D} - \sum_{i=1}^{K} \underset{\sim}{B}_{\varepsilon_{Ds_i}} \underset{\sim}{B}^{-1}_{\varepsilon_{s_i s_i}} \underset{\sim}{E}_{\varepsilon_{s_i}} \end{pmatrix} , \tag{77}$$

and

$$\underset{\sim}{\Delta p}_{ARC} = \begin{pmatrix} \underset{\sim}{\Delta p}_e \\ \underset{\sim}{\Delta p}_D \end{pmatrix} . \tag{78}$$

Arc parameter improvements are obtained from

$$\underset{\sim}{\Delta p}_{ARC} = \underset{\sim}{B}^{-1}_{ARC} \quad \underset{\sim}{E}_{ARC} . \tag{79}$$

7.1.2.1 Arc Normal Equation and Parameter Improvement (con't)

which can be used in equations (67) - (68) to obtain

$$\underset{\sim}{B}_{\varepsilon_{ee}} \underset{\sim}{\Delta p}_e + \underset{\sim}{B}_{\varepsilon_{eD}} \underset{\sim}{\Delta p}_D + \sum_{i=1}^{K} \underset{\sim}{B}_{\varepsilon_{es_i}} \underset{\sim}{B}^{-1}_{\varepsilon_{s_i s_i}} (\underset{\sim}{E}_{\varepsilon_{s_i}} - \underset{\sim}{B}_{\varepsilon_{s_i e}} \cdot$$

$$\underset{\sim}{\Delta p}_e - \underset{\sim}{B}_{\varepsilon_{s_i D}} \underset{\sim}{\Delta p}_D) = \underset{\sim}{E}_{\varepsilon_e} \qquad (71)$$

and

$$\underset{\sim}{B}_{\varepsilon_{De}} \underset{\sim}{\Delta p}_e + \underset{\sim}{B}_{\varepsilon_{DD}} \underset{\sim}{\Delta p}_D + \sum_{i=1}^{K} \underset{\sim}{B}_{\varepsilon_{Ds_i}} \underset{\sim}{B}^{-1}_{\varepsilon_{s_i s_i}} (\underset{\sim}{E}_{\varepsilon_{s_i}} - \underset{\sim}{B}_{\varepsilon_{s_i e}} \cdot$$

$$\underset{\sim}{\Delta p}_e - \underset{\sim}{B}_{\varepsilon_{s_i D}} \underset{\sim}{\Delta p}_D) = \underset{\sim}{E}_{\varepsilon_D} \qquad (72)$$

or

$$(\underset{\sim}{B}_{\varepsilon_{ee}} - \sum_{i=1}^{K} \underset{\sim}{B}_{\varepsilon_{es_i}} \underset{\sim}{B}^{-1}_{\varepsilon_{s_i s_i}} \underset{\sim}{B}_{\varepsilon_{s_i e}}) \underset{\sim}{\Delta p}_e + (\underset{\sim}{B}_{\varepsilon_{eD}} - \sum_{i=1}^{K} \underset{\sim}{B}_{\varepsilon_{es_i}} \cdot$$

$$\underset{\sim}{B}^{-1}_{\varepsilon_{s_i s_i}} \underset{\sim}{B}_{\varepsilon_{s_i D}}) \underset{\sim}{\Delta p}_D = \underset{\sim}{E}_{\varepsilon_e} - \sum_{i=1}^{K} \underset{\sim}{B}_{\varepsilon_{es_i}} \underset{\sim}{B}^{-1}_{\varepsilon_{s_i s_i}} \underset{\sim}{E}_{\varepsilon_{s_i}} \qquad (73)$$

and

$$(\underset{\sim}{B}_{\varepsilon_{De}} - \sum_{i=1}^{K} \underset{\sim}{B}_{\varepsilon_{Ds_i}} \underset{\sim}{B}^{-1}_{\varepsilon_{s_i s_i}} \underset{\sim}{B}_{\varepsilon_{s_i e}}) \underset{\sim}{\Delta p}_e + (\underset{\sim}{B}_{\varepsilon_{DD}} - \sum_{i=1}^{K} \underset{\sim}{B}_{\varepsilon_{Ds_i}} \cdot$$

$$\underset{\sim}{B}^{-1}_{\varepsilon_{s_i s_i}} \underset{\sim}{B}_{\varepsilon_{s_i D}}) \underset{\sim}{\Delta p}_D = \underset{\sim}{E}_{\varepsilon_D} - \sum_{i=1}^{K} \underset{\sim}{B}_{\varepsilon_{Ds_i}} \underset{\sim}{B}^{-1}_{\varepsilon_{s_i s_i}} \underset{\sim}{E}_{\varepsilon_{s_i}} \cdot \qquad (74)$$

7.1.2.1 Arc Normal Equation and Parameter Improvement (con't)

After the bias elimination has been performed upon the pass matrices they are added together, taking care to properly segregate the resulting station coordinate submatrices. For κ observing stations, the associated bias eliminated normal equations become

$$\begin{pmatrix} \underset{\sim}{B}_{\varepsilon_{ee}} & \underset{\sim}{B}_{\varepsilon_{eD}} & \underset{\sim}{B}_{\varepsilon_{es_1}} & \underset{\sim}{B}_{\varepsilon_{es_2}} & \cdots & \underset{\sim}{B}_{\varepsilon_{es\kappa}} \\ \underset{\sim}{B}_{\varepsilon_{De}} & \underset{\sim}{B}_{\varepsilon_{DD}} & \underset{\sim}{B}_{\varepsilon_{DS_1}} & \underset{\sim}{B}_{\varepsilon_{DS_2}} & \cdots & \underset{\sim}{B}_{\varepsilon_{Ds\kappa}} \\ \underset{\sim}{B}_{\varepsilon_{s_1e}} & \underset{\sim}{B}_{\varepsilon_{s_1D}} & \underset{\sim}{B}_{\varepsilon_{s_1s_1}} & \underset{\sim}{0} & \cdots & \underset{\sim}{0} \\ \underset{\sim}{B}_{\varepsilon_{s_2e}} & \underset{\sim}{B}_{\varepsilon_{s_2D}} & \underset{\sim}{0} & \underset{\sim}{B}_{\varepsilon_{s_2s_2}} & \cdots & \underset{\sim}{0} \\ \vdots & & & & & \\ \underset{\sim}{B}_{\varepsilon_{s_\kappa e}} & \underset{\sim}{B}_{\varepsilon_{s_\kappa D}} & \underset{\sim}{0} & \underset{\sim}{0} & \cdots & \underset{\sim}{B}_{\varepsilon_{s_\kappa s_\kappa}} \end{pmatrix} \begin{pmatrix} \underset{\sim}{\Delta p}_e \\ \underset{\sim}{\Delta p}_D \\ \underset{\sim}{\Delta p}_{s_1} \\ \vdots \\ \underset{\sim}{\Delta p}_{s_\kappa} \end{pmatrix} = \begin{pmatrix} \underset{\sim}{E}_{\varepsilon_e} \\ \underset{\sim}{E}_{\varepsilon_D} \\ \underset{\sim}{E}_{\varepsilon_{s_1}} \\ \underset{\sim}{E}_{\varepsilon_{s_2}} \\ \vdots \\ \underset{\sim}{E}_{\varepsilon_{s_\kappa}} \end{pmatrix} , \quad (66)$$

where the subscript "s_i" means the matrix is related to the i^{th} station. Thus one may write

$$\underset{\sim}{B}_{\varepsilon_{ee}} \underset{\sim}{\Delta p}_e + \underset{\sim}{B}_{\varepsilon_{eD}} \underset{\sim}{\Delta p}_D + \sum_{i=1}^{\kappa} \underset{\sim}{B}_{\varepsilon_{es_i}} \underset{\sim}{\Delta p}_{s_i} = \underset{\sim}{E}_{\varepsilon_e} \quad (67)$$

$$\underset{\sim}{B}_{\varepsilon_{De}} \underset{\sim}{\Delta p}_e + \underset{\sim}{B}_{\varepsilon_{DD}} \underset{\sim}{\Delta p}_D + \sum_{i=1}^{\kappa} \underset{\sim}{B}_{\varepsilon_{Ds_i}} \underset{\sim}{\Delta p}_{s_i} = \underset{\sim}{E}_{\varepsilon_D} \quad (68)$$

and

$$\underset{\sim}{B}_{\varepsilon_{s_ie}} \underset{\sim}{\Delta p}_e + \underset{\sim}{B}_{\varepsilon_{s_iD}} \underset{\sim}{\Delta p}_D + \underset{\sim}{B}_{\varepsilon_{s_is_i}} \underset{\sim}{\Delta p}_{s_i} = \underset{\sim}{E}_{\varepsilon_{s_i}} , \quad (i = 1, \ldots, \kappa). \quad (69)$$

Solving equation (69) for $\underset{\sim}{\Delta p}_{s_i}$ gives

$$\underset{\sim}{\Delta p}_{s_i} = \underset{\sim}{B}^{-1}_{\varepsilon_{s_is_i}} \left(\underset{\sim}{E}_{\varepsilon_{s_i}} - \underset{\sim}{B}_{\varepsilon_{s_ie}} \underset{\sim}{\Delta p}_e - \underset{\sim}{B}_{\varepsilon_{s_iD}} \underset{\sim}{\Delta p}_D \right), (i=1, \ldots, \kappa) \quad (70)$$

7.1.2.1 Arc Normal Equation and Parameter Improvement (con't)

where the subscript "α" represents all but the bias parameters (i.e. f_b, $\dot{f}_b$, C_R) which are represented by the subscript "b". Thus one may write

$$\underset{\sim}{B}_{\alpha\alpha} \quad \underset{\sim}{\Delta p}_{\alpha} + \underset{\sim}{B}_{\alpha b} \quad \underset{\sim}{\Delta p}_{b} = \underset{\sim}{E}_{\alpha} \tag{59}$$

and

$$\underset{\sim}{B}_{b\alpha} \quad \underset{\sim}{\Delta p}_{\alpha} + \underset{\sim}{B}_{bb} \quad \underset{\sim}{\Delta p}_{b} = \underset{\sim}{E}_{b} \quad . \tag{60}$$

The last equation may be solved for the bias correction to give

$$\underset{\sim}{\Delta p}_{b} = \underset{\sim}{B}_{bb}^{-1} \left(\underset{\sim}{E}_{b} - \underset{\sim}{B}_{b\alpha} \quad \underset{\sim}{\Delta p}_{\alpha}\right) \tag{61}$$

which can be substituted into equation (59) to give

$$\left(\underset{\sim}{B}_{\alpha\alpha} - \underset{\sim}{B}_{\alpha b} \quad \underset{\sim}{B}_{bb}^{-1} \quad \underset{\sim}{B}_{b\alpha}\right) \underset{\sim}{\Delta p}_{\alpha} = \underset{\sim}{E}_{\alpha} - \underset{\sim}{B}_{\alpha b} \quad \underset{\sim}{B}_{bb}^{-1} \quad \underset{\sim}{E}_{b} \quad . \tag{62}$$

The last equation is the bias eliminated pass normal equation which can be rewritten as

$$\underset{\sim}{B}_{\varepsilon_{\alpha\alpha}} \quad \underset{\sim}{\Delta p}_{\alpha} = \underset{\sim}{E}_{\varepsilon_{\alpha}} \quad , \tag{63}$$

where the subscript "ε" means that the associated matrices are the bias eliminated pass matrices defined as

$$\underset{\sim}{B}_{\varepsilon_{\alpha\alpha}} = \underset{\sim}{B}_{\alpha\alpha} - \underset{\sim}{B}_{\alpha b} \quad \underset{\sim}{B}_{bb}^{-1} \quad \underset{\sim}{B}_{b\alpha} \tag{64}$$

and

$$\underset{\sim}{E}_{\varepsilon_{\alpha}} = \underset{\sim}{E}_{\alpha} - \underset{\sim}{B}_{\alpha b} \quad \underset{\sim}{B}_{bb}^{-1} \quad \underset{\sim}{E}_{b} \quad . \tag{65}$$

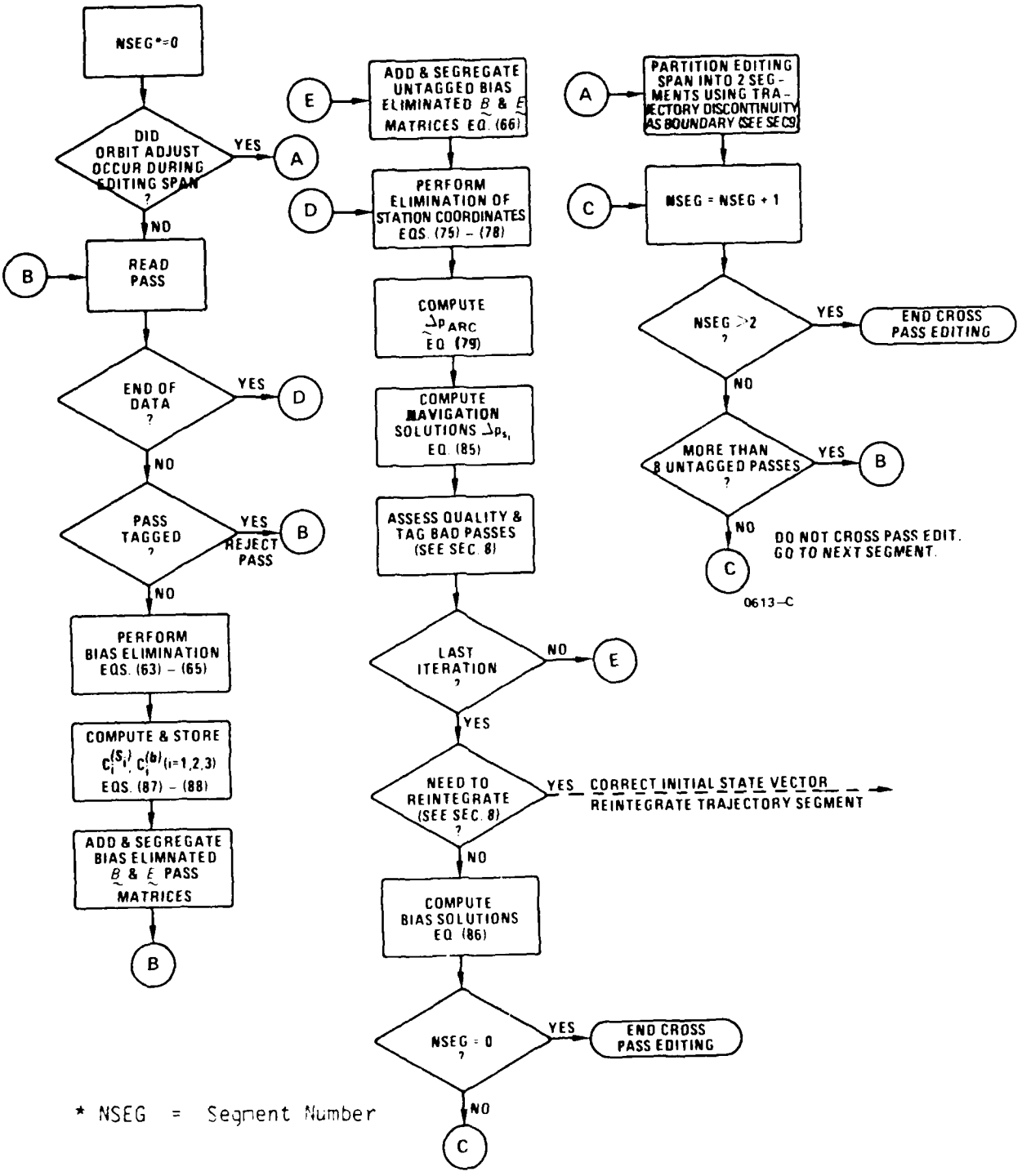

FIGURE 7-2. Cross Pass Editor Process Flow

7.1.2 APPLICATION TO THE CROSS PASS EDITING PROCESS (con't)

for the untagged passes. It should be noted that navigation solutions for all passes are obtained during each arc solution iteration and their quality assessed. Any pass which was tagged on a previous iteration, but is of adequate quality on the current iteration is untagged and used in the arc solution on the next iteration. Solutions for station bias parameters (i.e. f_b, $\dot{f}_b$, and C_R) are computed only on the final iteration. Upon convergence $\Delta\underset{\sim}{p}_{ARC}$ is checked to see if the initial state vector should be corrected by $\Delta\underset{\sim}{p}_{ARC}$ and the process repeated, beginning with the point editor. If so, the process diverts to the integrator and starts again. If not, the final file of edited tracking data is output and the process terminates. An overview of the cross pass editor process flow is presented in Figure 7-2. It should be pointed out that should an orbit adjust occur during the editing span, the cross pass editor will partition the span into two segments and cross pass edit each segment independently. However, if a segment is comprised of eight or fewer untagged passes, it will not be processed by the cross pass editor.

In this subsection, the mathematics associated with arc normal equation formation and solution, navigation solutions, and bias solutions are discussed. The methods used for quality assessment and convergence determination are developed in SECTION 8.

7.1.2.1 Arc Normal Equation and Parameter Improvement

The pass matrices contain elements which are station dependent. Since the arc matrices must be formed from the pass matrices, and yet be independent of station related elements, one must devise a method for eliminating the station dependencies. Consider first the elimination of the bias elements from the pass matrices. Let the pass normal equation be partitioned into submatrices as

$$\begin{pmatrix} \underset{\sim}{B}_{\alpha\alpha} & \underset{\sim}{B}_{\alpha b} \\ \underset{\sim}{B}_{b\alpha} & \underset{\sim}{B}_{bb} \end{pmatrix} \begin{pmatrix} \Delta\underset{\sim}{p}_{\alpha} \\ \Delta\underset{\sim}{p}_{b} \end{pmatrix} = \begin{pmatrix} \underset{\sim}{E}_{\alpha} \\ \underset{\sim}{E}_{b} \end{pmatrix} , \qquad (58)$$

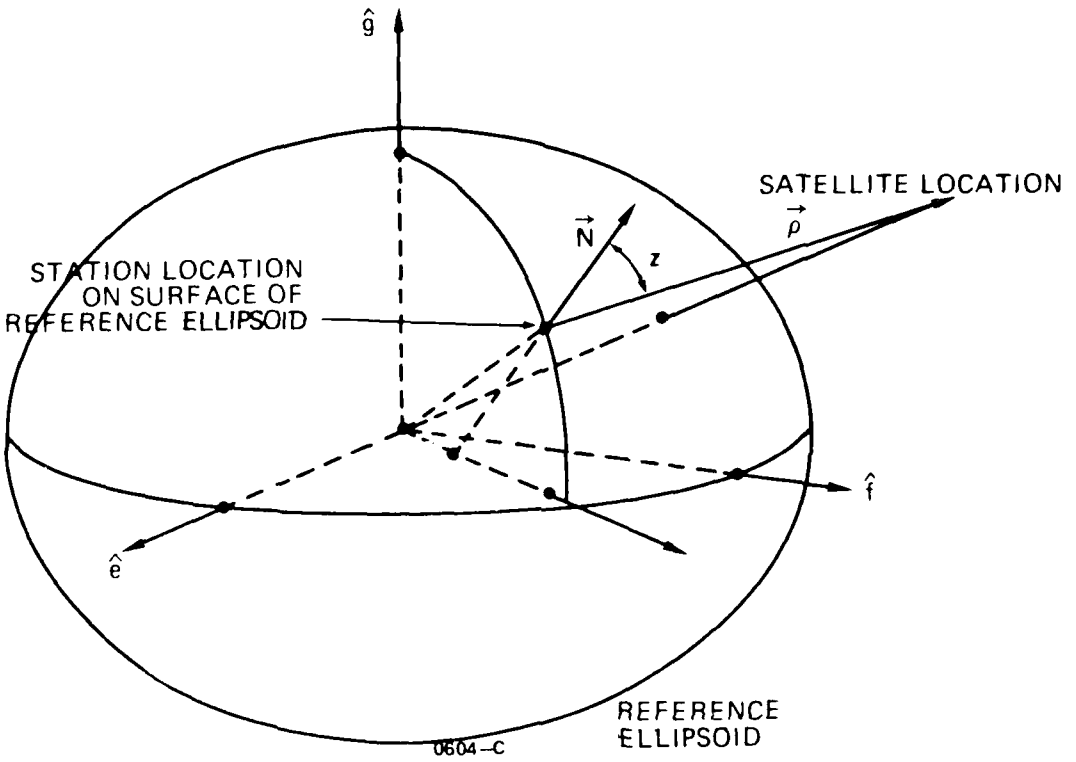

FIGURE 8-1. Zenith Angle Geometry

8.1.1 ZENITH ANGLE EDITING (con't)

then the zenith angle is obtained from

$$z = \tan^{-1}\left\{ \left[1 - (\hat{N} \cdot \hat{\rho})^2\right]^{\frac{1}{2}} / (\hat{N} \cdot \hat{\rho}) \right\} \quad . \tag{4}$$

To obtain $\hat{N}$, one uses the transformation from station geodetic latitude, height and longitude to earth-fixed cartesian coordinates (see SECTION 2) to find the earth-fixed coordinates of the station on the reference ellipsoid. This is done by setting the station's geodetic height above the reference ellipsoid to zero giving

$$\begin{pmatrix} e_s \\ f_s \\ g_s \end{pmatrix} = \frac{a_e}{(1 - \varepsilon^2 \sin^2 \phi)^{\frac{1}{2}}} \begin{pmatrix} \cos\phi \cos\lambda \\ \cos\phi \sin\lambda \\ (1 - \varepsilon^2) \sin\phi \end{pmatrix}$$

$$= k \begin{pmatrix} S_1 \\ S_2 \\ (1 - \varepsilon^2) S_3 \end{pmatrix} , \tag{5}$$

where ϕ, λ, and ε are the station's geodetic latitude, longitude and the eccentricity of the reference ellipsoid, respectively.

In general the equation for the surface of the reference ellipsoid is

$$\frac{e^2}{a_e^2} + \frac{f^2}{a_e^2} + \frac{g^2}{b_e^2} = 1 \quad , \tag{6}$$

8.1.1 ZENITH ANGLE EDITING (con't)

where b_e is the semi-minor axis of the reference ellipsoid. Since the eccentricity of the reference ellipsoid is given by

$$\varepsilon^2 = \frac{a_e^2 - b_e^2}{a_e^2} \quad , \tag{7}$$

then one may write

$$b_e^2 = a_e^2 (1 - \varepsilon^2) \quad . \tag{8}$$

Using this in equation (6) gives

$$(1 - \varepsilon^2)(e^2 + f^2) + g^2 = a_e^2 (1 - \varepsilon^2). \tag{9}$$

The gradient of the last equation evaluated at the station location on the reference ellipsoid is an outward normal to the surface at the point in question. Taking the gradient of the last expression gives

$$\vec{n} = \begin{pmatrix} (1 - \varepsilon^2)\, e_s \\ (1 - \varepsilon^2)\, fs \\ g_s \end{pmatrix} = (1 - \varepsilon^2) k \begin{pmatrix} S_1 \\ S_2 \\ S_3 \end{pmatrix} \quad , \tag{10}$$

where $\vec{n}$ is the normal in the earth-fixed reference frame. Applying the $\underset{\sim\sim\sim}{ABCD}$ transformations of SECTION 2, one obtains for $\vec{N}$:

$$\vec{N} = (\underset{\sim\sim\sim}{ABCD})^{-1} \vec{n} \quad . \tag{11}$$

8.1.1 ZENITH ANGLE EDITING (con't)

Equations (4), (10) and (11) are used to compute the zenith angle at t_{CA} and for each observation of a usable pass. The following two tests are applied directly to the computed zenith angles: if

$$z_{t_{CA}} \begin{cases} \leq z_{TOL}, & \text{accept pass of observations for further editing by point processor} \\ > z_{TOL}, & \text{reject all observations of pass,} \end{cases} \quad (12)$$

and if

$$z_t \begin{cases} \leq z_{TOL}, & \text{accept the observation} \\ > z_{TOL}, & \text{tag the observation,} \end{cases} \quad (13)$$

where $z_{t_{CA}}$ and z_t are the zenith angles computed from the reference trajectory at t_{CA} and observation time t, respectively.

8.1.2 ORBIT ADJUST INTERVAL EDITING

If tracking data falls within a period of time around an orbit adjust interval, then the pass (or passes) of data associated with that tracking data will be tagged as bad data. The test used to determine whether this condition exists is given as follows:

if

$$t_B \leq t_L \quad (14)$$

and

$$t_E \geq t_1, \quad \text{reject the pass.} \quad (15)$$

8.1.2 ORBIT ADJUST INTERVAL EDITING (con't)

In the above inequalities t_1 and t_L are the times of the first and last observation in the pass and

$$t_B = t_{OA_B} - m_1 h \tag{16}$$

and

$$t_E = t_{OA_E} + m_2 h \quad , \tag{17}$$

where t_{OA_B} and t_{OA_E} are the orbit adjust start and stop times, respectively, h is the integration step size, and the m_i (i = 1, 2) are integer constants.

8.1.3 OBSERVATION RESIDUAL QUALITY EDITING

Two different types of quality tests are performed upon the observation residuals in the point editing process. These are called the absolute and statistical residual quality edits, respectively. Consider first the absolute residual quality edit. This is a coarse check performed upon all observation residuals in each pass to identify those residuals which are associated with observations that are obviously of undesirable quality. This test is invoked upon the first iteration of the point editing process only and is stated as follows: if

$$|(\underset{\sim}{O} - \underset{\sim}{C})_i| > \rho_{TOL} \quad , \quad \text{tag the observation,} \tag{18}$$

where ρ_{TOL} is a pre-set tolerance value.

The statistical residual quality edit uses the weighted least squares method to fit a straight line through the observation residuals of a pass from which a standard error can be calculated and used in the test procedure. To elaborate upon this, let

8.1.3 OBSERVATION RESIDUAL QUALITY EDITING (con't)

$$y = at + b \tag{19}$$

be the linear function of time t which one wishes to fit to the observations. Using the results of SECTION 7 one finds that the required normal equation may be written as

$$\begin{pmatrix} \sum_{i=1}^{N} \frac{t_i^2}{\lambda\sigma_i^2} & \sum_{i=1}^{N} \frac{t_i}{\lambda\sigma_i^2} \\ \sum_{i=1}^{N} \frac{t_i}{\lambda\sigma_i^2} & \sum_{i=1}^{N} \frac{1}{\lambda\sigma_i^2} \end{pmatrix} \begin{pmatrix} a \\ b \end{pmatrix} = \begin{pmatrix} \sum_{i=1}^{N} \frac{t_i(\underset{\sim}{O}-\underset{\sim}{C})_i}{\lambda\sigma_i^2} \\ \sum_{i=1}^{N} \frac{(\underset{\sim}{O}-\underset{\sim}{C})_i}{\lambda\sigma_i^2} \end{pmatrix}, \tag{20}$$

where N is the number of observation residuals in the fit; λ is the multiplier defined by equation (38) of SECTION 7; and t_i is the time of the i^{th} observation. Matrix equation (20) is solved for a and b which are used with equation (19) to compute the standard error for the fit using the expressions:

$$r_i = (\underset{\sim}{O} - \underset{\sim}{C})_{i\ \text{corrected}} - y_i \quad (i = 1, 2, 3, \ldots, N), \text{ and} \tag{21}$$

$$\sigma = \left[\sum_{i=1}^{N} \frac{r_i^2}{N} \right]^{\frac{1}{2}} . \tag{22}$$

Equation (22) is used to perform the statistical residual quality edit on each point editor iteration but the first. This test is stated as follows: if

$$|r_i| > 2.5\ \sigma \quad , \text{ tag the observation .} \tag{23}$$

8.1.3 OBSERVATION RESIDUAL QUALITY EDITING (con't)

As noted in SECTION 7, the tagged observations are used in each iteration to perform the linear fit and in equations (21) - (23). They are not used in the formation of the pass normal equations.

The λ multiplier in equation (20) (and equation (38) of SECTION 7) is set equal to unity on the first iteration and is computed on successive iterations from the expression

$$\lambda_{new} = (S/N)_p^2 \quad \lambda_{previous} \quad , \tag{24}$$

where

$$(S/N)_p^2 = \left| V - \underset{\sim}{\varepsilon}_s^T \underset{\sim}{\varepsilon}_s \right| \Big/ \left[\text{MAX}\ (1,\ N_G - N_S) \right] \quad . \tag{25}$$

In this equation N_G is the number of untagged points in the pass; N_S is the number of best determined parameters used in the solution to the pass normal equations; $\underset{\sim}{\varepsilon}_S$ is a transformed $\underset{\sim}{E}$ matrix used in the solution to the pass normal equations; and V is the variance given by

$$V = \sum_{i=1}^{N_G} \left[\frac{(\underset{\sim}{O} - \underset{\sim}{C})_i^2 \text{ corrected}}{\lambda \sigma_i^2} \right] \quad . \tag{26}$$

The N_S number and the $\underset{\sim}{\varepsilon}_S$ matrix are discussed in the Cholesky decomposition subsection of SECTION 9.

8.1.4 OBSERVATION QUANTITY EDITING

As the point editor iterates during its processing, it will tag observations as being of insufficient quality. It may also untag previously tagged observations if they return to the quality bounds established during each iteration (see SECTION 8.1.2). This processing may produce a situation where too few observations remain in a pass for a successful solution to the associated pass

8.1.4 OBSERVATION QUANTITY EDITING (con't)

normal equation to be obtained. Such passes are then rejected. The standard used to determine this is straight-forward and given as follows: if

$$N_R < .01\ P \bullet N_o \quad \text{, reject the pass,} \tag{27}$$

where N_R is the number of untagged observations remaining; P is the predetermined percentage of original observations which must be untagged and below which the pass is rejected; and N_o is the original number of observations in the pass.

8.1.5 ITERATIVE CONVERGENCE CRITERIA

Observation data is processed by the point editor on a pass-by-pass basis. When the last pass has been processed, the point editing procedure is terminated. This termination is keyed from an end of file condition.

In order that the point editor exit at the proper time from the iterative loop for a pass, one of the following two conditions must be satisfied: if either

$$\left.\begin{array}{l} N_{I_p} > N_{I_{MAX_p}} \\ \text{or} \\ N_{G_j} = N_{G_{j-1}} = N_{G_{j-2}} \end{array}\right\} \text{, exit iteration loop normally and process next pass,} \tag{28}$$

where N_{I_p} is the number of iterations performed for a pass; $N_{I_{MAX_p}}$ is the maximum number of iterations allowed for a pass; and N_{G_k} is the number of untagged observations for iteration k.

8.2 CROSS PASS EDITOR METHODS AND CRITERIA

The cross pass editor uses the statistics of the navigation solutions for all passes to identify those passes of observation data which lack the quality required for post-PULSAR processing. The methods used to identify those passes are described below. The iterative convergence criteria used by the cross pass editor are also given. It should be mentioned that if an orbit adjust occurs during the editing span, then the tests and criteria discussed below are applied independently to each trajectory segment (refer to subsections 7.1.2 and 9.3.4).

8.2.1 NAVIGATION SOLUTION QUALITY EDITING

In order to identify those passes of data which are outliers, on each iteration the cross pass editor performs a coarse tolerance test to identify and to tag those passes which have tangential(ΔT_i) or radial (ΔR_i) navigation solutions (see equation (85) of Section 7) that are obvious outliers. The remaining untagged ΔT_i and ΔR_i are used to fit a quadratic equation from which a standard deviation is computed and used to edit the ΔT_i and ΔR_i for the remaining untagged passes.

To be more explicit, the coarse tolerance test used by the cross pass editor is as follows: if for the i^{th} pass

$$|\Delta R_i| > \eta_{TOL_{\Delta R_i}}$$

or , tag the pass, (29)

$$|\Delta T_i| > \eta_{TOL_{\Delta T_i}}$$

where the η_{TOL} are predetermined tolerance values. The remaining untagged ΔR_i and ΔT_i are fit with a quadratic of the form

$$y = at_{CA}^2 + bt_{CA} + C. \quad (30)$$

8.2.1 NAVIGATION SOLUTION QUALITY EDITING (con't)

The required normal equation may be written as

$$\begin{pmatrix} \sum_{i=1}^{N} t_{CA_i}^4 & \sum_{i=1}^{N} t_{CA_i}^3 & \sum_{i=1}^{N} t_{CA_i}^2 \\ \sum_{i=1}^{N} t_{CA_i}^3 & \sum_{i=1}^{N} t_{CA_i}^2 & \sum_{i=1}^{N} t_{CA_i} \\ \sum_{i=1}^{N} t_{CA_i}^2 & \sum_{i=1}^{N} t_{CA_i} & N \end{pmatrix} \begin{pmatrix} a \\ b \\ c \end{pmatrix} = \begin{pmatrix} \sum_{i=1}^{N} t_{CA_i}^2 \theta_i \\ \sum_{i=1}^{N} t_{CA_i} \theta_i \\ \sum_{i=1}^{N} \theta_i \end{pmatrix} \quad ,(31)$$

where N is the number of untagged navigation solutions and θ_i is either ΔR_i or ΔT_i, depending upon which is being fit. Using the definition

$$r_i = \left\{ \begin{array}{c} \Delta R_i \\ \text{or} \\ \Delta T_i \end{array} \right\} - y_i \qquad (i = 1, 2, \ldots, N), \tag{32}$$

the test used to quality edit the ΔR_i and ΔT_i navigation solutions may be stated as follows: if for the j^{th} arc solution

$$\frac{r_i^2}{\sigma_\theta^2 + \sigma_{j-1}^2} > 2 \sum_{i=1}^{N} \frac{r_i^2}{N(\sigma_\theta^2 + \sigma_{j-1}^2)} \quad \text{, tag the pass.} \tag{33}$$

8.2.1 NAVIGATION SOLUTION QUALITY EDITING (con't)

In this expression

$$\sigma_\theta^2 = \sum_{i=1}^{N} \frac{\theta_i^2}{N} \tag{34}$$

and σ_{j-1}^2 is the standard error for the $(j-1)^{th}$ arc solution given by

$$\sigma_{j-1}^2 = \begin{cases} \sum_{i=1}^{N} \frac{(\theta_i - y_i)^2}{N}_{j-1} & \text{for } j > 1 \\ 10^5 & \text{for } j = 1. \end{cases} \tag{35}$$

In the last two equations θ_i represents ΔR_i or ΔT_i, depending upon which is being edited, and N is the number of untagged passes. This process (i.e. equations (30) - (35)) is repeated m times, where m is a integer constant. Each of the m times this process is repeated only untagged passes are used to form the test conditions (i.e. (30), (31), (34), (35)), but both tagged and untagged passes are tested using inequality (33). Those passes which are tagged after the m^{th} iteration are omitted from the arc solution. However, during each arc solution iteration, those passes which were tagged are used again to generate new navigation solutions and their quality again assessed. If it is adequate the tags are removed and the passes are used in generating succeeding arc solutions.

8.2.2 ITERATIVE CONVERGENCE CRITERIA

In order that the cross pass editor exit from its iterative arc solution loop at the proper time, one of the following two conditions must be satisfied: if either

$$\left.\begin{array}{l} N_{I_C} > N_{I_{MAX_C}} \\ \text{or} \\ S_j = S_{j-1} \end{array}\right\} \quad , \quad \text{exit iteration loop normally,} \tag{36}$$

8.2.2 ITERATIVE CONVERGENCE CRITERIA (con't)

where N_{I_C} is the number of iteration loops completed by the cross pass editor; N_{IMAX_C} is the maximum number of iterations allowed for the cross pass editor; and S_k is the set of passes that were tagged on iteration k.

8.3 STATE VECTOR VALIDITY

As an option, the arc solution $\Delta\underset{\sim}{p}_{ARC}$ obtained from the last iteration of the cross pass editor can be tested to see if the initial state vector should be corrected to produce an improved reference trajectory. If the testing proves positive then the state vector at trajectory epoch t_0 is corrected using the results of SECTION 7.2; a new reference trajectory is generated; and the point and cross pass editing processes are repeated. It should be mentioned that when an orbit adjust occurs during the editing span, this process is repeated independently for each trajectory segment.

In order to devise a method for determining the acceptability of the initial state vector consider the pass variance defined by:

$$V(\underset{\sim}{p}_0) = \sum_{i=1}^{N} \frac{(\underset{\sim}{O} - \underset{\sim}{C})_i^2}{\lambda\sigma_i^2} = (\underset{\sim}{O} - \underset{\sim}{C}(\underset{\sim}{p}_0))^T \underset{\sim}{W} (\underset{\sim}{O} - \underset{\sim}{C}(\underset{\sim}{p}_0)) \quad , \tag{37}$$

where N is the number of observations during the pass and $\underset{\sim}{p}_0$ is the set of parameters to be corrected. Suppose the arc solution $\Delta\underset{\sim}{p}_{ARC}$ has been obtained upon convergence of the cross pass editor. If this arc solution is used to correct the initial state vector and regenerate a new reference trajectory, then some new $\Delta\underset{\sim}{p}$ will be introduced into the pass normal equations. The associated pass variance then becomes $V(\underset{\sim}{p}_0 + \Delta\underset{\sim}{p})$ which, when expanded in a Taylor series about $\underset{\sim}{p}_0$, has the form

8.3 STATE VECTOR VALIDITY (con't)

$$\mathbf{V}(\underset{\sim}{p}_0 + \Delta\underset{\sim}{p}) \simeq \mathbf{V}(\underset{\sim}{p}_0) + \left(\frac{\partial \mathbf{V}}{\partial \underset{\sim}{p}}\right)^T_{p_0} \Delta\underset{\sim}{p} + \frac{1}{2} \Delta\underset{\sim}{p}^T \left(\frac{\partial^2 \mathbf{V}}{\partial \underset{\sim}{p}^2}\right)_{p_0} \Delta\underset{\sim}{p} \cdot \tag{38}$$

Since

$$\frac{\partial V}{\partial \underset{\sim}{p}} = -2\underset{\sim}{E} \quad , \tag{39}$$

then

$$\frac{\partial^2 V}{\partial \underset{\sim}{p}^2} = -2\frac{\partial \underset{\sim}{E}}{\partial \underset{\sim}{p}} = 2\underset{\sim}{B} \quad , \tag{40}$$

so that one may write

$$\mathbf{V}(\underset{\sim}{p}_0 + \Delta\underset{\sim}{p}) \simeq \mathbf{V}(\underset{\sim}{p}_0) - 2\underset{\sim}{E}(\underset{\sim}{p}_0)^T \Delta\underset{\sim}{p} + \Delta\underset{\sim}{p}^T \underset{\sim}{B}(p_0)\, \Delta\underset{\sim}{p} \quad . \tag{41}$$

Using equation (58) of SECTION 7, the last equation may be rewritten as:

$$\mathbf{V}(\underset{\sim}{p}_0 + \Delta\underset{\sim}{p}) \simeq \mathbf{V}(\underset{\sim}{p}_0) - 2\underset{\sim}{E}^T_\alpha(\underset{\sim}{p}_0)\Delta\underset{\sim}{p}_\alpha - 2\underset{\sim}{E}^T_b(\underset{\sim}{p}_0)\Delta\underset{\sim}{p}_b + \Delta\underset{\sim}{p}^T_\alpha \underset{\sim}{B}_{\alpha\alpha}(\underset{\sim}{p}_0)\, \Delta\underset{\sim}{p}_\alpha$$

$$+ \Delta\underset{\sim}{p}^T_\alpha \underset{\sim}{B}_{\alpha b}(\underset{\sim}{p}_0)\Delta\underset{\sim}{p}_b + \Delta\underset{\sim}{p}^T_b \underset{\sim}{B}_{b\alpha}(\underset{\sim}{p}_0)\Delta\underset{\sim}{p}_\alpha + \Delta\underset{\sim}{p}^T_b \underset{\sim}{B}_{bb}(\underset{\sim}{p}_0)\Delta\underset{\sim}{p}_b \quad , \tag{42}$$

where as before subscript "α" represents all dynamic and station location parameters and subscript "b" represents the bias parameters. If equation (61) of SECTION 7 is substituted for $\Delta\underset{\sim}{p}_b$ in the last equation, one finds that after some algebraic manipulation:

8.3 STATE VECTOR VALIDITY (con't)

$$V(\underset{\sim}{p}_o + \Delta\underset{\sim}{p}) \approx V(\underset{\sim}{p}_o) + \Delta\underset{\sim}{p}_\alpha^T \left[\underset{\sim}{B}_{\alpha\alpha}(\underset{\sim}{p}_o) - \underset{\sim}{B}_{\alpha b}(\underset{\sim}{p}_o)\, \underset{\sim}{B}_{bb}^{-1}(\underset{\sim}{p}_o)\, \underset{\sim}{B}_{b\alpha}(\underset{\sim}{p}_o) \right] \Delta\underset{\sim}{p}_\alpha$$

$$- 2 \left[\underset{\sim}{E}_\alpha^T(p_o) - \underset{\sim}{E}_b^T(\underset{\sim}{p}_o)\, \underset{\sim}{B}_{bb}^{-1}(\underset{\sim}{p}_o)\, \underset{\sim}{B}_{b\alpha}(\underset{\sim}{p}_o) \right] \Delta\underset{\sim}{p}_\alpha$$

$$- \underset{\sim}{E}_b^T(\underset{\sim}{p}_o)\, \underset{\sim}{B}_{bb}^{-1}(\underset{\sim}{p}_o)\, \underset{\sim}{E}_b(\underset{\sim}{p}_o) \quad . \tag{43}$$

By inspection it is seen that the two terms in brackets in the last equation are the bias eliminated pass matrices given by equations (64) - (65) in SECTION 7. Thus

$$V(\underset{\sim}{p}_o + \Delta\underset{\sim}{p}) \approx V(\underset{\sim}{p}_o) + \Delta\underset{\sim}{p}_\alpha^T\, \underset{\sim}{B}_{\varepsilon_{\alpha\alpha}}(\underset{\sim}{p}_o)\, \Delta\underset{\sim}{p}_\alpha - 2\, \underset{\sim}{E}_{\varepsilon_\alpha}^T(\underset{\sim}{p}_o)\, \Delta\underset{\sim}{p}_\alpha$$

$$- \underset{\sim}{E}_b^T(\underset{\sim}{p}_o)\, \underset{\sim}{B}_{bb}^{-1}(\underset{\sim}{p}_o)\, \underset{\sim}{E}_b(\underset{\sim}{p}_o) \quad . \tag{44}$$

The last equation can be summed over all passes, taking care to properly segregate the resulting station coordinate submatrices. This gives

$$V'(\underset{\sim}{p}_o + \Delta\underset{\sim}{p}) \approx V'(\underset{\sim}{p}_o) + \Delta\underset{\sim}{p}'^T\, \underset{\sim}{B}'(\underset{\sim}{p}_o)\, \Delta\underset{\sim}{p}' - 2\, \underset{\sim}{E}'^T(\underset{\sim}{p}_o)\Delta\underset{\sim}{p}' -$$

$$- \sum_{\substack{\text{all} \\ \text{passes}}} \underset{\sim}{E}_b^T(\underset{\sim}{p}_o)\, \underset{\sim}{B}_{bb}^{-1}(\underset{\sim}{p}_o)\, \underset{\sim}{E}_b(\underset{\sim}{p}_o) \quad , \tag{45}$$

where $\Delta\underset{\sim}{p}'$, $\underset{\sim}{B}'(\underset{\sim}{p}_o)$, and $\underset{\sim}{E}'(\underset{\sim}{p}_o)$ have the form given by matrix equation (66) of SECTION 7. Station elimination can be performed using equation (70) of SECTION 7 to yield the final result:

TABLE 9-1. TABULATION OF COWELL COEFFICIENTS, C_j, AND ADAMS COEFFICIENTS a'_j

j	Cj	$a'j$
0	1/12	1/2
1	0	-1/12
2	-1/240	-1/24
3	-1/240	-19/720
4	-221/60480	-3/160
5	-19/6048	-863/60480
6	-9829/3628800	-275/24192
7	-407/172800	-33953/3628800
8	-330157/159667200	-8183/1036800
9	-24377/13305600	-3250433/479001600
10	-4281164477/2615348736000	-4671/788480
11	-70074463/47551795200	-13695779093/2615348736000
12	-1197622087/896690995200	-2224234463/475517952000
13	-97997951/80472268800	-132282840127/31384184832000

9.3.1 RUNNING PROCEDURE (con't)

$$\nabla^{-2}(h^2 \ddot{\vec{x}}_n) = \nabla^{-2}(h^2 \ddot{\vec{x}}_{n-1}) + \nabla^{-1}(h^2 \ddot{\vec{x}}_n) \tag{27}$$

and

$$\nabla^{-1}(h^2 \ddot{\vec{x}}_n) = \nabla^{-1}(h^2 \ddot{\vec{x}}_{n-1}) + \nabla^{0}(h^2 \ddot{\vec{x}}_n) \quad , \tag{28}$$

where $\nabla^{-2} h^2 \ddot{\vec{x}}_n$ and $\nabla^{-1} h^2 \ddot{\vec{x}}_n$ are called the second and first sums, respectively. They are computed during the starting procedure and are extrapolated forward as required during the running process.

These extrapolated differences are used to predict the position and velocity at t_{n+1} through the application of the predictor formulae

$$\vec{x}_{n+1} = \nabla^{-2}(h^2 \ddot{\vec{x}}_n) + \sum_{j=0}^{m} C_j \nabla^j (h^2 \ddot{\vec{x}}_{n+1}) \tag{29}$$

and

$$\dot{\vec{x}}_{n+1} = \frac{1}{h} \left\{ \nabla^{-1}(h^2 \ddot{\vec{x}}_n) + \sum_{j=0}^{m} a_j^* \nabla^j (h^2 \ddot{\vec{x}}_{n+1}) \right\} \quad , \tag{30}$$

where m is the order of integration, i.e. the number of acceleration values used in the predictors, and the C_j and a_j^* are the Cowell and Adams coefficients, respectively. These coefficients are tabulated in Table 9-1. These predicted position and velocity values are used in Equation (1) of SECTION 5 and equation (7) of SECTION 6 to produce the predicted accelerations $h^2 \ddot{\vec{x}}_{n+1_{pred.}}$. An extrapolated acceleration $h^2 \ddot{\vec{x}}_{n+1_{extrap.}}$ is obtained from equation (26) when $k = 0$ and the two are differenced to obtain the correction

$$\delta(h^2 \ddot{\vec{x}}) = h^2 \ddot{\vec{x}}_{n+1_{pred.}} - h^2 \ddot{\vec{x}}_{n+1_{extrap.}} \quad . \tag{31}$$

9.3 THE COWELL INTEGRATOR (con't)

trajectory epoch so that the eight point interpolation method described earlier can be used in the neighborhood of the start time. The following subsections describe the basic algorithm, the starting procedure, and those special procedures mentioned above.

9.3.1 RUNNING PROCEDURE

Once the starting procedure has been completed (see next subsection) the integrator operates in the running mode. The integration step from t_n to t_{n+1}, where

$$t_{n+1} = t_n + h \quad , \tag{22}$$

and h is a fixed integration step size, is initiated by extrapolating the backward difference table forward one time step. The backward differences $\nabla^k h^2 \ddot{\vec{x}}(t_n)$ are defined by the following relationships:

$$\nabla(h^2 \ddot{\vec{x}}_n) = \nabla\left(h^2 \ddot{\vec{x}}(t_n)\right) = h^2 \left[\ddot{\vec{x}}(t_n) - \ddot{\vec{x}}(t_{n-1}) \right] \tag{23}$$

and

$$\nabla^k(h^2 \ddot{\vec{x}}_n) = \nabla \left[\nabla^{k-1}(h^2 \ddot{\vec{x}}_n) \right] \quad . \tag{24}$$

(Here $\vec{x}$ will be used to represent both $\vec{r}$ and $\vec{\Psi}_{p_k}$, since both the equations of motion and the variational equations are integrated simultaneously using the same algorithm). The extrapolation is performed as follows by holding the highest difference fixed:

$$\nabla^m(h^2 \ddot{\vec{x}}_{n+1}) = \nabla^m(h^2 \ddot{\vec{x}}_n) \tag{25}$$

$$\nabla^k(h^2 \ddot{\vec{x}}_{n+1}) = \nabla^k(h^2 \ddot{\vec{x}}_n) + \nabla^{k+1}(h^2 \ddot{\vec{x}}_{n+1}), \quad k = m - 1, \cdots, 0 \tag{26}$$

9.2.2 COMPUTATION OF ECCENTRIC ANOMALY (con't)

This result can then be used with equation (16) to construct the $g(E')$ function and the following recursion relation:

$$E'_{n+1} = E'_n - \left\{ \frac{E'_n - e'' \sin E'_n - \ell''}{1 - e'' \cos E'_n} \right\} \quad . \tag{18}$$

The eccentric anomaly is computed by repeating the calculation of the last equation until

$$|E'_{n+1} - E'_n| \leq 10^{-8} \text{ radian} \quad . \tag{19}$$

When this condition is satisfied, then

$$E' = E'_{n+1} \quad . \tag{20}$$

The computations of equation (18) are initiated using

$$E'_1 = \ell'' + \left(\frac{e'' \sin \ell''}{1 - e'' \cos \ell''} \right) \quad . \tag{21}$$

9.3 THE COWELL INTEGRATOR

The Cowell predictor-corrector method is used by PULSAR to simultaneously numerically integrate the satellite equation of motion (see equation (1) of SECTION 5) and the associated variational equations (see equation (7) of SECTION 6). This numerical integrator is a fixed step/multistep algorithm based upon the integration of a backward difference formula fitted to a set of acceleration data. It is not a self starting process and uses a unique technique for supplying a backward difference table at the trajectory start time necessary for operating in the running mode. Furthermore, special procedures are required for trajectory generation in the neighborhood of orbit adjust intervals, as well as for generating trajectory data prior to the

9.2.1 COMPUTATION OF TIME OF CLOSEST APPROACH (t_{CA}) (Con't)

or until the maximum iteration count is reached. If equation (13) is satisfied then

$$t_{CA} = t_{i+1} \quad . \tag{14}$$

However if the maximum iteration count is reached, then

$$t_{CA} = t_{est} \quad , \tag{15}$$

where t_{est} is the estimated t_{CA} supplied for the pass by the observing station. This is obtained by sensing a change of sign in the range difference measurements. Should no sign change occur, t_{est} is set by the station to the time of the second observation. It is possible that this will be a frequent occurrence for the satellites supported by the PULSAR system, since their continuously varying attitudes can result in partial passes of observation data that may contain no t_{CA} which satisfies equation (10). It should be mentioned that equation (12) for $i = 1$ is initiated using $t_1 = t_{est}$.

9.2.2 COMPUTATION OF ECCENTRIC ANOMALY

As mentioned in SECTION 5, the Newton - Raphson iteration is used to compute the eccentric anomaly associated with the mean anomaly and eccentricity generated by the Brouwer orbit predictor. This is done by iteratively solving the Kepler equation given by equation (72) of SECTION 5. One rewrites this equation as

$$f(E') = E' - e'' \sin E' - \ell'' = 0 \quad , \tag{16}$$

where E', ℓ'' and e" are the eccentric anomaly, the mean anomaly, and the eccentricity, respecitvely. This expression may be differentiated with respect to E' to give

$$f'(E') = \frac{d\, f(E')}{dE'} = 1 - e'' \cos E' \quad . \tag{17}$$

9.2.1 COMPUTATION OF THE TIME OF CLOSEST APPROACH (t_{CA})

where

$$\dot{\vec{\rho}} = \dot{\vec{r}} - \dot{\vec{R}} \quad ,$$

$$\ddot{\vec{\rho}} = \ddot{\vec{r}} - \ddot{\vec{R}} \quad ,$$

$$\dot{\vec{R}} = \vec{\omega} \times \vec{R} \quad , \qquad (11)$$

and

$$\ddot{\vec{R}} = \vec{\omega} \times \dot{\vec{R}} \quad .$$

The satellite velocity and acceleration vectors are interpolated using equations (2) and (3). The angular velocity of the earth is given by equation (18) of Section 5.

Equations (11) are used to construct the $g(t)$ function and the associated recursion relation:

$$t_{i+1} = t_i - \left\{ \frac{\vec{\rho}(t_i) \cdot \dot{\vec{\rho}}(t_i)}{\dot{\vec{\rho}}(t_i) \cdot \dot{\vec{\rho}}(t_i) + \vec{\rho}(t_i) \cdot \ddot{\vec{\rho}}(t_i)} \right\} . \qquad (12)$$

To compute t_{CA} this recursion relation is repeated until

$$|t_{i+1} - t_i| < .05 \text{ second} \qquad (13)$$

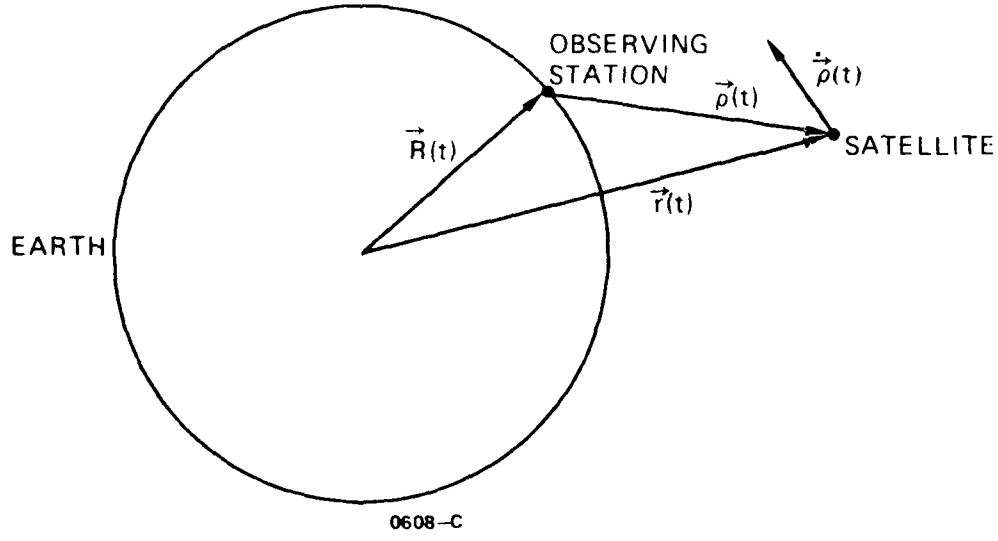

$\vec{r}(t)$ = INERTIAL POSITION VECTOR OF SATELLITE AT TIME t
$\vec{R}(t)$ = INERTIAL POSITION VECTOR OF STATION AT TIME t
$\vec{\rho}(t)$ = SATELLITE POSITION VECTOR RELATIVE TO THE STATION AT TIME t
$\dot{\vec{\rho}}(t)$ = SATELLITE VELOCITY VECTOR RELATIVE TO THE STATION AT TIME t

FIGURE 9-1. Satellite-Observing Station Relative Geometry

9.2 NEWTON - RAPHSON ITERATION

The Newton-Raphson method is an iterative technique which is used to find the zeroes of a differentiable function. It is used in PULSAR to find times of closest approach (t_{CA}) for individual passes, as well as to solve Kepler's equation for the eccentric anomalies of NAVSAT satellites at a specific time for the purpose of clock calibration (see SECTION 3). In general the method may be stated as follows: if $f(x)$ is a function such that $f'(x) = \frac{d\,f(x)}{dx} \neq 0$, and p_0 is an approximation to a solution of $f(x) = 0$, then the sequence $\{p_n\}$ which converges to the zero at $x = p$ can be generated recursively by the relation $p_n = g(p_{n-1})$, $n = 1, 2, \cdots$, where

$$g(x) = x - \frac{f(x)}{f'(x)} \quad . \tag{9}$$

The application of this method to finding t_{CA} and solving the Kepler equation are discussed below.

9.2.1 COMPUTATION OF TIME OF CLOSEST APPROACH (t_{CA})

The time of closest approach of a satellite to an observing station is the point in time at which the relative velocity component along the line of sight changes in sign. In order to formulate this in a precise way consider the geometry of Figure 9-1, where $\vec{\rho}(t)$ and $\dot{\vec{\rho}}(t)$ are the satellite position and velocity vectors relative to the observing station, respectively. By inspection one sees that the t_{CA} is the solution of the equation

$$\vec{\rho}(t) \cdot \dot{\vec{\rho}}(t) = 0 \quad . \tag{10}$$

To apply the Newton-Raphson method to solving this equation for t_{CA}, one takes the derivative with respect to time of the last equation giving

$$\frac{d}{dt}\left[\vec{\rho}(t) \cdot \dot{\vec{\rho}}(t)\right] = \dot{\vec{\rho}}(t) \cdot \dot{\vec{\rho}}(t) + \vec{\rho}(t) \cdot \ddot{\vec{\rho}}(t) \quad , \tag{11}$$

9.1 LAGRANGE INTERPOLATION (con't)

$$\mathcal{L}_i(t) = \prod_{\substack{j=0 \\ j\neq i}}^{n} \left(\frac{t - t_j}{t_i - t_j} \right) \quad , \tag{3}$$

$$\dot{\mathcal{L}}_i(t) = \prod_{\substack{j=0 \\ j\neq i}}^{n} \left(\frac{t - t_j}{t_i - t_j} \right) \left\{ \sum_{\substack{j=0 \\ j\neq i}}^{n} \left(\frac{1}{t - t_j} \right) \right\} \quad , \tag{4}$$

and

$$\ddot{\mathcal{L}}_i(t) = \prod_{\substack{j=0 \\ j\neq i}}^{n} \left(\frac{t - t_j}{t_i - t_j} \right) \left\{ \left[\sum_{\substack{j=0 \\ j\neq i}}^{n} \left(\frac{1}{t - t_j} \right) \right]^2 - \sum_{\substack{j=0 \\ j\neq i}}^{n} \left(\frac{1}{t - t_j} \right)^2 \right\} \quad . \tag{5}$$

In equations (1) - (6) n assumes the following values:

$$n = 7 \ , \quad \left\{ \begin{array}{l} \text{variational equations} \\ \text{satellite ephemerides} \end{array} \right. \quad ; \tag{6}$$

$$n = 5 \ , \quad \left\{ \begin{array}{l} \text{sun/moon ephemerides} \\ \text{nutation angles} \end{array} \right. \quad ; \tag{7}$$

and

$$n = 1 \ , \quad \left\{ \begin{array}{l} \text{pole wander values} \\ \text{UT1 - UTC time corrections.} \end{array} \right. \tag{8}$$

9.1 LAGRANGE INTERPOLATION

Numerical solutions to the variational equations, satellite ephemerides, sun and moon ephemerides, nutation angles, pole wander values, and UT1 - UTC time corrections are stored at discreet equally spaced times for use within PULSAR. In order to obtain these data at times other than those stored, it is necessary to employ an interpolation procedure. PULSAR utilizes the Lagrange interpolation method of various orders to obtain these data. This method involves fitting polynomials to the data points being interpolated and centering the fits such that equal numbers of points lie on either side of the interpolation time.

The polynomials for interpolating each type of data stored by PULSAR are of the form:

$$y(t) = \sum_{i=0}^{n} \mathcal{L}_i (t) y (t_i) . \qquad (1)$$

First time derivatives of satellite position and variational equation solutions and second time derivatives of satellite position are computed using:

$$\dot{y}(t) = \sum_{i=0}^{n} \dot{\mathcal{L}}_i (t) y (t_i)$$

and (2)

$$\ddot{y}(t) = \sum_{i=0}^{n} \ddot{\mathcal{L}}_i (t) y (t_i) \quad .$$

In the above expressions t is the interpolation time, t_i are the times for which the data to be interpolated exist, and

SECTION 9

NUMERICAL METHODS

In the previous sections a mathematical description of the PULSAR system has been developed and discussed. However, since the system is largely automated, a gap still exists between the purely analytical treatment of the preceeding text and the practical implementation of the analytics into the framework of the computational capability of the electronic computer. For example, the analytic development provides equations of motion which must be numerically integrated by the computer to generate a usable ephemeris; but the analytical development does not prescribe a method by which the computer can do this. It is the purpose of this section to close this gap by describing in some detail those special numerical techniques employed by the PULSAR system for use on the computer.

Presented in the following subsections are overviews of the numerical techniques used by PULSAR for:

(i) data point interpolation;

(ii) the solution of equations by fixed-point iteration;

(iii) numerically integrating the equations of motion and variational equations;

(iv) solving the pass normal equations; and

(v) compacting observation data.

Should further detail concerning these methods be required the reader is referred to several excellent numerical analysis texts. [1,2]

[1] Blum, E. K., Numerical Analysis and Computation Theory and Practice, Addison-Wesley Publishing Co., 1972.

[2] Moursund, D. G. and Duris, C. S., Elementary Theory and Application of Numerical Analysis, McGraw-Hill Book Company, 1967.

8.3 STATE VECTOR VALIDITY (con't)

In the above inequalities N_{CYCLE} is the number of times the editing cycle has been repeated; $N_{CYCLE_{MAX}}$ is the maximum number of such cycles allowed; and s_i (i = 1, 2) are predetermined tolerance values.

As noted in SECTION 7.2, if a recycling is required, the state vector for succeeding days should be improved using the correction propagation techniques discussed in that section.

8.3 STATE VECTOR VALIDITY (con't)

where $(S/N)_{SbR}$ is the station and bias reduced arc signal to noise given by:

$$(S/N)^2_{SbR} =$$

$$\frac{V'(\underset{\sim}{p}_o) - \sum_k \underset{\sim}{E}^T_{\varepsilon_{s_k}}(\underset{\sim}{p}_o)\underset{\sim}{B}^{-1}_{\varepsilon_{s_k}s_k}(\underset{\sim}{p}_o)\underset{\sim}{E}_{\varepsilon_{s_k}}(\underset{\sim}{p}_o) - \sum_{\substack{\text{all}\\ \text{passes}}} \underset{\sim}{E}^T_b(\underset{\sim}{p}_o)\ \underset{\sim}{B}^{-1}_{bb}(\underset{\sim}{p}_o)\ \underset{\sim}{E}_b(\underset{\sim}{p}_o)}{\sum_{i=1}^{M} N_i} \quad . \quad (49)$$

From this one may also compute the expected percent change in the arc variance due to a correction $\Delta\underset{\sim}{p}_{ARC}$ applied to the initial state vector. This is given by the expression

$$\Delta(S/N)^2_{ARC} = 100\left[\frac{(S/N)^2_{SbR} - (S/N)^2_{predicted}}{(S/N)^2_{SbR}}\right] \quad . \quad (50)$$

These results are used to formulate the criteria used by PULSAR to determine if a new reference trajectory need be generated and another editing cycle performed. If this option is selected, then the criteria may be stated as follows: if

$$N_{CYCLE} < N_{CYCLE_{MAX}}$$

and

$$(S/N)^2_{predicted} > \delta_1$$

and

$$\Delta(S/N)^2_{ARC} > \delta_2$$

then correct the initial state vector, regenerate reference trajectory, and recycle through point and cross pass editors. (51)

8.3 STATE VECTOR VALIDITY (con't)

$$V'(\underset{\sim}{p}_0 + \Delta\underset{\sim}{p}) \simeq V'(\underset{\sim}{p}_0) - \sum_k \underset{\sim}{E}^T_{\epsilon_{s_k}}(\underset{\sim}{p}_0)\, \underset{\sim}{B}^{-1}_{\epsilon_{s_k}s_k}(\underset{\sim}{p}_0)\, \underset{\sim}{E}_{\epsilon_{s_k}}(\underset{\sim}{p}_0)$$

$$- \sum_{\substack{\text{all} \\ \text{passes}}} \underset{\sim}{E}^T_b(\underset{\sim}{p}_0)\, \underset{\sim}{B}^{-1}_{bb}(\underset{\sim}{p}_0)\, \underset{\sim}{E}_b(\underset{\sim}{p}_0) - \underset{\sim}{E}^T_{ARC}(\underset{\sim}{p}_0)\, \Delta\underset{\sim}{p}_{ARC} \quad . \tag{46}$$

Thus an estimate of the variance for an orbit with corrected parameter values $\underset{\sim}{p}_0 + \Delta\underset{\sim}{p}$ can be predicted by using the variance for the uncorrected orbit and reducing it by station, bias, and arc solution terms.

To formulate in a concise way the two criteria used to determine if the trajectory must be regenerated from an improved state vector and the editing cycle repeated, one further definition is required: define the arc signal to noise ratio (S/N) as

$$(S/N)^2 = \frac{V'}{\sum_{i=1}^{M} N_i} \quad , \tag{47}$$

where N_i is the number of observations associated with the i^{th} pass and M is the number of passes. Then equation (46) can be used to obtain a prediction of the signal to noise value for a corrected orbit, i.e.

$$(S/N)^2_{predicted} = (S/N)^2_{SbR} - \frac{\underset{\sim}{E}^T_{ARC}(\underset{\sim}{p}_0)\, \Delta\underset{\sim}{p}_{ARC}}{\sum_{i=1}^{M} N_i} \quad , \tag{48}$$

9.3.1 RUNNING PROCEDURE (con't)

This difference is then used to correct the position and velocity by application of the expressions:

$$\vec{x}_{n+1_{corrected}} = \vec{x}_{n+1} + \delta\vec{x}_{n+1} \tag{32}$$

$$\dot{\vec{x}}_{n+1_{corrected}} = \dot{\vec{x}}_{n+1} + \delta\dot{\vec{x}}_{n+1} \quad , \tag{33}$$

where

$$\delta\vec{x}_{n+1} = \left(\sum_{j=0}^{m} C_j\right) \delta(h^2 \ddot{\vec{x}}) \tag{34}$$

and

$$\delta\dot{\vec{x}}_{n+1} = \frac{1}{h}\left(\sum_{j=0}^{m} a_j\right)\delta(h^2 \ddot{\vec{x}}) \quad . \tag{35}$$

Equations (32) - (33) are used to compute new accelerations and this process is continued until the number of such iterations exceeds that of an input control parameter. The extrapolated difference table is corrected using the expression

$$\nabla^j(h^2 \ddot{\vec{x}}_{n+1})_{corrected} = \nabla^j(h^2 \ddot{\vec{x}}_{n+1})_{extrapolated} + \delta(h^2 \ddot{\vec{x}}) \tag{36}$$

for $j = 0, 1, \ldots, m$. This completes the integration from t_n to t_{n+1}. The complete process is repeated for t_{n+2}, t_{n+3}, etc. A diagram is presented in Figure 9-2 which shows in flow form the running procedure (as well as the starting procedure described below).

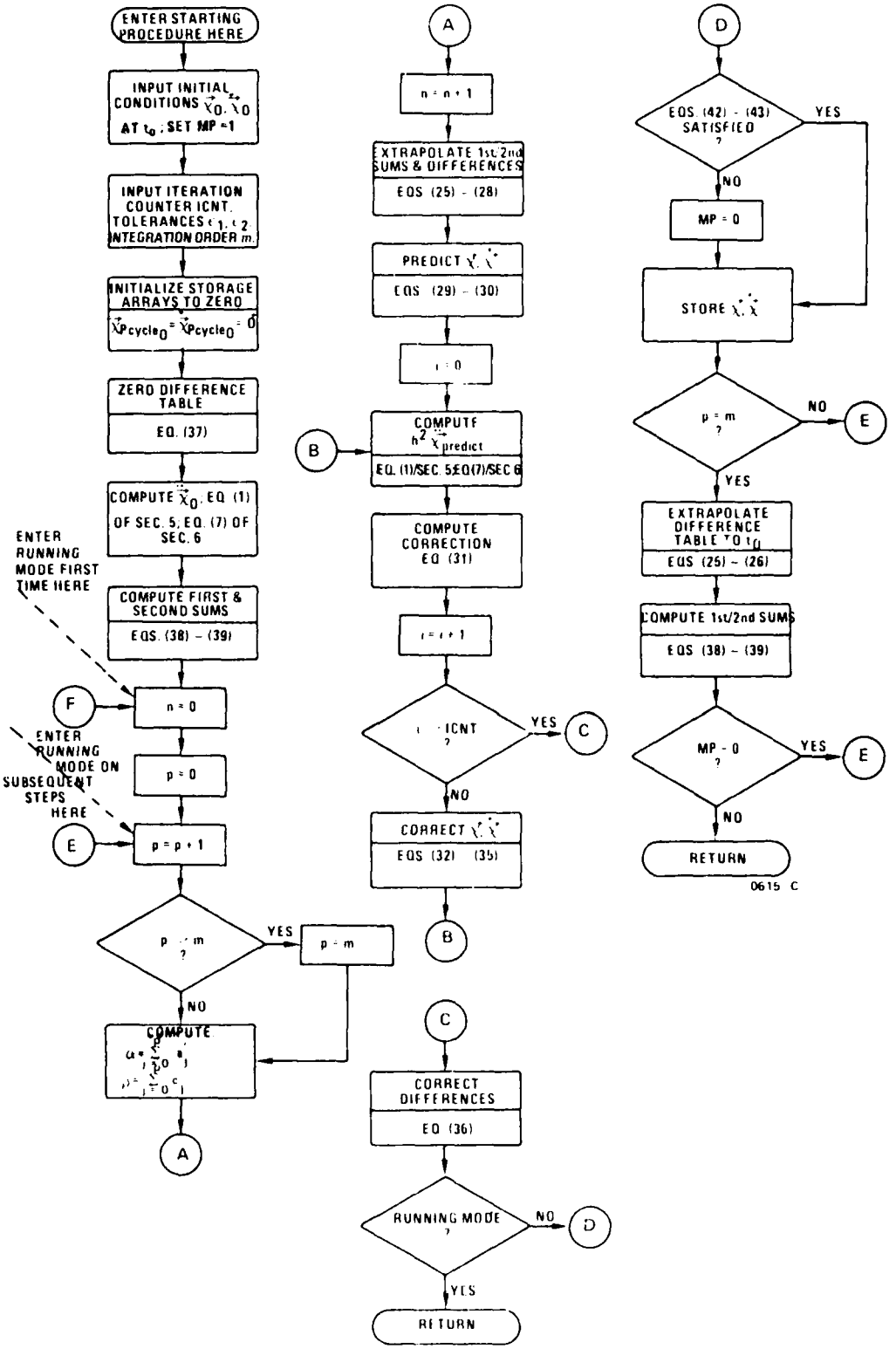

9-2 Starting Procedure and Running Procedure Flow

9.3.2 STARTING PROCEDURE

The Cowell integration process is initiated by using the initial conditions at trajectory epoch $\vec{x}_0 = \vec{x}(t_0)$ and $\dot{\vec{x}}_0 = \dot{\vec{x}}(t_0)$ to compute the accelerations $h^2 \ddot{\vec{x}}_0$ from equation (1) of SECTION 5 and equation (7) of SECTION 6. The difference table is initialized to zero for $k > 0$, i.e.

$$\nabla^k (h^2 \ddot{\vec{x}}_0) = 0 , \quad k = 1, 2, 3, \cdots, m, \tag{37}$$

and the first and second sums are computed by transposing equations (29) - (30), i.e.

$$\nabla^{-1} (h^2 \ddot{\vec{x}}_{-1}) = h \dot{\vec{x}}_0 - \sum_{j=0}^{m} a'_j \nabla^j (h^2 \ddot{\vec{x}}_0) \tag{38}$$

and

$$\nabla^{-2} (h^2 \ddot{\vec{x}}_{-1}) = \vec{x}_0 - \sum_{j=0}^{m} C_j \nabla^j (h^2 \ddot{\vec{x}}_0) \quad . \tag{39}$$

Integration is then performed for m time steps as described in the previous subsection for the running procedure, except that the corrections to $\vec{x}$ and $\dot{\vec{x}}$ are given by

$$\delta \vec{x}_p = \left(\sum_{j=0}^{p} C_j \right) \delta (h^2 \ddot{\vec{x}}) \tag{40}$$

and

$$\delta \dot{\vec{x}}_p = \frac{1}{h} \left(\sum_{j=0}^{p} a'_j \right) \delta (h^2 \ddot{\vec{x}}) \quad , \tag{41}$$

9.3.2 STARTING PROCEDURE (con't)

and only the first p differences are corrected by $\delta(h^2 \ddot{\vec{x}})$, i.e. equation (36) applies for $j = 0, 1, \cdots, p \leq m$. After the m^{th} time step has been completed, the difference table is extrapolated backward, holding the m^{th} difference constant, to obtain an improved difference table at the trajectory epoch using equations (25) - (26).

This completes the first cycle of the starting procedure. Cycling, which starts with the computation of the first and second sums using equations (38) - (39), is repeated until the conditions

$$\left| \vec{x}_{p_{\text{cycle } i}} - \vec{x}_{p_{\text{cycle } i-1}} \right| < \varepsilon_1 \tag{42}$$

and

$$\left| \dot{\vec{x}}_{p_{\text{cycle } i}} - \dot{\vec{x}}_{p_{\text{cycle } i-1}} \right| < \varepsilon_2 \tag{43}$$

are met for all p, where the ε_i $(i = 1, 2)$ are tolerance values. The starting procedure is then terminated and the running procedure is invoked. It should be noted that during the first m steps of the running mode the procedure for the starting mode is followed in that equations (40) - (41) apply and only the first p differences are corrected. Figure 9-2 shows the flow of the starting and running procedures.

9.3.3 BACKWARD INTEGRATION

In order to apply the eight point Lagrange interpolation method in the vicinity of the trajectory epoch t_0 it is necessary to integrate the satellite equations of motion (equation (1)/SECTION 5) and the variational equations (equation (7)/SECTION 6) for several time steps backward in time from t_0. It should be noted that the integration should also extend several time steps beyond the trajectory stop time t_e so that the interpolation technique can be applied in the neighborhood of t_e. The latter case presents no problem, since the normal integration process described in the previous subsections can be continued for some Δt

9.3.3 BACKWARD INTEGRATION (con't)

beyond t_e. However the backward integration case must be treated in a special fashion.

The backward integration process for integrating the equations of motion is initiated by changing the initial conditions from $\left(\vec{r}(t_o), \dot{\vec{r}}(t_o)\right)$ to $\left(\vec{r}(t_o), -\dot{\vec{r}}(t_o)\right)$. This sets the satellite's motion in the proper direction as the time is stepped backwards. However in order to produce the proper earth fixed/inertial reference frame transformations and the correct atmospheric drag acceleration it is also necessary to change the earth rotation vector's sign, i.e. use $-\vec{\omega}$ instead of $\vec{\omega}$, and the sign of the drag coefficient, i.e. use -D instead of D. As the time is stepped backward, the time for the n^{th} backward step given by

$$t = t_o - nh \quad , \qquad n = 1, 2, \ldots, \tag{44}$$

where h is the integration step size, should be used to compute the associated luni-solar gravitational accelerations, as well as the earth-fixed/inertial reference frame transformations (see SECTION 2). These modifications apply to the variational equations as well.

As a result of the changes to the initial conditions for the equations of motion, new variational equation initial conditions must be used which are consistent with those for the equations of motion. This can be seen more clearly by first noting the convolutions introduced into the Keplerian element set by making a velocity sign reversal. Consider Figure 9-3 which depicts the orbit configuration and associated Keplerian elements before and after the velocity sign reversal. The following relationships between the elements for the two cases can be obtained by inspection:

$$a' = a \quad ,$$

$$e' = e \quad ,$$

$$i' = \pi - i,$$

$$\omega' = \pi - \omega,$$

$$\Omega' = \pi + \Omega.$$

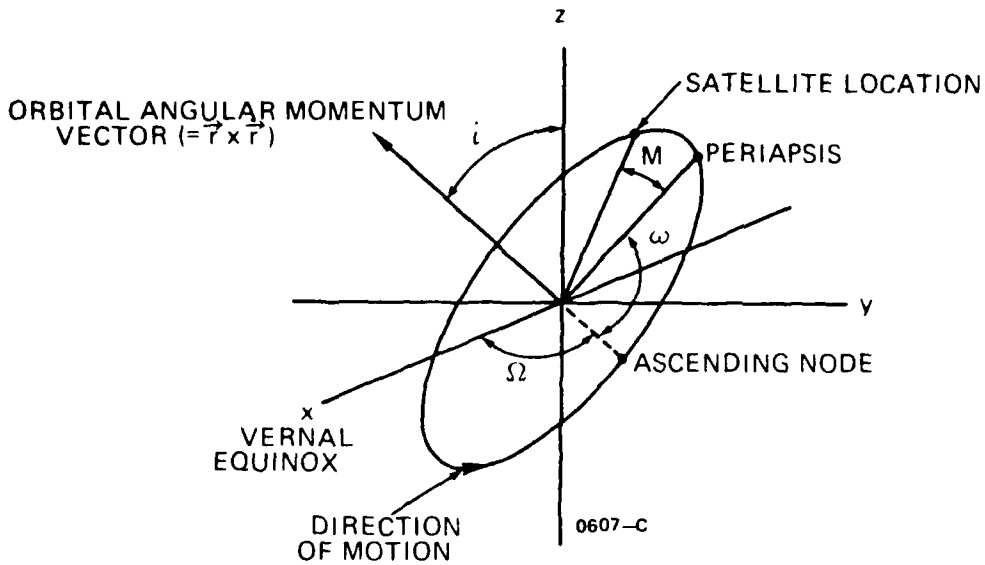

(a) BEFORE VELOCITY SIGN REVERSAL

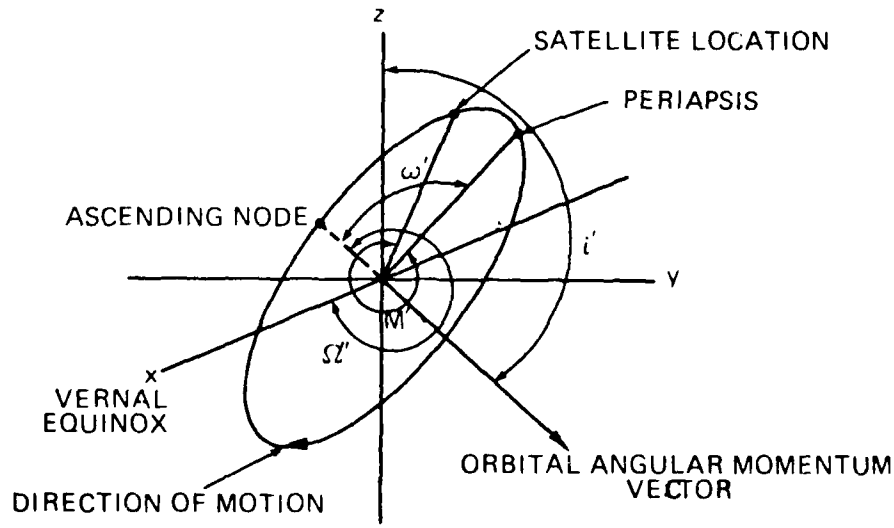

(b) AFTER VELOCITY SIGN REVERSAL

FIGURE 9-3. Keplerian Orbital Element Convolutions Due to a Velocity Sign Reversal.

9.3.3 BACKWARD INTEGRATION (con't)

and

$$M' = 2\pi - M \quad , \tag{45}$$

where the primed elements are those resulting from the sign reversal. These results may be used to generate the following relationships between the primed and unprimed element sets given by equation (9) of SECTION 6:

$$\begin{aligned} a' &= a \quad , \\ e' \sin\omega' &= e \sin\omega \quad , \\ e' \cos\omega' &= -e \cos\omega \quad , \\ \dot{i}' &= \pi - \dot{i} \quad , \\ M' + \omega' &= \pi - (M + \omega) \quad , \\ \Omega' &= \pi + \Omega \quad . \end{aligned} \tag{46}$$

Of course, when position and velocity components are used one has:

$$\begin{aligned} x' &= x \quad , \\ y' &= y \quad , \\ z' &= z \quad , \\ \dot{x}' &= -\dot{x} \quad , \\ \dot{y}' &= -\dot{y} \quad , \end{aligned} \tag{47}$$

and

$$\dot{z}' = -\dot{z} \quad .$$

9.3.3 BACKWARD INTEGRATION (con't)

To obtain a new set of initial conditions for the variational equations that are consistent with the equation of motion initial conditions and still referenced to the unprimed element set at trajectory epoch, one must use the following transformation:

$$\underset{\sim}{\Phi}_{t_o}(t_o) = \underset{\sim}{\Phi}'_{t_o}(t_o)\,\underset{\sim}{K}, \tag{48}$$

where $\underset{\sim}{\Phi}_{t_o}(t_o)$ and $\underset{\sim}{\Phi}'_{t_o}(t_o)$ are given by equation (62) of SECTION 6, with the prime indicating that the primed element set is used in that equation. The $\underset{\sim}{K}$ matrix is given by

$$\underset{\sim}{K} = \begin{pmatrix} 1 & 0 & 0 & 0 & 0 & 0 \\ 0 & 1 & 0 & 0 & 0 & 0 \\ 0 & 0 & -1 & 0 & 0 & 0 \\ 0 & 0 & 0 & -1 & 0 & 0 \\ 0 & 0 & 0 & 0 & -1 & 0 \\ 0 & 0 & 0 & 0 & 0 & 1 \end{pmatrix}, \tag{49}$$

The primed matrix in equation (48) is computed using $\vec{r}(t_o)$, $-\dot{\vec{r}}(t_o)$, and the primed element set in equations (43) - (54) of SECTION 6. When coordinates are being used instead of orbital elements, the following relationship is used:

9.3.3 BACKWARD INTEGRATION (con't)

$$\underset{\sim}{\Phi}(t_o)_{t_o} = \begin{pmatrix} 1 & 0 & 0 & 0 & 0 & 0 \\ 0 & 1 & 0 & 0 & 0 & 0 \\ 0 & 0 & 1 & 0 & 0 & 0 \\ 0 & 0 & 0 & -1 & 0 & 0 \\ 0 & 0 & 0 & 0 & -1 & 0 \\ 0 & 0 & 0 & 0 & 0 & -1 \end{pmatrix} . \quad (50)$$

9.3.4 THRUST INTERVAL INTEGRATION

PULSAR does not consider thrusting in its force model or variational equations and thus does not numerically integrate through an orbit adjust interval using a thrust acceleration model. It instead uses a time t'_{OA_E} near the orbit adjust end time (t_{OA_E}), where $t'_{OA_E} \geq t_{OA_E}$, to partition the trajectory into two segments. The first segment is integrated in the normal fashion using the pre-orbit adjust state vector at the trajectory start epoch t_o until time t'_{OA_E} is reached. At this time a predicted post-orbit adjust state vector is used as the initial state vector to generate the second trajectory segment using the Cowell integration algorithm.

It should be mentioned that backward integration from time t'_{OA_E} is not required, since no point or cross pass editing will be done for some time period around the orbit adjust interval (see subsection 8.1.2). Also one should note that cross pass editing is done independently on each trajectory segment and that state vector improvements cannot be propagated across a segment boundary.

The logical flow of the integration path controller is shown in Figure 9-4. This controller determines whether an orbit adjust has occurred during the editing span and directs the integrator through the associated required logic paths.

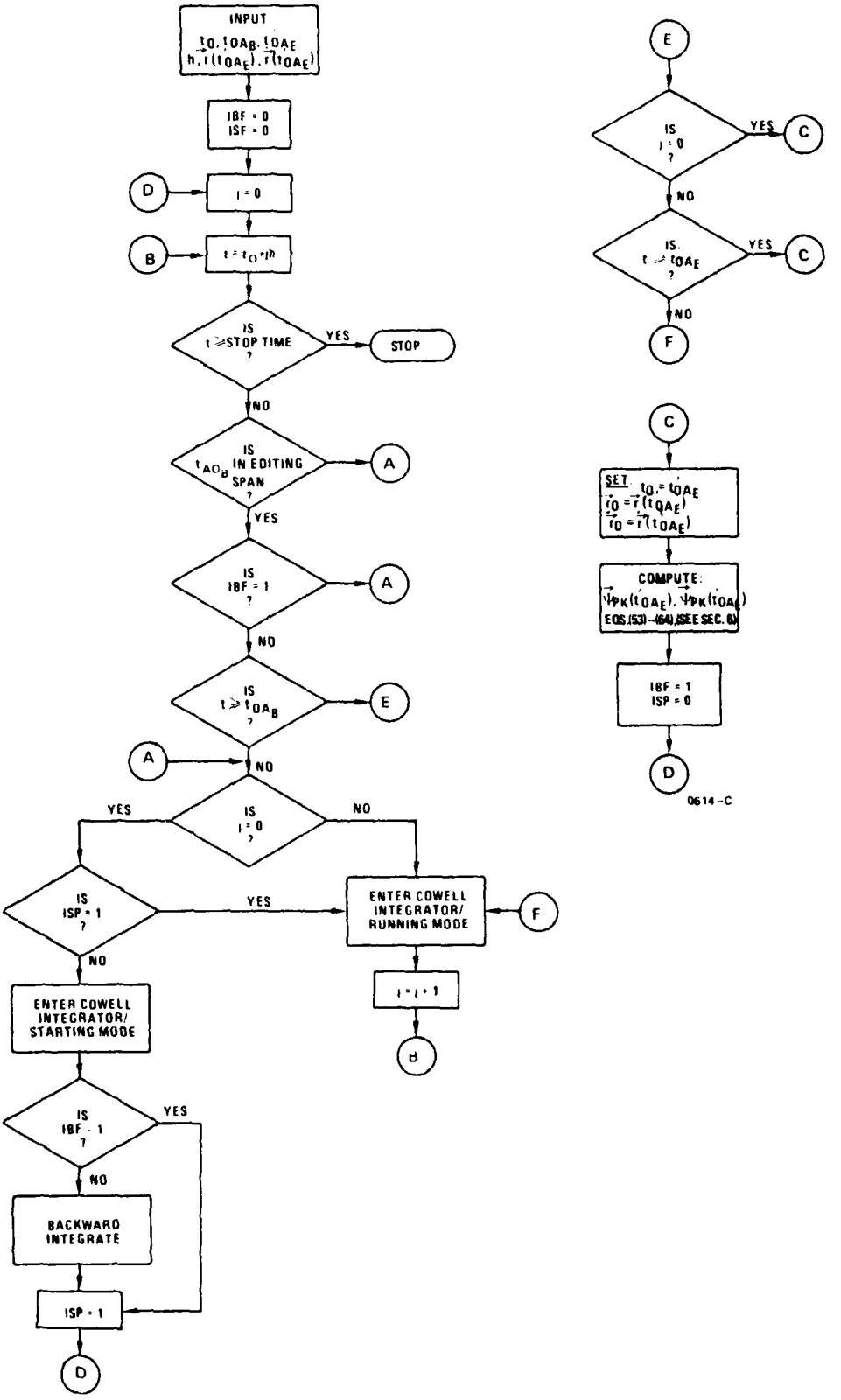

FIGURE 9-4. Integration Controller Logic Flow

9.4 CHOLESKY'S METHOD

Since $\underset{\sim}{\beta}$ is real and symmetric, a Cholesky decomposition is used in PULSAR to solve the pass normal equations (see equations (53) - (55) of SECTION 7). The method has been modified to identify and solve for only those parameters which are well determined.

In general the method involves solving the equation

$$\underset{\sim}{S} \begin{pmatrix} \underset{\sim}{\Delta b}'_{t_{CA}} \\ \\ \underset{\sim}{\Delta e}'_{t_{CA}} \end{pmatrix} = \underset{\sim}{\varepsilon}_s(t_{CA}) \quad , \tag{51}$$

where $\underset{\sim}{S}$ is a triangular matrix which satisfies the following relationships:

$$\underset{\sim}{S}^T \underset{\sim}{S} = \underset{\sim}{\beta}(t_{CA}) \tag{52}$$

and

$$\underset{\sim}{S}^T \underset{\sim}{\varepsilon}_s(t_{CA}) = \underset{\sim}{\varepsilon}(t_{CA}) \quad . \tag{53}$$

Note that in the equations above the matrices have been rearranged so that $\underset{\sim}{\beta}(t_{CA})$ and $\underset{\sim}{\varepsilon}(t_{CA})$ are given by equations (53) - (54) of SECTION 7, respectively, with the subscripts 'b' and 'e' interchanged. Once $\underset{\sim}{S}$ is determined, then the parameter corrections are given by:

$$\begin{pmatrix} \underset{\sim}{\Delta b}'_{t_{CA}} \\ \\ \underset{\sim}{\Delta e}'_{t_{CA}} \end{pmatrix} = \underset{\sim}{S}^{-1} \underset{\sim}{\varepsilon}_s(t_{CA}) \quad . \tag{54}$$

9.4 CHOLESKY'S METHOD (con't)

In order to identify those parameters which are well determined, the quantity d is used to perform a relative size test, where

$$d = \underset{\sim}{\beta}_{ii} \text{ for bias parameters,}$$

$$d = \sum_{\substack{\vec{r} \\ \text{components}}} \underset{\sim}{\beta}_{ii} \text{ for position parameters,} \tag{55}$$

or

$$d = \sum_{\substack{\dot{\vec{r}} \\ \text{components}}} \underset{\sim}{\beta}_{ii} \text{ for velocity parameters.}$$

This test assumes that all parameters are well determined unless the condition

$$\frac{\tau_i}{d} \leq 10^{-4} \tag{56}$$

is satisfied for the i^{th} parameter, where

$$\tau_i = \underset{\sim}{\beta}_{ii} - \sum_{k=1}^{i-1} \underset{\sim}{S}_{ki}^2 \quad , \tag{57}$$

and the summation vanishes for $i = 1$. Then the i^{th} parameter is not well determined and is suppressed as a solution parameter.

When equation (56) is satisfied, the i^{th} parameter is suppressed by setting all elements associated with it in the $\underset{\sim}{S}$ matrix to zero, i.e.

CHOLESKY'S METHOD (con't)

$$\underset{\sim}{S}_{ij} = 0 \quad (j = 1, 2, \cdots, N_p + 1), \tag{58}$$

re N_p is the number of original solution parameters. The number of para-
ers to solve for, N_s, is also reduced by one, i.e.

$$N_{s_{new}} = N_{s_{old}} - 1. \tag{59}$$

elements of the $\underset{\sim}{S}$ and $\underset{\sim}{\varepsilon}_s$ matrices for well determined parameters are
puted as follows:

$$\underset{\sim}{S}_{ii} = \left[\underset{\sim}{\beta}_{ii} - \sum_{k=1}^{i-1} \underset{\sim}{S}_{ki}^2 \right]^{-\frac{1}{2}}, \tag{60}$$

$$\underset{\sim}{S}_{ij} = \frac{1}{\underset{\sim}{S}_{ii}} \left[\underset{\sim}{\beta}_{ij} - \sum_{k=1}^{i-1} \underset{\sim}{S}_{ki} \underset{\sim}{S}_{kj} \right], \quad (j > i), \tag{61}$$

$$\underset{\sim}{\varepsilon}_{S_i} = \left[\underset{\sim}{\varepsilon}_i - \sum_{k=1}^{i-1} \underset{\sim}{S}_{ki} \underset{\sim}{\varepsilon}_{s_k} \right] \left[\underset{\sim}{S}_{ii} - \sum_{k=1}^{i-1} \underset{\sim}{S}_{ki}^2 \right]^{-\frac{1}{2}}, \tag{62}$$

re, as before, the summations vanish for $i = 1$. The inverse of the $\underset{\sim}{S}$ matrix
computed from:

$$\underset{\sim}{S}_{ji}^{-1} = \left[(i/j) - \sum_{k=i}^{j-1} \underset{\sim}{\gamma}_{ki} \underset{\sim}{\gamma}_{kj} \right] \underset{\sim}{S}_{jj}, \tag{63}$$

9.4 CHOLESKY'S METHOD (con't)

where

$$\underset{\sim}{Y}_{\ell m} = \begin{cases} \underset{\sim}{S}^{-1}_{\ell m} & \text{for } \ell \geq m \\ \\ \underset{\sim}{S}_{\ell m} & \text{for } \ell < m \end{cases} .$$

The t_{CA} parameter corrections Δp_i are then computed from:

$$\Delta p_i = \sum_{k=i}^{Np} \underset{\sim}{S}^{-1}_{ki} \; \underset{\sim}{\varepsilon}_{s_k} . \tag{65}$$

9.5 DATA COMPACTION

In order that any required post-PULSAR processing be performed more efficiently, the PULSAR data editor can compact its edited and untagged range difference tracking data. This process combines successive good data points produced by the PULSAR editing processes into a smaller and more compact output data set. The data compaction procedure merely involves adding together successive untagged (and valid) data points within an untagged and edited pass until a time span Δt_c from the time tag of the first point in the sum is reached, or until the last good point within Δt_c has been added. This process is repeated using the next set of data points within a Δt_c time span from the new first point until the end of the pass is reached. This procedure is restarted and repeated on a pass-by-pass basis until all good passes have been processed.

AD-A154 601 A MATHEMATICAL DESCRIPTION OF THE PULSAR DOPPLER SATELLITE TRACKING DATA EDITOR(U) NAVAL SURFACE WEAPONS CENTER DAHLGREN VA A D PARKS ET AL. SEP 82 3/3

UNCLASSIFIED NSWC/TR-82-391 F/G 17/3 NL

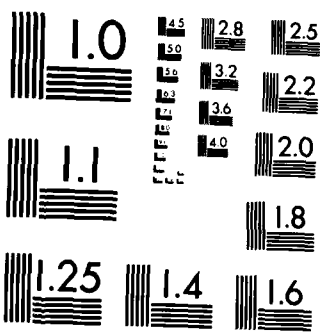

9.5 DATA COMPACTION (con't)

Also included with the compacted data points are the associated compacted observation sigmas, oscillator bias corrections, tropospheric corrections, and antenna offset corrections. To see how these compacted corrections are computed, consider the compacted data point P given by

$$P = \sum_i \mathcal{C}_i = \sum_i \left[\mathcal{D}(p_j, t_i) - \mathcal{D}(p_j, t_{i-1}) + \delta\Delta R_i \right] , \qquad (66)$$

where $\mathcal{D}(p_j, t)$ is defined by equation (17) of SECTION 7 and the summation is carried out over the good data points within the Δt_c time span. The last equation can be rewritten as

$$P = \sum_i \left\{ |\vec{\rho}_i| - |\vec{\rho}_{i-1}| \right\} - \frac{C}{f_o} f_b \sum_i \left| t_i - t_{i-1} \right|$$

$$- \frac{C}{2f_o} \dot{f}_b \sum_i \left| (t_i - t_{i-1}) (t_i + t_{i-1} - 2t_1) \right|$$

$$+ (1 + C_R) \sum_i \left| \Delta f_{R_i} - \Delta f_{R_{i-1}} \right| + \sum_i \delta\Delta R_i \quad . \qquad (67)$$

The second and fourth terms in this equation are the compacted oscillator bias and tropospheric corrections that are provided with the compacted data points. Although not required for post-PULSAR processing, it should be noted that compacted antenna offset and general relativity corrections are obtained from a Taylor expansion of the first term in the last equation. Using Equation (18) of Section 7, one may write

9.5 DATA COMPACTION (con't)

$$|\vec{\rho}_j| \simeq \mathbb{X}_j + \vec{\Delta r}_{A_j} \cdot \hat{\mathbb{X}}_j + \Delta\rho_{GR_j} , \tag{68}$$

where

$$\vec{\mathbb{X}}_j = \vec{r}_j - \vec{r}_{s_j} . \tag{69}$$

Thus the first term in equation (67) becomes

$$\sum_i \left\{ |\vec{\rho}_i| - |\vec{\rho}_{i-1}| \right\} \approx \sum_i (\mathbb{X}_i - \mathbb{X}_{i-1}) + \sum_i (\hat{\mathbb{X}}_i \cdot \vec{\Delta r}_{A_i} - \hat{\mathbb{X}}_{i-1} \cdot \vec{\Delta r}_{A_{i-1}})$$

$$+ \sum_i (\Delta\rho_{GR_i} - \Delta\rho_{GR_{i-1}}) . \tag{70}$$

The second and third sums in the last equation are the compacted antenna offset correction and compacted general relativity correction, respectively. The compacted observation sigma is given by

$$\sigma_c = (\Delta T)^{-\frac{1}{2}} , \tag{71}$$

where ΔT is the range difference time interval spanned by the compaction summation. The flow of the compaction process is presented in Figure 9-5.

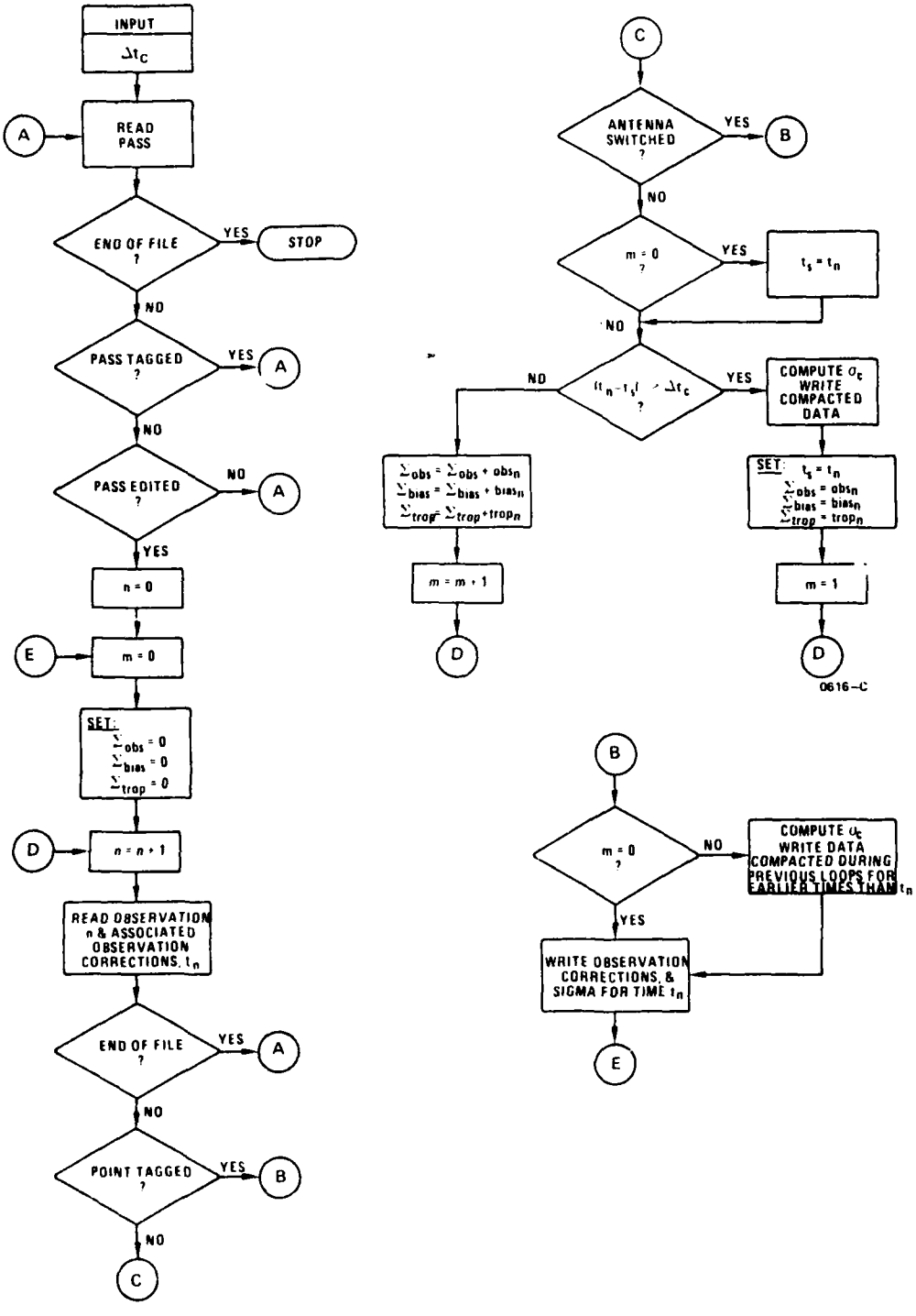

FIGURE 9-5. Data Compaction Process Flow

DISTRIBUTION

Library of Congress
ATTN: Gift and Exchange Division (4)
Washington, DC 20540

National Aeronautics and Space Administration
Scientific and Technical Library
Code NHS 22, Rm. BA39
600 Independence Avenue, SW
Washington, DC 20546 (2)

Defense Mapping Agency
ATTN: Mr. Jack Calender (10)
Washington, DC 20305

Defense Mapping Agency
Hydrographic/Topographic Center
ATTN: Mr. Patrick Fell (10)
Washington, DC 20390

Defense Mapping Agency Aerospace Center
ATTN: Dr. Robert Ballew (8)
St. Louis, MO 63118

Naval Electronics Systems Command
Navy Space Project, PME106
Washington, DC 20360 (3)

Office of Chief of Naval Operations
Naval Oceanography Division (NOP-952)
Bldg. 1, U.S. Naval Observatory (2)
Washington, DC 20390

Office of Naval Operations
Navy Space Systems Division (NOP-943) (2)
Washington, DC 20350

Naval Research Laboratory
ATTN: Mr. Al Bartholomew (3)
Washington, DC 20375

Naval Oceanographic Office
Bay St. Louis, MS 39522 (2)

DISTRIBUTION (Continued)

Office of Naval Research
Physical Sciences Division
800 N. Quincy St. (2)
Arlington, VA 22217

Air Force Geophysics Laboratory
Hanscom Field
Bedford, MA 01731 (2)

Goddard Space Flight Center
ATTN: Dr. David Smith (1)
Greenbelt, MD 20771

The University of Texas at Austin
ATTN: Dr. Byron Tapley (1)
Austin, TX 78712

Applied Research Laboratory
University of Texas
ATTN: Dr. Arnold Tucker (5)
Austin, TX 78712

Physical Sciences Laboratory
New Mexico State University
Box 3 - PSL
ATTN: Dan Martin (3)
Las Cruces, NM 88003

Applied Physics Laboratory
Johns Hopkins University
Johns Hopkins Road
ATTN: Harold Black (3)
Laurel, MD 20810

Local:

E31 (GIDEP)
E431 (10)
F14 (4)
K05 (2)
K12 (10)
K13 (30)
K14 (5)

END

FILMED

7-85

DTIC